รายงานการวิจัยฉบับสมบูรณ์

การคัดเลือกลักษณะเด่นของสัญญาณไฟฟ้ากล้ามเนื้อเพื่อระบุท่าทางการเคลื่อนไหวของมือ

ผู้วิจัย รศ.ดร.ชูศักดิ์ ลิ่มสกุล
ผู้ร่วมวิจัย ผศ.ดร.พรชัย พฤกษ์ภัทรานนต์

งานวิจัยนี้ได้รับทุนอุดหนุนการวิจัย จากเงินรายได้
คณะวิศวกรรมศาสตร์ ประจำปีงบประมาณ 2552

บทคัดย่อ

การวิจัยครั้งนี้ มีวัตถุประสงค์เพื่อคัดเลือกวิธีการหาลักษณะเด่นของสัญญาณไฟฟ้ากล้ามเนื้อ ในการระบุท่าทางการเคลื่อนไหวของมือ เพื่อนำไปประยุกต์ใช้สำหรับระบบจดจำสัญญาณไฟฟ้ากล้ามเนื้อ เพื่อใช้ประโยชน์ในการนำไปควบคุมอุปกรณ์ภายนอก เช่น รถเข็นไฟฟ้า เคอร์เซอร์เมาส์คอมพิวเตอร์ หรืออุปกรณ์เครื่องใช้ไฟฟ้าภายในบ้าน เป็นต้น รูปแบบการวิจัยในครั้งนี้ เป็นการวิจัย โดยใช้การประมวลผล และทำการประเมินแบบออฟไลน์ โดยในการประเมินหาวิธีการวัดลักษณะเด่นของสัญญาณที่ดีที่สุดนั้น ได้แบ่งการประเมินออกเป็น 3 ประเด็น คือ 1. ความแม่นยำในการระบุท่าทางการเคลื่อนไหว 2. ความสามารถในการทนต่อสัญญาณรบกวน 3. เวลา และความซับซ้อนในการคำนวณ ซึ่งในทั้ง 3 ประเด็นนั้น จะมีการประเมินวิธีการวัดลักษณะเด่นของสัญญาณ ทั้งจากการประเมินวิธีการวัดลักษณะเด่นของสัญญาณที่มีการใช้งานอยู่ในปัจจุบัน ทั้งจากวิธีการทางสถิติ และวิธีการใช้ตัวจำแนก การปรับปรุงวิธีการวัดลักษณะเด่นของสัญญาณที่มีอยู่เดิม ให้มีคุณสมบัติบางประการที่ดีขึ้น รวมทั้งการหาวิธีการวัดลักษณะเด่นของสัญญาณชนิดใหม่มาประยุกต์ใช้งาน อย่างไรก็ตามจากข้อจำกัดที่ว่า ไม่มีวิธีการวัดลักษณะเด่นของสัญญาณชนิดใดที่จะได้ผลดีที่สุดในทั้ง 3 ประเด็นนั้น ในขั้นของการทดลอง และสรุปผลวิธีการวัดลักษณะเด่นของสัญญาณที่ดีที่สุด จึงแยกวิเคราะห์ในแต่ละประเด็น โดยในการนำไปประยุกต์ใช้งานจริง มีความจำเป็นต้องเลือกใช้ให้เหมาะสมกับงานต่อไป สำหรับวิธีการวัดลักษณะเด่นของสัญญาณที่นำมาประเมินในงานวิจัยที่ได้จากการทบทวนวรรณกรรมมีด้วยกัน 16 วิธี มีการปรับปรุงวิธีการวัดลักษณะเด่นของสัญญาณ 2 วิธี และนำเสนอวิธีการวัดลักษณะเด่นของสัญญาณชนิดใหม่อีก 1 วิธี ซึ่งสามารถสรุปผลของการวิจัย แบ่งตามประเด็นได้ดังนี้

1. ในประเด็นความแม่นยำในการระบุท่าทางการเคลื่อนไหว คณะผู้วิจัยได้ทำการเลือก และรวมกลุ่มวิธีการวัดลักษณะเด่นของสัญญาณในแกนเวลา 3 ชนิด ซึ่งประกอบด้วย วิธี Waveform Length (WL) วิธี Root Mean Square (RMS) และวิธี Auto Regressive อันดับที่ 4 (AR4) ซึ่งให้ผลค่าความแม่นยำในการจำแนกท่าทางขณะไม่มีสัญญาณรบกวนสูงถึง 98-99% โดยการประเมินด้วยตัวจำแนกชนิด Linear Discriminant Analysis (LDA) หลังจากนั้นคณะผู้วิจัยได้ทำการประเมินวิธีการวัดลักษณะเด่นของสัญญาณที่มีอยู่เดิมจากการทบทวนวรรณกรรม 15 วิธี ทั้งบนแกนเวลาและแกนความถี่ โดยการใช้วิธีการประเมินทางสถิติ ซึ่งพบว่า วิธีการวัดลักษณะเด่นของสัญญาณแบบ WL ให้ผลดีที่สุด ตามมาด้วยวิธี RMS และวิธี Willison Amplitude (WAMP) ดังนั้น ในแง่มุมของความแม่นยำในการระบุท่าทาง สามารถสรุปได้ว่าวิธีการวัดลักษณะเด่นของสัญญาณแบบ WL ให้ผลดีที่สุด ในประเด็นความแม่นยำของการจำแนกท่าทาง

2. ในประเด็นความสามารถในการทนต่อสัญญาณรบกวน คณะผู้วิจัยได้เริ่มศึกษาเพิ่มเติมในขั้นของการเตรียมสัญญาณ ก่อนนำมาคำนวณหาวิธีการวัดลักษณะเด่นของสัญญาณ โดยการใช้การลดสัญญาณรบกวนด้วยวิธีการแปลงเวฟเล็ต ซึ่งทำให้ยังคงค่าความแม่นยำในการระบุท่าทางการเคลื่อนไหวอยู่ได้ แม้ขณะที่มีสัญญาณรบกวนเข้ามาในระบบ นอกจากนี้ ทางคณะผู้วิจัยได้มีการปรับปรุงวิธีการวัดลักษณะเด่นของสัญญาณ ในแกนความถี่ 2 วิธี คือ วิธี Modified Mean Frequency (MMNF) และวิธี Modified Median Frequency (MMDF) ซึ่งพบว่าสามารถเพิ่มประสิทธิภาพในการทนต่อสัญญาณรบกวนได้ดีขึ้น เมื่อเทียบกับวิธีการวัดลักษณะเด่นของ

สัญญาณแบบเดิม 16 วิธี นอกจากนี้ในการประเมินวิธีการวัดลักษณะเด่นของสัญญาณชนิดเดิม 16 วิธีนั้น พบว่าวิธีการวัดลักษณะเด่นของสัญญาณแบบ WAMP และ Histogram of EMG (HIST) ให้ผลในการทนต่อสัญญาณรบกวนที่ดี

3. ในประเด็นเวลาและความซับซ้อนในการคำนวณ พบว่าวิธีการวัดลักษณะเด่นของสัญญาณ แบบ Integrated EMG (IEMG) ใช้เวลาในการคำนวณน้อยที่สุด และพบว่าวิธีการวัดลักษณะเด่นของสัญญาณบนแกนเวลาจะใช้เวลาในการคำนวณน้อยกว่าบนแกนความถี่ แต่ถึงอย่างไรก็ตามวิธีการวัดลักษณะเด่นของสัญญาณบนแกนเวลา ซึ่งสามารถคำนวณได้ทันเวลานั้นจะไม่สามารถเข้าถึงคุณลักษณะ Non-stationary ของสัญญาณได้ แต่วิธีการวัดลักษณะเด่นของสัญญาณแบบทั้งแกนเวลาและความถี่ จะสามารถเข้าถึง Non-stationary ของสัญญาณได้ แต่ก็พบว่าจะใช้เวลาในการคำนวณสูงกว่าหลายร้อยเท่า ดังนั้นทางคณะผู้วิจัยจึงได้เลือกทำการศึกษาวิธีการวัดลักษณะเด่นของสัญญาณชนิดใหม่เพิ่มเติม คือ วิธี Detrended Fluctuation Analysis (DFA) ซึ่งเป็นวิธีที่สามารถเข้าถึงความเป็น Non-stationary ของสัญญาณได้ เหมือนกับวิธีการวัดลักษณะเด่นของสัญญาณบนแกนเวลาและความถี่ แต่ใช้เวลาในการคำนวณ และความซับซ้อนที่น้อยกว่าวิธีบนแกนเวลาและความถี่มาก และใช้เวลาในการคำนวณสูงกว่าวิธีบนแกนเวลา และวิธีบนแกนความถี่เพียงเล็กน้อย นอกจากนี้วิธี DFA ยังคงให้ความแม่นยำในการระบุท่าทาง และความสามารถในการทนต่อสัญญาณรบกวนที่ดีด้วย

Abstract

The objective of this research is a selection of an optimal Electromyography (EMG) feature extraction in order to determine the different kinds of hand movement for applying with EMG recognition and control system i.e. electric powered wheelchair, mouse cursor, and electric equipment. The evaluation process in this study is an offline test. In order to find an optimal EMG feature, three criterions should be addressed including class separability, robustness, and computational complexity. Firstly, we evaluated the existed EMG features from the literatures. In addition, the modification of the existed EMG features and a novel EMG feature are presented. However, from the limitation that it does not have the best feature in the whole criterions. In this study, discussion and summary are presented for each criterion. In practice, we should select the optimal EMG features depending on the interested application. In summary, we evaluated sixteen existed EMG features, modified two existed EMG feature, and introduced a novel feature. The discussion and summary are presented in each criterion of the following:

1. In class separability view point, we selected and grouped three well-known EMG features in time domain including Root Mean Square (RMS), Waveform Length (WL), and the forth order of Auto Regressive (AR4). In addition, classification task is evaluated by Linear Discriminant Analysis (LDA). The accuracy of recognition is about 98-99% with free noise environment. After that we evaluated fifteen EMG features from the previous literatures in both of time domain and frequency domain by using statistic criterion method. From the experimental results, WL is the best feature comparing with the other features. RMS and Willison Amplitude (WAMP) are useful augmenting features for a more powerful feature vector. In conclusion, for a single feature, WL is the best feature in class separability point of view.

2. In robustness viewpoint, we firstly used pre-processing stage based on denoising method using wavelet transform. The results show the improving of hand movement recognition accuracy among the noisy environment. Furthermore, we also modified two types of feature extraction based on frequency domain, namely Modified Mean Frequency (MMNF) and Modified Median Frequency (MMDF). From the experimental results, it is shown that MMNF and MMDF can be used for the new robust feature extraction. Its robustness performance is better than the other existing features. In addition, WAMP and Histogram of EMG (HIST) are the existed features that are better in robustness point of view.

3. In computational complexity and time, Integrated EMG (IEMG) uses less computational cost. In addition, we found that time domain features have low computational complexity compared to features in frequency domain. Moreover, we introduced a novel feature based on non-linear analysis, namely Detrended Fluctuation Analysis (DFA). DFA is suitable for analyzing the non-stationary (EMG) signals same as time-frequency features that features in time domain and frequency domain are not suitable. However, DFA takes

less CPU time than feature in frequency domain and time-frequency features and a few more CPU time than feature in time domain.

กิตติกรรมประกาศ

ขอขอบพระคุณ คณะวิศวกรรมศาสตร์ มหาวิทยาลัยสงขลานครินทร์ วิทยาเขตหาดใหญ่ ที่ให้การสนับสนุนทุนอุดหนุนในการทาวิจัย ตลอดจนบุคลากร นักศึกษาระดับปริญญาเอก และปริญญาตรีของห้องปฏิบัติการวิศวกรรมฟื้นฟู ภาควิชาวิศวกรรมไฟฟ้า คณะวิศวกรรมศาสตร์

รายงานฉบับนี้ เกิดขึ้นได้จากการสนับสนุนช่วยเหลือจากบุคคลต่างๆ ดังกล่าวข้างต้น อย่างไรก็ตาม หากมีบุคคลอื่นใดที่ข้าพเจ้ามิได้กล่าวไว้ ณ ที่นี้ ข้าพเจ้าต้องขออภัยและขอขอบคุณไว้ ณ โอกาสนี้

ชูศักดิ์ ลิ่มสกุล
หัวหน้าโครงการ

คำนำ

รายงานการวิจัย เรื่อง การคัดเลือกลักษณะเด่นของสัญญาณไฟฟ้ากล้ามเนื้อ เพื่อระบุท่าทางการเคลื่อนไหวของมือเล่มนี้ จัดทำขึ้นเพื่อรายงานการคัดเลือกวิธีการหาลักษณะเด่นของสัญญาณไฟฟ้ากล้ามเนื้อ ในการระบุท่าทางการเคลื่อนไหวของมือ ซึ่งประกอบไปด้วย ข้อมูลเบื้องต้นของโครงการวิจัย หลักการและเหตุผล ประโยชน์ที่คาดว่าจะได้รับ การทบทวนวรรณกรรมและโครงการวิจัยที่เกี่ยวข้อง ระเบียบวิธีการวิจัย ผลการวิจัย และวิเคราะห์ผลการวิจัย และสรุปผลการวิจัย

ผลจากการคัดเลือกวิธีการหาลักษณะเด่นของสัญญาณไฟฟ้ากล้ามเนื้อ ได้ทำการประเมินและปรับปรุงวิธีการวัดลักษณะเด่นของสัญญาณที่เหมาะสม ในการนำไประบุท่าทางการเคลื่อนไหวของมือ ซึ่งสามารถนำไปประยุกต์ใช้สำหรับระบบจดจำสัญญาณไฟฟ้ากล้ามเนื้อต่อไปได้ ซึ่งในระบบจดจำสัญญาณไฟฟ้ากล้ามเนื้อนั้น ถ้าเลือกวิธีการวัดลักษณะเด่นของสัญญาณที่เหมาะสมแล้วจะทำให้ประสิทธิภาพของระบบจดจำถูกปรับปรุงขึ้น ทั้งในแง่มุมของความแม่นยำในการจำแนก ความทนต่อสัญญาณรบกวนชนิดต่างๆ รวมถึงเวลาและความซับซ้อนในการประมวลผลของระบบ นอกจากนี้ในรายงานฉบับนี้ ยังได้รวบรวมวิธีการหาลักษณะเด่นของสัญญาณไฟฟ้ากล้ามเนื้อแต่ละวิธีที่มีใช้อยู่ในงานวิจัยในปัจจุบัน ซึ่งสามารถใช้เป็นแหล่งสำหรับอ้างอิง และศึกษาเพิ่มเติมเกี่ยวกับวิธีการวัดลักษณะเด่นของสัญญาณไฟฟ้ากล้ามเนื้อได้ต่อไป

ชูศักดิ์ ลิ่มสกุล
หัวหน้าโครงการ

สารบัญ

สารบัญ (ต่อ)

1. บทนำ

1.1 ประเภทของงานวิจัย ประยุกต์

1.2 คำหลัก (Keywords) EMG, Electromyography, Feature Extraction, Hand Movement

1.3 หลักการและเหตุผล (Importance and motivation of this research)

ในผู้ป่วยหรือผู้พิการหรือผู้สูงอายุ พบว่ามีความยากลำบากในการใช้งานอุปกรณ์ช่วยเหลือภายนอก ซึ่งเป็นอุปกรณ์ที่ใช้การควบคุมด้วยมือ เช่น แป้นพิมพ์ หรือคันบังคับ ดังนั้น จึงมีความพยายามในการพัฒนาส่วนในการควบคุมอุปกรณ์ภายนอกที่ไม่ต้องใช้มือควบคุม (Hand-free) ขึ้นมา โดยใช้สัญญาณทางชีวการแพทย์ ซึ่งสัญญาณที่สำคัญสัญญาณหนึ่ง คือ สัญญาณไฟฟ้ากล้ามเนื้อ (Electromyography (EMG) signal หรือ Myoelectric signal) ซึ่งเป็นสัญญาณที่สามารถวัดได้จากอิเล็กโทรดชนิดพื้นผิว (Surface electrode) โดยประกอบด้วยข้อมูลของสัญญาณจำนวนมาก ดังนั้น ในการจะนำสัญญาณเหล่านี้มาใช้งานในการจำแนกท่าทางของผู้ใช้งาน จึงต้องใช้ระเบียบวิธีในการคำนวณ (Algorithm) ต่างๆ

การประยุกต์ใช้งานสัญญาณกล้ามเนื้อถูกพัฒนามาอย่างต่อเนื่องตลอดช่วงเวลา 50 ปี โดยในช่วงแรก เป็นเพียงการนำสัญญาณไฟฟ้ากล้ามเนื้อจากเพียงหนึ่งจุดกล้ามเนื้อ เพื่อควบคุมการทำงานฟังก์ชันหนึ่งอย่าง เช่น การเปิดหรือปิด โดยมีอัตราเร็วค่าหนึ่ง ต่อมามีการนำสัญญาณไฟฟ้ากล้ามเนื้อจากหลายจุดกล้ามเนื้อ เพื่อใช้ในการควบคุมการทำงานได้หลายฟังก์ชัน (Multifunction control) เช่น การควบคุมอวัยวะเทียมทั้งมือเทียม แขนเทียม และขาเทียม (Prostheses) การควบคุมหุ่นยนต์ที่สามารถสวมใส่ได้เพื่อใช้ผ่อนแรงผู้ใช้ (Exoskeleton robot control) ซึ่งล้วนแล้วแต่ต้องการความแม่นยำสูงในการควบคุม การนำวิธีการทางคณิตศาสตร์มาช่วยในการจำแนกสัญญาณต่างๆ จึงถูกนำมาใช้ เพื่อให้มีความแม่นยำสูง ทนต่อสัญญาณรบกวนได้ดี และสามารถตอบสนองต่อการทำงานอย่างรวดเร็วได้ ดังนั้นจึงมีแนวคิดในการคัดเลือกวิธีการวัดลักษณะเด่นของสัญญาณ (Feature extraction) ที่เหมาะสมในการระบุท่าทางการเคลื่อนไหวของมือ เพื่อนำไปประยุกต์ใช้ในการควบคุมอุปกรณ์ภายนอกที่มีประสิทธิภาพต่อไป

1.4 ประโยชน์ที่คาดว่าจะได้รับ (Expected benefits)

1. ได้วิธีการวัดลักษณะเด่นของสัญญาณไฟฟ้ากล้ามเนื้อที่เหมาะสมที่จะใช้ในการระบุท่าทางการเคลื่อนไหวของมือ

2. สามารถนำการระบุท่าทางการเคลื่อนไหวของมือ เพื่อนำไปสู่การสร้างระบบเชื่อมต่อระหว่างผู้ใช้กับอุปกรณ์ภายนอกสำหรับผู้พิการ และผู้สูงอายุได้

1.5 การทบทวนวรรณกรรม และโครงการวิจัยที่เกี่ยวข้อง (Literature review)

การวัดลักษณะเด่นของสัญญาณ (Feature extraction) ในการระบุท่าทางการเคลื่อนไหวของมือ ถือเป็นส่วนสำคัญในการที่จะประสบความสำเร็จในการควบคุมอุปกรณ์ภายนอก [1, 3] ดังนั้น จึงมีนักวิจัยจำนวนมากที่ได้ทำการพัฒนาวิธีการวัดลักษณะเด่นของสัญญาณ โดยในยุคเริ่มแรกนั้น [4] วิธีการวัดลักษณะเด่นของสัญญาณ

จะมีการวิเคราะห์บนแกนเวลา (Time domain) เป็นส่วนใหญ่ เนื่องจากมีความง่ายในการเขียนโปรแกรม ในการทำความเข้าใจ และใช้เวลาในการประมวลผลที่น้อย ซึ่งเหมาะสมกับอุปกรณ์ทางฮาร์ดแวร์ แต่ด้วยเนื่องจากข้อจำกัดของสัญญาณไฟฟ้ากล้ามเนื้อที่มีความแปรปรวนสูง โดยเฉพาะเมื่อต้องอ้างอิงในเชิงเวลา ดังนั้นจึงมีการนำการวิเคราะห์สัญญาณบนแกนความถี่ (Frequency domain) เข้ามาใช้งาน แต่ก็จะพบว่า วิธีการวัดลักษณะเด่นของสัญญาณในแกนความถี่ จะทำให้เสียข้อมูลในแกนเวลาไป [5] นักวิจัยในยุคต่อมาจึงได้มีการพัฒนาการวิเคราะห์สัญญาณบนทั้งแกนเวลาและความถี่เข้ามาใช้งาน ซึ่งทำให้ผลการระบุการท่าทางการเคลื่อนไหวของมือสามารถระบุได้แม่นยำมากขึ้น แต่ข้อจำกัดที่มีก็คือ เรื่องของเวลาในการคำนวณที่มีมากขึ้นตามไปด้วย [6]

ดังนั้น ในการจะเลือกว่าวิธีการวัดลักษณะเด่นของสัญญาณชนิดใดจะเหมาะสมนั้น จึงไม่สามารถใช้เฉพาะเกณฑ์ความแม่นยำในการจำแนกเพียงอย่างเดียวได้ จึงมีคณะผู้วิจัยทีมหนึ่ง [7] ได้ระบุเกณฑ์ในการที่จะระบุว่าวิธีการวัดลักษณะเด่นของสัญญาณชนิดใดมีความเหมาะสมที่สุด โดยใช้เกณฑ์ที่สำคัญ 3 อย่าง ได้แก่ 1. ความแม่นยำในการระบุท่าทางการเคลื่อนไหว (Class separability) 2. ความสามารถทนต่อสัญญาณรบกวน (Robustness)

3. เวลา และความซับซ้อนในการคำนวณ (Computational complexity) ซึ่งในปัจจุบันพบว่าวิธีการวัดลักษณะเด่นของสัญญาณมีการพัฒนามากขึ้นเป็นจำนวนมาก ซึ่งข้อจำกัดในปัจจุบันคือ นักวิจัยได้ทำการนำเสนอวิธีการวัดลักษณะเด่นของสัญญาณชนิดใหม่ โดยใช้ข้อมูลสัญญาณไฟฟ้ากล้ามเนื้อที่แตกต่างกันออกไป และไม่ได้ใช้เกณฑ์ในการเปรียบเทียบด้วยหลักเกณฑ์เดียวกัน ทำให้เราไม่สามารถเปรียบเทียบกันได้โดยตรงว่าวิธีการวัดลักษณะเด่นของสัญญาณชนิดใดให้ผลที่ดีกว่ากัน ตัวอย่างเช่น ในเรื่องของความแม่นยำในการจำแนกท่าทาง ค่าของความแม่นยำเอง นอกจากจะขึ้นกับชนิดของวิธีการวัดลักษณะเด่นของสัญญาณแล้ว ยังขึ้นอยู่กับชนิดของวิธีการจำแนก (Classifier) ด้วย ซึ่งปัจจุบันยังมีการใช้การเปรียบเทียบจากวิธีการจำแนกคนละแบบกัน ซึ่งไม่ยุติธรรมในการเปรียบเทียบ หรือนักวิจัยบางกลุ่มที่ใช้หลักเกณฑ์เดียวกัน แต่ก็ทำการเปรียบเทียบกลุ่มของวิธีการวัดลักษณะเด่นของสัญญาณที่ไม่มากนัก [8] เมื่อเทียบกับจำนวนของวิธีการวัดลักษณะเด่นของสัญญาณที่มีใช้ในปัจจุบัน นอกจากนี้การประเมินวิธีการวัดลักษณะเด่นของสัญญาณ ในมุมของการทนต่อสัญญาณรบกวน ยังไม่มีการทดสอบที่เป็นรูปธรรม ดังนั้น ในงานวิจัยนี้จะทำการสรรหาวิธีการคัดเลือกวิธีการวัดลักษณะเด่นของสัญญาณที่เหมาะสมจากทั้งใน 3 เกณฑ์ โดยใช้ฐานข้อมูลเดียวกัน โดยทำการทดสอบกับวิธีการวัดลักษณะเด่นของสัญญาณที่ครอบคลุมมากที่สุด จนถึงการสำรวจบทความวิชาการในปัจจุบัน

การวัดลักษณะเด่นของสัญญาณ (Feature Extraction)

การวัดลักษณะเด่นของสัญญาณ คือ กระบวนการวัดคุณสมบัติของวัตถุ โดยคุณสมบัติที่กล่าวถึงนี้หมายถึง ลักษณะเฉพาะตัวของวัตถุ (Feature) นั้นๆ ซึ่งจะต้องเป็นปริมาณที่สามารถวัดค่าได้ และมีค่าเป็นตัวเลข และเนื่องจากการจำแนกท่าทางหลายท่า อาจมีท่าทางบางท่าที่มีลักษณะเฉพาะตัวบางอย่างคล้ายคลึงกัน ดังนั้น จึงมีความจำเป็นต้องใช้คุณสมบัติหลายๆ ประการ มาจำแนกท่าทางหลายชนิดออกจากกัน ดังนั้น จึงจำเป็นต้องทำการเลือกลักษณะเด่น (Salient features) เพียงไม่กี่ชนิดที่สามารถใช้จำแนกลักษณะท่าทางต่างๆ ออกจากกันได้อย่างชัดเจน แทนที่จะทำการวัดคุณสมบัติทุกอย่าง เพื่อลดความสิ้นเปลืองดังกล่าว และเมื่อในกรณีของสัญญาณไฟฟ้ากล้ามเนื้อ คือ แรงดันไฟฟ้าที่วัดได้ภายในช่วงระยะเวลาหนึ่ง จะพบว่าสัญญาณไฟฟ้ากล้ามเนื้อมี

ลักษณะเฉพาะตัวหลายๆ ชนิด เช่น ขนาดของแรงดันสูงสุด ขนาดของแรงดันเฉลี่ยในหนึ่งหน่วยเวลา ขนาดขององค์ประกอบสัญญาณที่ได้จากการแปลงฟูเรียร์อย่างรวดเร็ว เป็นต้น

กระบวนการวัดคุณสมบัติของวัตถุ หรือ Feature extraction ผลที่ได้จากกระบวนการนี้ คือ ค่าคุณสมบัติต่างๆ ของวัตถุ ซึ่งหากนำมาจัดวางในรูปแบบเวกเตอร์ก็จะได้ Feature vector ซึ่งเป็นการแสดงค่าคุณสมบัติทั้งหมดที่วัดจากวัตถุนั้นๆ ที่อยู่ในรูปของเวกเตอร์ เช่น

$$V = \begin{bmatrix} 0.5 \\ 0.05 \end{bmatrix}$$

การคำนวณทางคณิตศาสตร์ เพื่อหาลักษณะต่างๆ ของสัญญาณแรงดันไฟฟ้าซึ่งถูกสุ่มเข้ามาสู่คอมพิวเตอร์ด้วยค่าความถี่ในการสุ่มคงที่ มีหลายรูปแบบ โดยสามารถแบ่งออกได้เป็น 3 กลุ่ม คือ การวิเคราะห์บนแกนเวลา (Time domain), การวิเคราะห์บนแกนความถี่ (Frequency domain) และการวิเคราะห์บนทั้งแกนเวลาและความถี่ (Time-Frequency representation)

สมมุติให้ x_n คือ ค่าแรงดันไฟฟ้าที่คอมพิวเตอร์ทำการสุ่มเข้ามาครั้งที่ n ดังนั้นสัญญาณที่สุ่มเข้ามาภายในช่วงเวลาหนึ่งจำนวน N ค่า จะสามารถแทนด้วยชุดแรงดันไฟฟ้า $[x_1, x_2, \ldots, x_n]$ ซึ่งเราจะสามารถคำนวณลักษณะต่างๆ ของสัญญาณได้ดังนี้

1.5.1 ตัวอย่างวิธีการวัดลักษณะเด่นของสัญญาณบนแกนเวลา (Time domain)

1. Root Mean Square (RMS) เป็นการหาค่ารากของค่าเฉลี่ยของกำลังสองของสัญญาณไฟฟ้ากล้ามเนื้อ ได้ผลลัพธ์ 1 feature vector

$$\mathrm{RMS} = \sqrt{\frac{1}{N}\sum_{n=1}^{N} x_n^2}$$

2. Mean Absolute Value (MAV) เป็นการหาค่าเฉลี่ยของค่าสัมบูรณ์ของสัญญาณไฟฟ้ากล้ามเนื้อ หรืออาจเรียกเป็นอย่างอื่น เช่น Integral of absolute value (IAV) ได้ผลลัพธ์ 1 feature vector

$$\mathrm{MAV} = \frac{1}{N}\sum_{n=1}^{N} |x_n|$$

โดยที่วิธีการวัดลักษณะเด่นของสัญญาณแบบได้เพิ่มเติมมาจากการหาค่าผลรวมของค่าสัมบูรณ์ของสัญญาณไฟฟ้ากล้ามเนื้อ ซึ่งมีชื่อเรียกวิธีการวัดลักษณะเด่นของสัญญาณวิธีดังกล่าวว่า Integrated EMG (IEMG)

$$\mathrm{IEMG} = \sum_{n=1}^{N} |x_n|$$

นอกจากนี้ยังมีการพัฒนาการหาค่าเฉลี่ยของค่าสัมบูรณ์ของสัญญาณไฟฟ้ากล้ามเนื้อ โดยการให้ค่าน้ำหนัก (Modified Mean Absolute Value: MMAV1 and MMAV2) อีก 2 วิธี ซึ่งนิยามของการคำนวณ แสดงได้ดังนี้

$$\text{MAV1} = \frac{1}{N}\sum_{n=1}^{N} w_n |x_n|, \qquad \text{MAV2} = \frac{1}{N}\sum_{n=1}^{N} w_n |x_n|,$$

$$w_n = \begin{cases} 1, & if\ 0.25N \le n \le 0.75N \\ 0.5, & otherwise. \end{cases} \qquad w_n = \begin{cases} 1, & if\ 0.25N \le n \le 0.75N \\ 4n/N, & if\ 0.25N > n \\ 4(n-N)/N, & if\ 0.75N < n. \end{cases}$$

3. Mean Absolute Value Slope (MAVS) เป็นการหาค่าผลต่างระหว่างค่าของวิธีการวัดลักษณะเด่นของสัญญาณแบบ MAV ของค่าในตำแหน่งปัจจุบันกับค่าในตำแหน่งถัดไป โดยความละเอียดของวิธีการวัดลักษณะเด่นของสัญญาณชนิดนี้ จะขึ้นกับจำนวนของ Segment ที่กำหนด ได้ผลลัพธ์เท่ากับจำนวนของ Segment -1 feature vectors

$$\text{MAVS}_i = \text{MAV}_{i+1} - \text{MAV}_i; \quad i = 1, \ldots, I-1.$$

เมื่อ i = Segment ตัวที่ i

4. Simple Square Integral (SSI) เป็นการหาค่าพลังงานของสัญญาณไฟฟ้ากล้ามเนื้อ เพื่อใช้แทนลักษณะเด่นของสัญญาณ ได้ผลลัพธ์ 1 feature vector

$$\text{SSI} = \sum_{n=1}^{N} |x_n|^2$$

5. Variance (VAR) ใช้วัดความหนาแน่นของพลังงานของสัญญาณไฟฟ้ากล้ามเนื้อ ถ้าค่าสูง แสดงว่าสัญญาณไฟฟ้ากล้ามเนื้อมีความเปลี่ยนแปลงมาก และบ่งชี้ว่ามีความหนาแน่นของพลังงานมาก ได้ผลลัพธ์ 1 feature vector

$$\text{VAR} = \frac{1}{N-1}\sum_{n=1}^{N} x_n^2$$

6. Waveform Length (WL) เป็นการหาค่าสะสมของผลต่างระหว่างแรงดันปัจจุบันกับค่าก่อนหน้า เป็นค่าที่บ่งชี้ว่าสัญญาณไฟฟ้ากล้ามเนื้อมีการเปลี่ยนแปลงไปมากน้อยเพียงใด ได้ผลลัพธ์ 1 feature vector

$$\text{WL} = \sum_{n=1}^{N-1} |x_{n+1} - x_n|$$

7. Zero Crossing (ZC) เป็นการหาจำนวนครั้งที่รูปคลื่นสัญญาณไฟฟ้ากล้ามเนื้อตัดผ่านระดับแรงดันไฟฟ้าเท่ากับศูนย์ โดยทั่วไปแล้วจะใช้การนับจำนวนครั้งที่แรงดันไฟฟ้ามีการเปลี่ยนเครื่องหมายจากลบเป็นบวก หรือเปลี่ยนจากบวกเป็นลบ มีการกำหนดค่า Threshold อยู่ในช่วง 20–40 mV ได้ผลลัพธ์ 1 feature vector

$$\text{ZC} = \sum_{n=1}^{N-1} \left[\text{sgn}\left(x_n \times x_{n+1}\right) \cap \left|x_n - x_{n+1}\right| \ge threshold \right];$$

$$\text{sgn}(x) = \begin{cases} 1, & if\ x \ge 0 \\ 0, & otherwise. \end{cases}$$

8. Willison Amplitude (WAMP) เป็นการหาจำนวนครั้งที่สัญญาณไฟฟ้ากล้ามเนื้อมีการเปลี่ยนแปลงขนาดมากกว่าค่าที่กำหนดไว้ (Threshold) ส่วนใหญ่แล้วจะกำหนดค่า Threshold = 30 mV โดยที่ปริมาณนี้จะบ่งชี้ถึงระดับความรุนแรงของกล้ามเนื้อมีการหดตัว ในขณะที่ร่างกายออกแรงกระทำ ได้ผลลัพธ์ 1 feature vector

$$\text{WAMP} = \sum_{n=1}^{N-1} f\left(\left|x_n - x_{n+1}\right|\right);$$

$$f(x) = \begin{cases} 1, & if\ x \geq threshold \\ 0, & otherwise. \end{cases}$$

9. Slope Sign Change (SSC) เป็นวิธีการวัดลักษณะเด่นของสัญญาณที่มีความสัมพันธ์กับวิธีการหาค่า ZC โดยเป็นการหาจำนวนครั้งที่สัญญาณไฟฟ้ากล้ามเนื้อมีการเปลี่ยนแปลงขนาดระหว่างค่าความชันที่เป็นบวกกับลบของสัญญาณในสามลำดับที่ติดต่อกัน ซึ่งจะมีการกำหนดให้นับเมื่อค่ามากกว่าค่าที่กำหนดไว้ (Threshold) ส่วนใหญ่แล้วจะกำหนดค่า Threshold = 30 mV ได้ผลลัพธ์ 1 feature vector

$$\text{SSC} = \sum_{n=2}^{N-1}\left[f\left[\left(x_n - x_{n-1}\right)\times\left(x_n - x_{n+1}\right)\right]\right];$$

$$f(x) = \begin{cases} 1, & if\ x \geq threshold \\ 0, & otherwise. \end{cases}$$

10. Auto Regressive (AR) Model เป็นการหาค่าสัมประสิทธิ์ของแบบจำลอง ที่มีแนวคิดพื้นฐานที่ว่าสำหรับสัญญาณหนึ่งๆ ที่ได้ถูกสุ่มอ่านเข้ามานั้น สามารถแทนค่าแรงดันที่จุดปัจจุบันที่กำลังพิจารณา x_n ด้วยผลรวมของผลคูณระหว่างสัมประสิทธิ์ (α) และค่าแรงดันก่อนหน้าหลายๆ พจน์ และสัญญาณรบกวนที่มีการกระจายตัวแบบ Gaussian (w_n) ซึ่งจำนวนพจน์ของแรงดันก่อนหน้าที่ต้องการสำหรับคำนวณค่าของแรงดันปัจจุบันที่กำลังพิจารณานั้น จะถูกกำหนดโดยลำดับของแบบจำลอง

$$x_n = -\sum_{i=1}^{p} a_i x_{n-i} + w_n$$

1.5.2 ตัวอย่างวิธีการวัดลักษณะเด่นของสัญญาณบนแกนความถี่ (Frequency domain)

1. Mean Frequency (MNF) เป็นการใช้ FFT เพื่อให้ได้ Power spectrum แล้วหาค่าเฉลี่ยของความถี่ ได้ผลลัพธ์ 1 feature vector

$$\text{MNF} = \sum_{j=1}^{M} f_j P_j \Big/ \sum_{j=1}^{M} P_j$$

เมื่อ P_j = Power Spectrum ตัวที่ j

f_j = ความถี่ตัวที่ j

2. Median Frequency (MDF) เป็นการใช้ FFT เพื่อให้ได้ Power spectrum แล้วหาค่าที่ทำให้ผลรวมเป็นของความถี่เป็นครึ่งหนึ่งพอดี ได้ผลลัพธ์ 1 feature vector

$$\sum_{j=1}^{\text{MDF}} P_j = \sum_{j=\text{MDF}}^{M} P_j = \frac{1}{2}\sum_{j=1}^{M} P_j$$

1.5.3 ตัวอย่างวิธีการวัดลักษณะเด่นของสัญญาณบนแกนเวลาและความถี่ (Time-Frequency representation)

1. Fast Fourier Transform (FFT) หรือ การแปลงฟูเรียร์อย่างรวดเร็ว อยู่บนแนวคิดพื้นฐานที่ว่า สัญญาณเชิงเวลาใดๆ เกิดจากการรวมตัวกันขององค์ประกอบสัญญาณย่อยๆ ที่เป็นสัญญาณกระแสตรง และสัญญาณรูปคลื่นซายน์หลายๆ สัญญาณ ซึ่งมีค่าขนาดแรงดันไฟฟ้าสูงสุด ความถี่ของสัญญาณและมุมเฟสที่แตกต่างกันไป

2. Short Time Fourier Transform (STFT) สัญญาณไฟฟ้ากล้ามเนื้อนั้น องค์ประกอบสัญญาณแต่ละความถี่ไม่ได้ปรากฏขึ้นตลอด แต่จะเกิดขึ้นเป็นช่วงๆ และบางช่วงก็จะหายไป ซึ่งการแปลงฟูเรียร์ไม่สามารถให้ข้อมูลได้ว่าองค์ประกอบสัญญาณแต่ละความถี่นั้นเกิดขึ้น และหายไปในช่วงเวลาใดบ้าง จึงมีการคำนวณสัญญาณดังกล่าวจะเริ่มจากการแบ่งสัญญาณที่สุ่มเข้ามาออกเป็นกลุ่มย่อยๆ ซึ่งแต่ละกลุ่มมีจำนวนจุดของสัญญาณไฟฟ้าที่สุ่มเข้ามาเท่ากัน หลังจากนั้นจึงคูณค่าแรงดันไฟฟ้าด้วยค่าที่เหมาะสม และจึงทำการแปลงฟูเรียร์ในแต่ละกลุ่มย่อยๆ เหล่านั้น ซึ่งจะพบว่า จากผลที่ได้เราจะได้ข้อมูลว่า สัญญาณที่มีความถี่ “ช่วง” ใด เกิดขึ้นระหว่าง “ช่วง” เวลาใดบ้าง

3. Wavelet Transform (WT) เป็นวิธีการวิเคราะห์สัญญาณที่มีลักษณะไม่คงที่ และเป็นการวิเคราะห์ข้อมูลระหว่างแกนเวลาและแกนความถี่ ซึ่ง Wavelet Transform นั้นสามารถปรับขนาดหน้าต่างได้แบบอัตโนมัติ โดยจะใช้หน้าต่างที่สั้นกับความถี่สูง และหน้าต่างที่กว้างกับความถี่ต่ำ ทำให้สามารถเลือกคุณลักษณะเด่นทางเวลาและความถี่ได้

2. วัตถุประสงค์ของโครงการวิจัย

2.1 เพื่อศึกษากล้ามเนื้อแขนที่มีผลต่อการเคลื่อนไหวของมือใน 6 ท่าทาง ได้แก่ ท่าแบบมือ ท่ากำมือ ท่างอมือ ท่ายืดมือ ท่าหงายมือ และท่าคว่ำมือ

2.2 เพื่อศึกษาหาวิธีการวัดลักษะของสัญญาณที่ใช้ในการระบุท่าทางการเคลื่อนไหวของมือทั้ง 6 ท่า โดยการประเมินคุณสมบัติ 3 อย่าง ได้แก่ 1. ความแม่นยำในการจำแนกท่าทาง 2. ความคงทนต่อสัญญาณรบกวน 3. ทรัพยากรและเวลาในการคำนวณ

3. ระเบียบวิธีการวิจัยของโครงการวิจัย

3.1 ศึกษาบทความทางวิชาการที่เกี่ยวข้อง และศึกษาทฤษฎีของวิธีการวัดลักษณะเด่นของสัญญาณ ทั้งบนแกนเวลา ความถี่ และเวลาและความถี่ เพื่อทำการศึกษาถึงคุณลักษณะต่างๆ ของวิธีการวัดลักษณะเด่นของสัญญาณ โดยจะทำการเขียนโปรแกรมของวิธีการวัดลักษณะเด่นของสัญญาณต่างๆ บนโปรแกรม MATLAB

3.2 กำหนดจุดจับสัญญาณบริเวณกล้ามเนื้อแขนที่เหมาะสมกับรูปแบบการเคลื่อนไหวของมือทั้ง 6 ท่าที่จะใช้ในการศึกษา และทำการเตรียมอุปกรณ์ในการทดลอง เช่น วงจรขยายสัญญาณไฟฟ้ากล้ามเนื้อ, การ์ดแปลงสัญญาณอนาลอกเป็นดิจิตอล เป็นต้น

3.3 ออกแบบการเก็บข้อมูล และเก็บข้อมูลสัญญาณไฟฟ้ากล้ามเนื้อจากจุดที่กำหนดไว้ โดยการทำการทดลองกับอาสาสมัคร

3.4 นำวิธีการทางคณิตศาสตร์ที่ได้ศึกษาไว้ในข้อ 3.1 มาใช้ในการวิเคราะห์สัญญาณที่ตรวจจับได้ในข้อ 3.3 เพื่อหาวิธีที่ให้ความแม่นยำในการระบุท่าทางการเคลื่อนไหวของมือที่เหมาะสมที่สุด สามารถทนต่อสัญญาณรบกวนได้ดี และใช้เวลาในการคำนวณน้อย

3.5 สรุปวิธีการวัดลักษณะเด่นของสัญญาณที่เหมาะสมในแต่ละประเด็น และเขียนรายงาน

4. ผลการวิจัยและวิเคราะห์ผลการวิจัย

การทำงานโดยรวมของระบบจดจำสัญญาณไฟฟ้ากล้ามเนื้อ อธิบายได้โดยแผนภาพในรูปที่ 1 ดังนี้

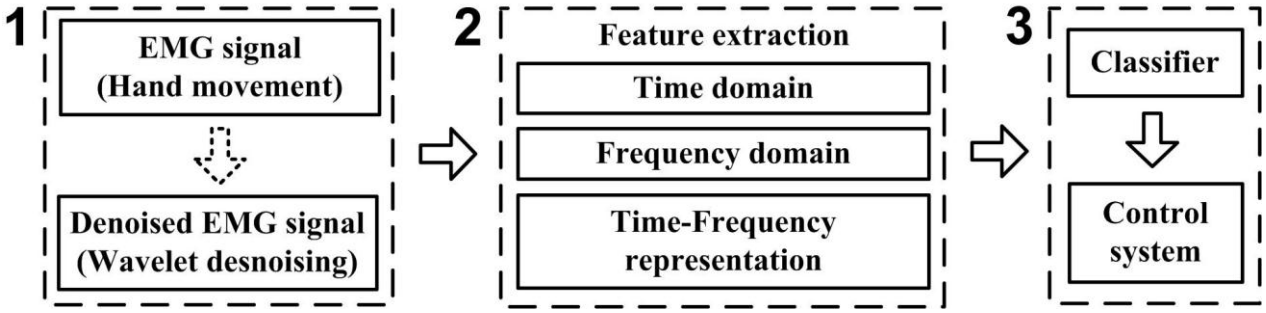

รูปที่ 1 องค์ประกอบในกระบวนการจดจำสัญญาณไฟฟ้ากล้ามเนื้อ สำหรับควบคุมอุปกรณ์ภายนอก

จากแผนภาพ พบว่ากระบวนการของการคัดเลือกลักษณะเด่นของสัญญาณจะอยู่ในขั้นตอนที่ 2 โดยที่ในขั้นตอนที่ 1 นั้น สัญญาณไฟฟ้ากล้ามเนื้อ จะถูกบันทึกจากอาสาสมัคร หรือผู้ใช้งาน โดยการใช้อิเล็กโทรดชนิดพื้นผิว นำสัญญาณจากบริเวณกล้ามเนื้อแขนท่อนล่าง รวมถึงแขนท่อนบนบางส่วน ตามช่องจำนวนที่กำหนด โดยที่ในงานวิจัยนี้ จะมีข้อมูลอยู่ 2 ชุด คือ ชุดหนึ่งนำสัญญาณจากแขนท่อนล่าง 2 จุด และอีกชุดหนึ่งนำสัญญาณจากแขนท่อนล่าง 7 จุดและจากท่อนบนอีก 1 จุด หลังจากนั้นสัญญาณจะเข้าสู่ระบบเก็บข้อมูล โดยการแปลงสัญญาณในรูปของอนาลอก เปลี่ยนเป็นสัญญาณในรูปของดิจิตอล ในกรณีที่สัญญาณไฟฟ้ากล้ามเนื้อที่ได้มีสัญญาณรบกวนเข้ามาปน ในงานวิจัยได้มีการทำการกรองสัญญาณในบางช่วงความถี่ออก และได้มีการใช้วิธีการลดสัญญาณรบกวน ด้วยวิธีการแปลงเวฟเล็ตร่วมด้วย หลังจากได้สัญญาณที่ถูกสุ่มเข้ามาในคอมพิวเตอร์แล้ว สัญญาณที่ได้ก็จะถูกนำไปคำนวณด้วยสมการทางคณิตศาสตร์ เพื่อหาตัวเลขที่ใช้เป็นตัวแทนของสัญญาณที่ได้จากการแสดงท่าทาง ในแต่ละท่าทาง โดยในขั้นนี้เนื่องจากมีวิธีการคำนวณได้หลายวิธี งานวิจัยนี้จึงมุ่งเน้นเพื่อทำการค้นหาวิธีการที่เหมาะสม เพราะจะเห็นได้ว่าถ้าเราได้ตัวเลขที่แทนลักษณะเด่นของสัญญาณที่ไม่เหมาะสมแล้ว ประสิทธิภาพของการจดจำท่าทางในขั้นตอนที่ 3 จะไม่สามารถให้ผลที่ดีได้ เนื่องจากทำการรับค่าเข้ามาจากในขั้นตอนที่ 2 ซึ่งในขั้นตอนที่ 3 หลังจากได้ค่าของลักษณะเด่นของสัญญาณแล้ว ตัวจำแนกจะทำการจดจำและจำแนกสัญญาณเข้ากับท่าทางและคำสั่งที่กำหนด แล้วนำไปใช้ในการควบคุมอุปกรณ์ภายนอกต่อไป

ในการศึกษาหาวิธีการวัดลักษณะเด่นของสัญญาณที่ใช้ในการระบุท่าทางการเคลื่อนไหวของมือทั้ง 6 ท่า ดังที่ได้กล่าวไว้ข้างต้นว่า สามารถทำการประเมินคุณสมบัติของวิธีการวัดลักษณะเด่นของสัญญาณได้ด้วยเกณฑ์ 3 อย่าง ได้แก่

1. ความแม่นยำในการจำแนกท่าทาง
2. ความคงทนต่อสัญญาณรบกวน

3. ทรัพยากรและเวลาในการคำนวณ

ดังนั้น คณะผู้วิจัย จึงได้ทำการคัดเลือกลักษณะเด่นที่เหมาะสมในแต่ละแง่มุมไว้ เนื่องจากไม่มีวิธีการวัดลักษณะเด่นใดที่จะให้ผลดีที่สุดในทั้ง 3 เกณฑ์ ดังนั้น ในการนำไปประยุกต์ใช้งานจริง ผู้ใช้จำเป็นต้องเลือกวิธีการวัดลักษณะเด่นของสัญญาณที่เหมาะสมกับงานประยุกต์นั้นๆ ต่อไป เช่น ในระบบที่ต้องการทำงานแบบทันเวลาได้ (Real time) ผู้ใช้ก็จำเป็นต้องเลือกวิธีการวัดลักษณะเด่นที่ใช้เวลาในการคำนวณน้อย สามารถประมวลผลแบบทันเวลาได้ แต่อาจมีคุณสมบัติในการจำแนกท่าทาง และการทนต่อสัญญาณรบกวนลดลง แต่ยังอยู่ในระดับที่รับได้ ซึ่งจะถูกอธิบายด้วยบทความวิชาการต่างๆ ต่อไป โดยบทความวิชาการ จะถูกอธิบายแบ่งตามเกณฑ์ทั้ง 3 อย่างข้างต้น แต่ถึงอย่างไรก็ตาม ในทุกบทความจะมีการอธิปรายด้วยเกณฑ์ทั้ง 3 แต่จะเน้นหนัก เพื่อหาวิธีการวัดลักษณะเด่นของสัญญาณที่เหมาะสมในแต่ละเกณฑ์ โดยที่สามารถจัดแบ่งบทความตามเกณฑ์ทั้ง 3 ข้างต้นได้ดังนี้

4.1 ความแม่นยำในการจำแนกท่าทาง

ในแง่มุมของความแม่นยำในการจำแนกท่าทาง ได้มีการใช้วิธีการของการลดสัญญาณรบกวนของสัญญาณก่อนการจำแนกด้วยวิธี Wavelet Denoising เข้ามาช่วย (บทความที่ 1 และ 2) ซึ่งทำให้สามารถเพิ่มความแม่นยำของการจำแนกท่าทางของวิธีการคัดเลือกลักษณะเด่น 3 ชนิด ที่ได้เลือกมาใช้ คือ Root Mean Square (RMS) Waveform Length (WL) และ Autoregressive Coefficients อันดับที่ 4 (AR4) โดยที่ในขณะที่ระบบมีสัญญาณรบกวนอยู่ที่ระดับต่างๆ ค่าความแม่นยำในการจำแนกท่าทาง เพิ่มขึ้นในช่วงตั้งแต่ 6.5 จนถึง 78.5 เปอร์เซ็นต์ เมื่อเทียบกับไม่มีการลดสัญญาณรบกวนก่อนการจำแนก และความแม่นยำขณะไม่มีสัญญาณรบกวนสูงถึง 98-99 เปอร์เซ็นต์ อย่างไรก็ตาม วิธีการวัดลักษณะเด่นของสัญญาณข้างต้นนั้นได้หาค่าความแม่นยำของการจำแนกท่าทางด้วยวิธีการวัดค่าความแม่นยำ โดยการใช้ตัวจำแนกชนิด Linear Discriminant Analysis (LDA) ซึ่งจากการทบทวนวรรณกรรมพบว่าประสิทธิภาพของความแม่นยำของวิธีการวัดลักษณะเด่นของสัญญาณแต่ละชนิด จะขึ้นกับชนิดของตัวจำแนก ดังนั้น ในการประเมินประสิทธิภาพที่เป็นกลาง ไม่ขึ้นกับชนิดของตัวจำแนก จึงจำเป็นต้องใช้วิธีการทางสถิติเข้ามาช่วยในการประเมินแทน ทางคณะผู้วิจัยจึงเลือกวิธีการทางสถิติอย่างง่าย 2 ตัวมาใช้ในการประเมิน คือ Euclidean Distance และ Standard Deviation (บทความที่ 3) โดยนำมาประเมินในรูปของอัตราส่วนระหว่างตัวประเมินทั้งสอง ซึ่งนำมาใช้ในการประเมินวิธีการวัดลักษณะเด่นของสัญญาณบนแกนเวลาและบนแกนความถี่จำนวน 15 ชนิด ซึ่งประกอบด้วย 1.Integrated EMG (IEMG) 2.Mean Absolute Value (MAV) 3.Modified Mean Absolute Value 1 (MAV1) 4.Modified Mean Absolute Value 2 (MAV2) 5.Mean Absolute Value Slope (MAVS) 6.Simple Square Integral (SSI) 7.Variance (VAR) 8.Root Mean Square (RMS) 9.Waveform length (WL) 10.Zero crossing (ZC) 11.Slope Sign Change (SSC) 12.Willison amplitude (WAMP) 13.Auto-regressive (AR) coefficients 14.Median Frequency (MDF) 15.Mean Frequency (MNF) ผลที่ได้พบว่าวิธีการวัดลักษณะเด่นของสัญญาณ แบบ WL ให้ผลดีที่สุด ตามมาด้วย RMS และ Willison Amplitude (WAMP) และเนื่องจากเวลาในการคำนวณที่สูงมากของวิธีการวัดลักษณะเด่นของสัญญาณแบบทั้งแกนเวลาและความถี่ และการที่ต้องใช้สมการในการหาค่าตัวแทนของลักษณะสัญญาณบนแกนเวลาและความถี่ ทำให้วิธีการวัดลักษณะเด่นของสัญญาณด้วยวิธีในกลุ่มนี้จึงไม่ได้ถูกพิจารณาในงานวิจัยนี้

บทความที่ 1 เรื่อง EMG Denoising Estimation Based on Adaptive Wavelet Thresholding for Multifunction Myoelectric Control

บทความที่ 2 เรื่อง EMG Signal Estimation Based on Adaptive Wavelet Shrinkage for Multifunction Myoelectric Control

บทความที่ 3 เรื่อง Evaluation of EMG Feature Extraction for Hand Movement Recognition Based on Euclidean Distance and Standard Deviation

EMG Denoising Estimation Based on Adaptive Wavelet Thresholding for Multifunction Myoelectric Control

Angkoon Phinyomark, *Student Member, IEEE,* Chusak Limsakul,
and Pornchai Phukpattaranont, *Member, IEEE*

***Abstract*—Wavelet denoising algorithms have been received considerable attention in the removal of noises of surface electromyography (sEMG) signal. Wavelet denoising algorithms proposed by Donoho's method is more often used in sEMG signal. However, Donoho's method is limited especially for multifunction myoelectric control. It does not only remove noises but it also removes some important part of sEMG signals. This study proposes an improved threshold estimation method. Six modified threshold estimation methods associated with the selected thresholding rescaling are evaluated. SEMG signal from six hand motions with additive WGN at various signal-to-noise ratios (SNRs) were applied to evaluate the efficient of method. Features of the estimated signal are sent to classification task. Evaluations of the performance of these algorithms are mean squared error (MSE) and classification rate. The results show that Global Scale Modified Universal (GSMU) method provides better performance than traditional Donoho's method. It produces sEMG signals that remain important information of the original sEMG signal and can eliminate lots of noises. The average MSE are 0.0024 at 20 dB SNR, low noise, and 0.074 at 0 dB, high noise. The accuracy of hand movement recognition of sEMG signal that estimates from GSMU is improved. It improves 1 to 4% of the classification accuracy depend on level of noise. In addition, performance of level dependent method is better than the others rescaling method. In the experiment, GSMU threshold estimation method is an efficient method for producing useful sEMG signal without noise and improving the application of hand movement recognition.**

I. Introduction

SURFACE Electromyography (sEMG) signal is one of physiological signal that is very complex, nonlinear, non-stationary, and non-periodic [1]. Because the use of sEMG signal is very easy, fast and convenient, it is currently becoming increasingly a powerful indication to get important information and to diagnose about the muscular and nervous systems. However, varieties of noises originated from measure instruments are major problems in analysis of sEMG signals. Therefore, methods to eliminate or reduce the effect of noises have been one of the most important problems. Power line interference or instability of electrode-skin contact can be removed using typical filtering procedures but the interference of white Gaussian noise (WGN) is difficult to remove using previous procedures. Wavelet denoising algorithms, an advance signal processing method, have been received considerable attention in the removal of WGN [2], [13].

In this study, we propose a wavelet denoising based estimation technique to generate the useful sEMG signal without noise. The general wavelet based denoising procedures are composed of three steps: decomposition, denoising wavelet's detail coefficients, and reconstruction. To achieve and optimize the above procedures, four points must be addressed, namely selection of the suitable wavelet function, level of decomposition, threshold estimation, and threshold transformation. Most wavelet based denoising literatures are proposed by Donoho's method [3]-[4]. However, Donoho's method in denoising of sEMG signal is limited especially for multifunction myoelectric control. The limitation of Donoho's method is the large value of threshold that is not suitable for sEMG signal. It does not only remove noises but it removes some important part of sEMG signals. As shown in Fig.1, loss of geometrical characteristics and amplitude of sEMG signal can be observed.

This study proposes an improved threshold estimation method based on Donoho's method. Traditional Donoho's method is modified and combined with existing techniques for providing higher classification rate and less error. It means that useful information is remained and undesirable parts of sEMG signal are removed. The aim of this paper is to show the comparison results of the different threshold estimation methods found in previous research [4]-[8]. Moreover, thresholding rescaling methods including global, first-level, and level dependent estimation are evaluated using both standard deviation of noise and length of wavelet coefficients parameters [9]-[10]. Getting higher performance in denoising assumes that mean square error between the estimated of original sEMG signal and denoising sEMG signal is the lowest.

After evaluating the threshold estimation method in denoising point view and for evaluating the efficiency of classification task, the estimated sEMG signals are sent to the hand recognition system in order to identify six hand movements. Lots of methods are used to model and analyze

Manuscript received April 14, 2009. This work was supported in part by the Thailand Research Fund through the Royal Golden Jubilee Ph.D. Program (Grant No. PHD/0110/2550) and in part by NECTEC-PSU center of excellence for rehabilitation engineering and Faculty of Engineering, Prince of Songkla University.

A. Phinyomark is with the Electrical Engineering Department, Prince of Songkla University, Hatyai, Songkhla 90110 Thailand (phone: 668-4195-8591; fax: 6674-459-395; e-mail: angkoon.p@hotmail.com).

C. Limsakul and P. Phukpattaranont, are with the Electrical Engineering Department, Prince of Songkla University, Hatyai, Songkhla 90110 Thailand.

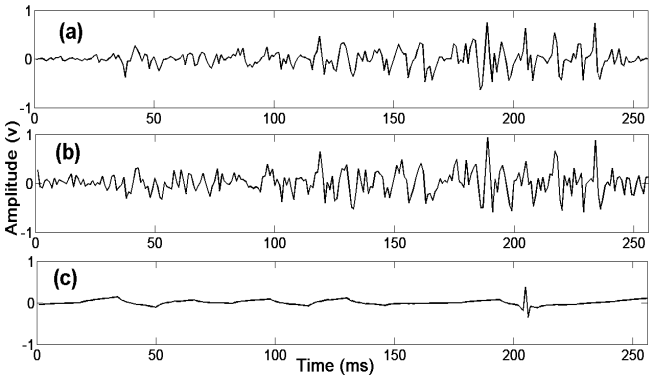

Fig. 1. (a) Original sEMG signal (b) Noisy sEMG signal with 5 dB signal-to-noise ratio (c) sEMG signal estimated by traditional Donoho's method.

sEMG signal that called feature extraction. Time domain and frequency domain features are used to describe the characteristics of the sEMG signal. Three well-known features are Root Mean Square (RMS), Waveform Length (WL), and the forth order of Auto Regressive (AR4) [11]-[12]. After feature extraction task, classification task is evaluated by Linear Discriminant Analysis (LDA). When high performance is obtained, classification rate should be the highest value.

II. Wavelet Denoising and Signal Estimation

The objective of wavelet denoising algorithm is to suppress the noise part of the signal *s(n)* by discarding the white Gaussian noise *e(n)* and to recover the signal of interest *f(n)*. The model is basically of the following form:

$$s(n) = f(n) + e(n) . \quad (1)$$

The procedure of wavelet denoising follows three steps. Firstly, sEMG signal is decomposed by discrete wavelet transform. Detail and approximation coefficient are obtained. Secondly, estimated threshold is applied to the detail coefficients, zeroing all coefficients below their associated thresholds. Finally, denoised signal is reconstructed based on modified detail coefficients.

The first significant step of wavelet denoising procedure is selection of wavelet function or mother wavelet. The right

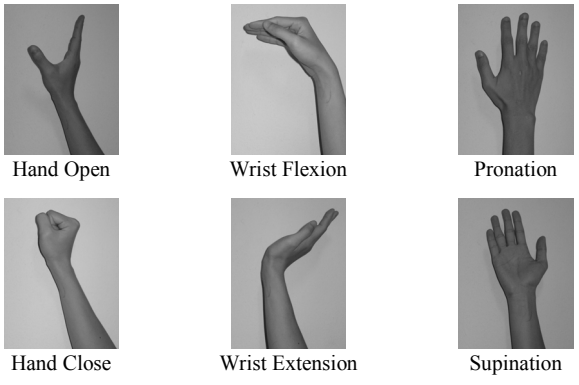

Fig. 2. Estimated six hand motions.

wavelet function determines perfect reconstruction and performs better analysis. Next step is the selection of the number of decomposition levels of signal. Instead of focusing on the selection of the wavelet function and decomposition level, we have presented in previous work that the Daubechies wavelet with second orders (db2) and the forth decomposition level provide the lowest mean square error [13].

A. Wavelet Threshold Estimation Method

Estimation of detail coefficient threshold is selected with estimator methods for each level from 1 to 4. Universal threshold estimation method proposed by Donoho's method has been shown that its denoising capability is better than other classical methods such as SURE method, Hybrid method, and minimax method [13]. Universal threshold estimation method uses a fixed form threshold, which can be expressed as [3]

$$THR_{UNI} = \sigma\sqrt{2\log(N)} , \quad (2)$$

where N is the length in samples of time-domain signal, σ is standard deviation of noise, and log is a natural logarithm. The parameter σ can be estimated using median parameter which can be calculated as

$$\sigma = \frac{median\left(\left|cD_j\right|\right)}{0.6745} , \quad (3)$$

where *cDj* is the detail wavelet coefficients at scale level *j* and 0.6475 is a normalization factor.

Six modified threshold estimation methods were applied in this study as described in the following. In this study, we provide specific name to each method because modified threshold estimation methods do not have specific names.

1) Length Modified Universal Method: Length Modified Universal (LMU) was modified by Donoho to be used in soft-thresholding transformation [4]. It is defined as

$$THR_{LMU} = \sigma \cdot \frac{\sqrt{2\log(N)}}{\sqrt{N}} . \quad (4)$$

2) Scale Modified Universal Method: Scale Modified Universal (SMU) was modified by Donoho to be used in level dependent [5]. It can be expressed as

$$THR_{SMU} = \sigma \cdot 2^{\frac{j-J}{2}} \cdot \sqrt{2\log(N)} , \quad (5)$$

where *j* is scale level from 1 to 4 and *J* is maximum level, 4.

3) Global Scale Modified Universal Method: Global Scale Modified Universal (GSMU) was modified by Zhong and Cherkassky to be used in image denoising [6]. It is given by

$$THR_{GSMU} = \sigma \cdot 2^{\frac{-J}{2}} \cdot \sqrt{2\log(N)} . \quad (6)$$

4) Scale Length Modified Universal Method: Scale Length Modified Universal (SLMU) was modified by Donoho. It is combined between LMU and SMU [5]. It is shown as

$$THR_{SLMU} = 2\sigma \cdot \frac{\sqrt{2\log(N)}}{\sqrt{N} \cdot 2^{\frac{J-j}{2}}} . \quad (7)$$

5) Log Scale Modified Universal Method: Log Scale Modified Universal (LSMU) was modified by Song and Zhao [7]. It takes the different thresholds at different scales.

$$THR_{LSMU} = \sigma \cdot \frac{\sqrt{2\log(N)}}{\log(j+1)} . \quad (8)$$

6) Log Variable Modified Universal Method: Log Variable Modified Universal (LVMU) was modified by Qingju and Zhizeng [8]. It uses the constant *d* to adapt the threshold value. Their experiments show that the value of constant *d* is associated to the wavelet function and *SNR*. It should be ranging between 0 and 3. In this study, we used 3 for the constant *d*. The equation can be defined as

$$THR_{LVMU} = \sigma \cdot \frac{\sqrt{2\log(N)}}{\log[e+(j-1)^d]} . \quad (9)$$

where e is the mathematical constant (2.71828).

A. Wavelet Threshold Rescaling Method

Seven threshold estimation methods, six modified and classical one, can be improving using rescaling method. In wavelet threshold rescaling, three categories can be identified: global (GL), first-level (FL) and level dependent (LD) thresholding [9]-[10]. In the first one, standard deviation of noise (σ) can be adapted to three categories. While the second one, length of wavelet coefficients (*N*) can be adapted to only GL and LD thresholding.

In addition, to identify the threshold rescaling method, GL defines σ as the estimated standard deviation of all the wavelet coefficients and *N* as length of the total wavelet coefficients. FL defines σ_1 as the estimated standard deviation of first-level detail coefficients (cD_1). LD defines σ_j as the estimated standard deviation for every decomposition level and N_j as length of the total wavelet coefficients.

After threshold values are determined, thresholding can be done using soft transformation,

$$cD_j = \begin{cases} \text{sgn}(cD_j)(cD_j - THR_j), & if \ |cD_j| > THR_j \\ 0, & otherwise \end{cases} . \quad (10)$$

Combining seven threshold estimation methods, six threshold rescaling methods, and a threshold transformation method, forty-two possible wavelet denoising estimators exist. All of wavelet denoising procedures are presented in Table I. After denoising procedure, the reconstructed signal computes wavelet reconstruction based on the original approximation coefficients of level 4 and the modified detail coefficients of levels from 1 to 4.

TABLE I
WAVELET DENOISING PROCEDURES (METHOD FORMAT: THRESHOLD ESTIMATION / σ RESCALING / *N* RESCALING)

#	TE	σ	N	#	TE	σ	N
1	UNI	GL	GL	22	UNI	FL	LD
2	LMU			23	LMU		
3	SMU			24	SMU		
4	SLMU			25	SLMU		
5	GSMU			26	GSMU		
6	LSMU			27	LSMU		
7	LVMU			28	LVMU		
8	UNI	GL	LD	29	UNI	LD	GL
9	LMU			30	LMU		
10	SMU			31	SMU		
11	SLMU			32	SLMU		
12	GSMU			33	GSMU		
13	LSMU			34	LSMU		
14	LVMU			35	LVMU		
15	UNI	FL	GL	36	UNI	LD	LD
16	LMU			37	LMU		
17	SMU			38	SMU		
18	SLMU			39	SLMU		
19	GSMU			40	GSMU		
20	LSMU			41	LSMU		
21	LVMU			42	LVMU		

B. Experiment

In this section, we describe our experimental procedure for recording sEMG signals. The sEMG signals were recorded from flexor carpi radialis and extensor carpi radialis longus of a healthy volunteer by two pairs of surface electrodes (3M red dot 2.5 cm. foam solid gel). Each electrode was separated from the other by 20 mm. A band-pass filter of 1-500 Hz bandwidth and an amplifier with 500 times gain were used. Sampling rate was set at 1000 samples per second using a 16 bit A/D converter board (National Instruments, USA, model 6024E). Volunteers performed six hand motions including hand open (ho), hand close (hc), wrist extension (we), wrist flexion (wf), pronation (pr), and supination (su) as shown in Fig. 2. Hand close and wrist flexion were analyzed using signals from extensor carpi radialis longus and the others motions were analyzed using signals from flexor carpi radialis because each motion has strong signal depending upon electrode position. Ten datasets were collected for each motion.

C. Evaluation

The mean squared error (*MSE*) used to evaluate the quality of the denoising signals can be given by

$$MSE = \frac{\sum_{i=1}^{N} (f_i - fe_i)^2}{N} , \quad (11)$$

where f_i represents the estimated original sEMG signal and fe_i is estimated denoising sEMG signal.

The classification rate used to evaluate the quality of the recognition system from the estimated sEMG signal. The performance of the algorithms is the best when *MSE* is small

and classification rate closes to 100 percents. To guarantee the best wavelet denoising method optimized for estimated sEMG signals, we calculated *MSE* and classification rate averages for each motion with 5 times of additional WGN and each time was varied from 20-0 dB *SNRs*. *SNR* is calculated by

$$SNR = 10\log\frac{P_{clean}}{P_{noise}}, \qquad (12)$$

where P_{clean} is the power of original sEMG signals and P_{noise} is the power of WGN.

III. Multifunction Myoelectric Control Based on Estimated sEMG Signal

Estimated sEMG signal that were denoised from all of wavelet denoising procedures in previous section were sent to hand movement recognition. In this work, we evaluated the performance of adaptive wavelet thresholding technique in pattern recognition point view with Myoelectric Control development (MEC) toolbox [14]. MEC Toolbox has example data that is collected from 30 subjected. SEMG signal is recorded from seven electrode positions on the arm and volunteers perform six motions same as the above experiment as shown in Fig. 2. More details of experiment and data acquisition are described in [14]. The window size is 256 ms and window slide is 32 ms for the real-time constraint that the response time should be less than 300 ms. The feature vector is six features per channel (1 RMS, 1 WL, and 4 AR4). The classification was evaluated by LDA and majority vote post-processing was performed.

The classification rates were calculated for each estimated sEMG signals. The improved classification rate (ICR) was calculated the improvement of wavelet thresholding method, which can be expressed as

$$ICR = CR_{denoised} - CR_{no\ denoised}, \qquad (13)$$

where $CR_{denoised}$ is classification rate of estimated sEMG signal and $CR_{no\ denoised}$ is classification rate of noisy sEMG signal. The performance of the algorithms is the best when improved classification rate is high and classification rate closes to 100 percents.

IV. Results and Discussion

This paper presents a complete comparative study of wavelet denoising for estimated sEMG signal using modified wavelet threshold estimation methods and wavelet threshold rescaling methods. The objectives of this study were to investigate the suitable wavelet denoising procedure in two point views: 1) denoising 2) pattern recognition.

A. Wavelet Denoising and Signal Estimation

In denoising point view, *MSE* is used to present the high performance when *MSE* is small. The results of *MSE* of all 42 possible combinations of wavelet denoising procedures in Table I at 20, 10, 0 db *SNR* are shown in Fig. 3 (a)-(c) that presents the low, medium, and high noise, respectively. By comparing Fig. 3(a)-(c), results of wavelet denoising procedures in each *SNR* level is the same trend. As *SNR* increases, the *MSE* of each wavelet denoising procedures increases. We can evaluate the results in Fig. 3 in three groups: 1) the suitable wavelet threshold estimation method 2) the suitable threshold rescaling method for σ 3) the suitable threshold rescaling method for *N*. The evaluation of

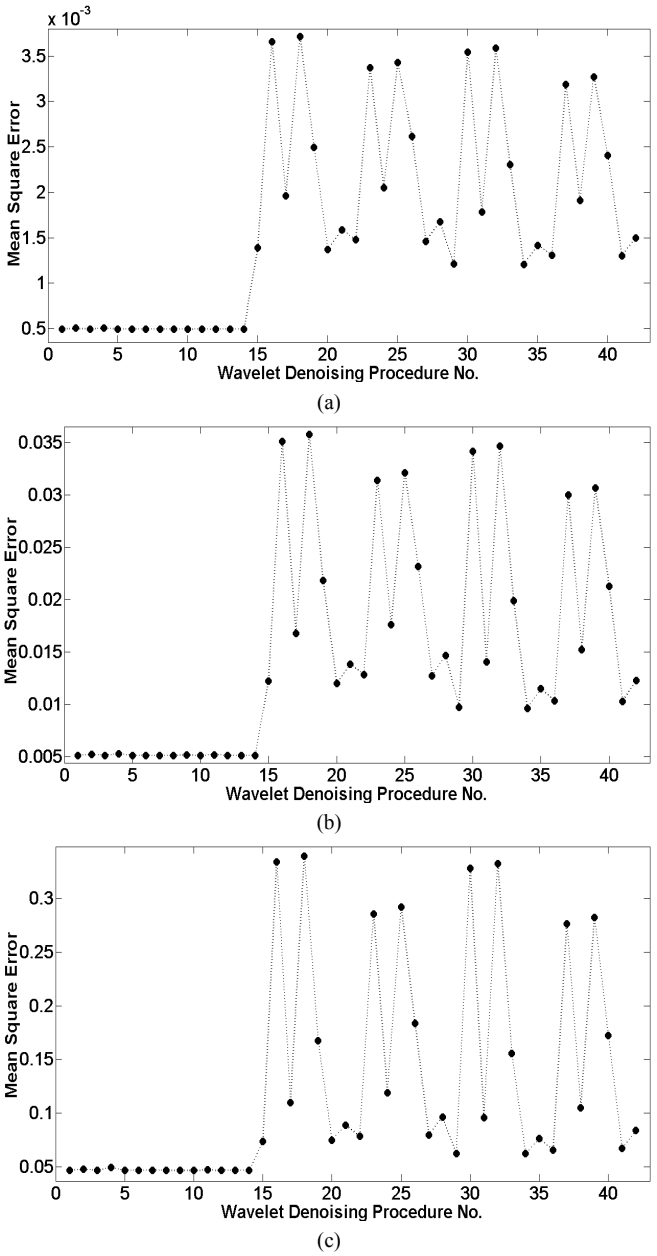

Fig. 3. Mean Square Error (*MSE*) of all 42 possible combinations of wavelet threshold estimation methods and wavelet threshold rescaling methods (wavelet denoising procedure numbers refer to the wavelet denoising procedures in Table I, i.e. #1-Universal threshold estimation method (UNI), global threshold rescaling of σ, and global threshold rescaling of N) at (a) 20 dB *SNR* (b) 10 dB *SNR* (c) 0 dB *SNR*.

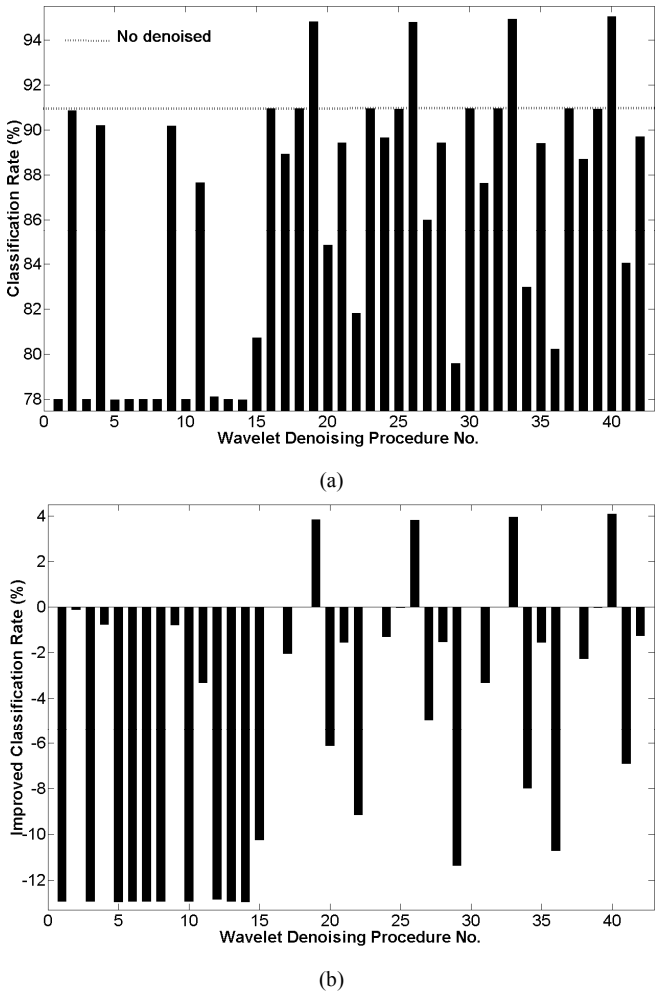

Fig. 4. (a) Classification rate (*CR*) (b) Improved classification rate (*ICR*) of all 42 possible combinations of wavelet threshold estimation methods and wavelet threshold rescaling methods (wavelet denoising procedure numbers refer to the wavelet denoising procedures in Table I, i.e. #1-Universal threshold estimation method (UNI), global threshold rescaling of σ, and global threshold rescaling of N) at 0 dB *SNR*.

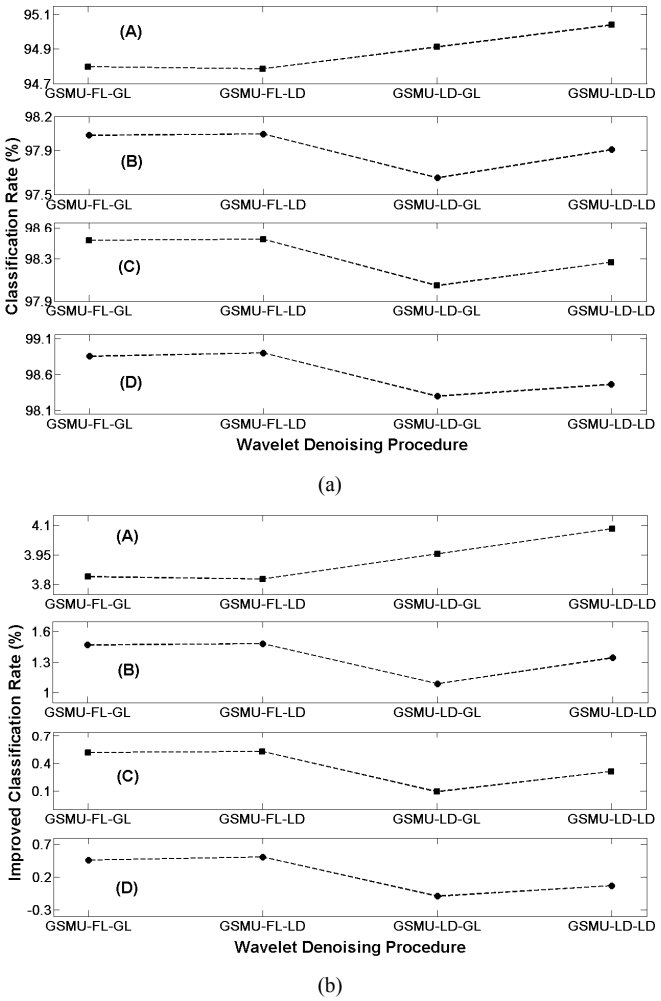

Fig. 5. (a) Classification rate (*CR*) (b) Improved classification rate (*ICR*) of Global Scale Modified Universal (GSMU) method, σ threshold rescaling, and N of global threshold rescaling at (A) 0 dB *SNR* (B) 5 dB *SNR* (C) 10 dB *SNR* (D) 15 dB *SNR*.

threshold estimation methods shows that all methods have the same value when rescaling method of σ was set to GL. When rescaling method of σ is FL or LD, the results of threshold estimation method are difference. *MSE* of UNI is the lowest, followed closely by the LSMU and LVMU. SMU and GSMU have slightly larger error compared to the UNI, LSMU, and LVMU. The *MSE* of LMU and SLMU are large. Their *MSE* are as much as two of the minimum *MSE*.

The *MSE* of threshold rescaling of σ is the smallest when it is set to GL. However, it makes the big value of threshold value. The sEMG signal that estimated from this method loses lots of useful information. It will make the bad performance in pattern recognition that we discuss in section B. By comparing FL and LD, the LD is slightly better than FL. The results of threshold rescaling of *N* have the same result with threshold rescaling of σ. The *MSE* of LD is slightly smaller than FL. However, the *MSE* can evaluate only for denoising point view that it maybe has the different result in pattern recognition point view.

B. Multifunction Myoelectric Control Based on Estimated sEMG Signal

In pattern recognition point view, *CR* and *ICR* are used to - present the high performance when *CR* closes to 100 % and *ICR* is high. The results of *CR* and *ICR* of all 42 possible combinations of wavelet denoising procedures in Table I at 0 dB *SNR* are shown in Fig. 4 (a)-(b). From the results of *CR* and *ICR* at various SNR, it has the same trend. Therefore, we present only at 0 dB, very high noise. Fig. 4 (a) shows that only four wavelet denoising procedures have the classification rate more than no denoising procedure. GSMU-FL-GL, GSMU-FL-LD, GSMU-LD-GL, and GSMU-LD-LD are the wavelet denoising procedures that improve the classification rate. Their *ICR* are about 4%.

Consequently, evaluations of four wavelet denoising procedures were considered. Fig. 5 (a)-(b) show results of the effect of level of noises. At 0 dB *SNR*, very high noise, GSMU-LD-LD can improve classification rate about 4%. It shows the best performance. However, at 5, 10, and 15 dB

SNR, high to low noise, GSMU-FL-LD is the best performance. The best *CR* is 98.9% at low noise and 95% at very high noise. It improves classification rate between 1 to 4% depend on level of noises.

From these experimental results, we can conclude that GSMU is only one threshold estimation method that can improve the classification rate. When the threshold rescaling of *N* is GL, the *CR* is better than LD. However, the threshold rescaling of σ is depending on the level of noise. At very high noise, LD is better than FL. On the other hand, at high to low noise, FL is better than LD. In addition, at very low noise, more than 20 dB *SNR*, the wavelet denoising procedure does not improve classification rate. It has the same results.

V. CONCLUSION

In this work, we introduced and evaluated adaptive wavelet thresholding technique for estimating useful information of sEMG signal and improve the application of multifunction myoelectric control system. The results show that Global Scale Modified Universal (GSMU) method provides better performance than traditional Donoho's method and others modified threshold estimation methods. In addition, performance of level dependent method is better than the others rescaling method. This paper is a starting idea to find the optimal threshold value for denoising and estimating sEMG signal. In the future work, a new equation should be formulated.

REFERENCES

[1] R. Merletti and P. Parker, *Electromyography Physiology, Engineering, and Noninvasive Applications*. New Jersey: John Wiley & Sons, Hoboken, 2004.

[2] M. C. E. Rosas-Orea, M. Hernandez-Diaz, V. Alarcon-Aquino, and L. G. Guerrero-Ojeda, "A Comparative simulation study of wavelet based denoising algorithms," In *Proc. 15th Int. Conf. Electronics, Communications and Computers*, 2005, pp. 125-130.

[3] D. L. Donoho and I. M. Johnstone, "Ideal spatial adaptation by wavelet shrinkage," *Biometrika*, vol. 81, no. 3, 1994, pp. 425-455.

[4] D. L. Donoho, "De-noising by soft-thresholding," *IEEE Trans. Information Theory*, vol. 41, no. 3, May. 1995, pp. 613-627.

[5] D. L. Donoho, "Wavelet analysis and WVD: a ten minute tour," In *Proc. Int. Conf. Wavelets and Applications*, France, 1992.

[6] S. Zhong and V. Cherkassky, "Image denoising using wavelet thresholding and model selection," In *Proc. Int. Conf. Image Processing*, 2000, pp. 262-265.

[7] G. Song and R. Zhao, "Three novel models of threshold estimator for wavelet coefficients," In *Proc. 2nd Int. Conf. Wavelet Analysis and Its Applications*, Berlin: Springer-Verlag, 2001, pp. 145-150.

[8] Z. Qingju and L. Zhizeng, "Wavelet De-Noising of Electromyography," In *Proc. IEEE Int. Conf. Mechatronics and Automation*, Luoyang, 2006, pp.1553-1558.

[9] M. M. Elena, J. M. Quero, and I. Borrego, "An optimal technique for ECG noise reduction in real time applications," *Computers in Cardiology*, vol. 33, 2006, pp. 225-228.

[10] I. M. Johnstone and B. W. Silverman, "Wavelet threshold estimators for data with correlated noise," *J. Royal Statist. Soc.,* vol. B 59, no. 2, 1997, pp. 319-351.

[11] R. Boostani and M. H. Moradi, "Evaluation of the forearm EMG signal features for the control of a prosthetic hand," *Physiological Measurement*, vol. 24, 2003, pp. 309-319.

[12] A. Phinyomark, C. Limsakul, and P. Phukpattaranont, "A novel EMG feature extraction for tolerance of interference," In *Proc. 13th Int. Annu. Sym. Computational Science and Engineering,* Bangkok, 2009, pp. 407-413.

[13] A. Phinyomark, C. Limsakul, and P. Phukpattaranont, "A Comparative Study of Wavelet Denoising for Multifunction Myoelectric Control," In *Proc. Int. Conf. Computer and Automation Engineering,* Bangkok, 2009, pp. 21-25.

[14] A. D. C. Chan and G. C. Green, "Myoelectric control development toolbox," In *Proc. 30th Conf. Canadian Medical and Biological Engineering Society*, Toronto, 2007.

EMG Signal Estimation Based on Adaptive Wavelet Shrinkage for Multifunction Myoelectric Control

A. Phinyomark, C. Limsakul, P. Phukpattaranont
Department of Electrical Engineering, Faculty of Engineering, Prince of Songkla University
110/5, Kanchanavanid Road, Hat Yai, Songkhla 90112 Thailand
E-mail: angkoon.p@hotmail.com, chusak.l@psu.ac.th, pornchai.p@psu.ac.th

***Abstract*-Electromyography (EMG) signal is interfered with different kinds of noise and wavelet denoising algorithm is a powerful method to reduce noises in EMG signal. Hard and soft shrinkage, traditional wavelet transformation, are applied to wavelet coefficients with threshold value. From the limitation of hard and soft shrinkage, this study proposes nine improved wavelet shrinkage methods that achieve a compromise between two standards. EMG signal from six hand motions with additive noise at different signal-to-noise ratios were applied to evaluate the efficiency of the methods in denoising viewpoint. In addition, features of estimated denoising signal are sent to classification task to measure the performance in myoelectric control. The experimental results show that adaptive wavelet shrinkage method (ADP) provides the better performance than traditional methods and other modified methods in both of denoising and pattern recognition viewpoints. Accuracy of recognition of EMG signal transformed by ADP is improved about 6.5-78.5% depending on the level of noise. ADP is an efficient method for producing useful EMG signal without noise and improving application of myoelectric control.**

I. INTRODUCTION

Electromyography (EMG) signal is physiological signal that is a powerful indication to get useful information. It can be used to control the prosthetic or assistive devices. However, EMG signal is interfered with different kinds of noises and becomes the major problem in EMG analysis. Therefore, methods that used to remove or reduce the effect of noises are the significant step before performing EMG analysis. Wavelet denoising algorithm is an effective method to remove or reduce noises in EMG signal. Generally, the wavelet based denoising schemes are composed of three stages, namely decomposition, modified wavelet's detail coefficients, and reconstruction. To achieve the above schemes, four points must be addressed: wavelet function, decomposition levels, wavelet threshold estimation, and wavelet threshold transformation or shrinkage [1-2].

This study proposes improved wavelet shrinkage methods based on Donoho and Johnson's method [3]. It is influenced by the fact that the available results of comparative study of wavelet shrinkage methods were not effective enough [1-6]. From literatures, it has been shown that all of them used only standard transformation methods, hard and soft shrinkage. Moreover, our previous work [6], the two modified wavelet transformation methods, namely hyperbolic and non-negative Garrote shrinkage have been tested. However, this was not powerful enough to make the comparison reasonable with respect to the available techniques today. In this study, nine shrinkage methods that modified and compromised between hard and soft shrinkage and two traditional shrinkage methods are evaluated in both of denoising and pattern recognition points of view. In other words, the wavelet denoising method is used as an estimation technique to generate the useful EMG signal in pattern recognition that improving in both of accuracy and robustness.

II. WAVELET DENOISING AND ESTIMATION

The aim of wavelet denoising algorithm is used to suppress the noise part of signal by rejecting white Gaussian noise (WGN) and recover signal of interest. The first significant step of wavelet denoising schemes is the selection of wavelet function. The right wavelet function determines perfect reconstruction and performs better analysis. Next step is the selection of suitable decomposition levels. Instead of focusing on the selection of wavelet function and decomposition level, we have already presented in our previous work [2], [6] that the Daubechies wavelet with second orders (db2) and the forth decomposition level provide the best result in denoising point of view. The third step is the estimation of wavelet's detail coefficients threshold value. Universal threshold method proposed by Donoho's method has been shown that its denoising capability is better than other classical methods [2]. Universal threshold method can be expressed as [3]

$$THR = \sigma\sqrt{2\log(N)}, \tag{1}$$

where N is the length in samples of the signal in time domain and σ is standard deviation of noise that can be estimated using median parameter which can be calculated as

$$\sigma = \frac{median\left(\left|cD_j\right|\right)}{0.6745}, \tag{2}$$

where cD_j is the wavelet's detail coefficients at scale level j and 0.6745 is a normalization factor [3]. Moreover, threshold value is improved using rescaling method [2].

A. Wavelet Shrinkage Approach

After threshold values are determined, thresholding can be done using wavelet shrinkage method. The eleven wavelet shrinkage methods were described in the following.

1) *Hard Shrinkage (HAD):* It is a simple shrinkage method. All wavelet's detail coefficients whose absolute values are

lower than threshold are set to be zero and other wavelet's detail coefficients are kept [3]. It is calculated by

$$cD_j = \begin{cases} cD_j, & if\ |cD_j| > THR_j \\ 0, & otherwise \end{cases}. \quad (3)$$

2) *Soft Shrinkage (SOF):* It is an extension of HAD [3]. It can be done by zeroing all wavelet's detail coefficients whose absolute values are lower than threshold same as HAD. Then, non-zero coefficients are shrunk towards zero. It is defined as

$$cD_j = \begin{cases} \mathrm{sgn}(cD_j)(|cD_j| - THR_j), & if\ |cD_j| > THR_j \\ 0, & otherwise \end{cases}, \quad (4)$$

where sgn(x) is a sign function that extracts the sign of a real number x.

3) *Mid Shrinkage (MID):* It is an extension of SOF [7], small wavelet's coefficients are zeroed, and then large wavelet's coefficients are not affected. However, intermediate wavelet's coefficients are reduced. MID can be expressed as

$$cD_j = \begin{cases} cD_j, & |cD_j| > 2THR_j \\ 2\,\mathrm{sgn}(cD_j)(|cD_j| - THR_j), & THR_j < |cD_j| \le 2THR_j \\ 0, & otherwise \end{cases}. \quad (5)$$

4) *Modulus Squared Shrinkage (MSQ):* It is attempted to address the limitation of SOF. It is described in [8] and its equation is defined same as Hyperbolic shrinkage that is given by [9],

$$cD_j = \begin{cases} \mathrm{sgn}(cD_j)\sqrt{(cD_j^2 - THR_j^2)}, & if\ |cD_j| > THR_j \\ 0, & otherwise \end{cases}. \quad (6)$$

5) *Non-negative Garrote Shrinkage (NNG):* It combines Donoho and Johnstone's wavelet shrinkage with Breiman's non-negative garrote. The equation is modified by Gao [10]. It is expressed as

$$cD_j = \begin{cases} cD_j - \dfrac{THR_j^2}{cD_j}, & if\ |cD_j| > THR_j \\ 0, & otherwise \end{cases}. \quad (7)$$

6) *Compromising of Hard- and Soft- Shrinkage (CHS):* It estimates wavelet's coefficients by weighted average of HAD and SOF [8]. For $0<\alpha<1$, when α is 0, it changed into HAD and when α is 1, it changed into SOF. In this study, we used 0.5 for the constant α.

$$cD_j = \begin{cases} \mathrm{sgn}(cD_j)(|cD_j| - \alpha THR_j), & if\ |cD_j| > THR_j \\ 0, & otherwise \end{cases}. \quad (8)$$

7) *Weighted Averaging Shrinkage (WAV):* It estimates coefficients by weighted average of MSQ and HAD [5]. It is given by

$$cD_j = \begin{cases} (1-\alpha)\,\mathrm{sgn}(cD_j)\sqrt{(cD_j^2 - THR_j^2)} + \alpha(cD_j), & if\ |cD_j| > THR_j \\ 0, & otherwise \end{cases}, \quad (9)$$

where $0<\alpha<1$. If α is 0, (9) will change to MSQ and (9) will change to HAD, if α is 1. We used 0.5 for the constant α.

8) *Adaptive Denoising Shrinkage (ADP):* It is modified based on SOF [11]. It is given by

$$cD_j = cD_j - THR_j + \frac{2THR_j}{1 + e^{2.1cD_j/THR_j}}. \quad (10)$$

9) *Improved Shrinkage (IMP):* It is attempted to address the deficiency of HAD and SOF [12]. It can be defined as

$$cD_j = \begin{cases} \mathrm{sgn}(cD_j)(|cD_j| - \beta^{(THR_j - |cD_j|)} \cdot THR_j), & if\ |cD_j| > THR_j \\ 0, & otherwise \end{cases}, \quad (11)$$

where $\beta \in \Re^+$ and $\beta>1$. In this study, we used 15 from the suggestion of [12].

10) *Modified Hyperbolic Shrinkage (MHP):* It is obtained from the results in variance pattern resembling HAD and means resembling SOF removing the bias problem. It is modified by Poornachandra et al. [13] and is shown as

$$cD_j = \begin{cases} (k \cdot cD_j)\left[1 + (\dfrac{cD_j^2}{6})\right], & if\ |cD_j| > THR_j \\ 0, & otherwise \end{cases}, \quad (12)$$

where k is the scaling function and we used 1 for the constant k in this study.

11) *Custom Shrinkage (CUT):* Idea of this transformation is similar to that of NNG method, in the sense that CUT and NNG are continuous and can adapt to the signal characteristics. The equation can be expressed as

$$cD_j = \begin{cases} cD_j + \mathrm{sgn}(cD_j)(1-\alpha)THR_j, & if\ |cD_j| \ge THR_j \\ 0, & if\ |cD_j| \le \gamma, \\ \alpha \cdot THR_j \left(\dfrac{|cD_j| - \gamma}{THR_j - \gamma}\right)^2 \left\{(\alpha - 3)\left(\dfrac{|cD_j| - \gamma}{THR_j - \gamma}\right) + 4 - \alpha\right\}, & otherwise \end{cases} \quad (13)$$

where $0 < \gamma < THR_j$ and $0 < \alpha < 1$. In this study, we used the same threshold as [14] with $\alpha = 1$ and $\gamma = THR_j/2$.

B. Experiments

The EMG signals in this study were divided into two sets. The first set is used to evaluate the denoising viewpoint using mean square error (*MSE*) criterion and the second set is used to evaluate the recognition viewpoint using classification rate criterion. The EMG signals in both data sets are from six upper limb motions including wrist flexion, wrist extension, hand close, hand open, forearm pronation, and forearm supination. The EMG signals in the first set were recorded from two channels on the right forearm namely, flexor carpi radialis and extensor carpi radialis longus by two pairs of Ag-AgCl Red Dot surface electrodes. Each electrode was separated from the other by 2 cm. The EMG signals were sampled at 1 kHz by using an analog-to-digital converter board (DAQCard-6024E, NI). A band-pass filter of 10-500 Hz bandwidth and an amplifier with 60 dB gain were used. Ten datasets were collected for each motion. The second set of EMG signals was recorded from eight channels on the right

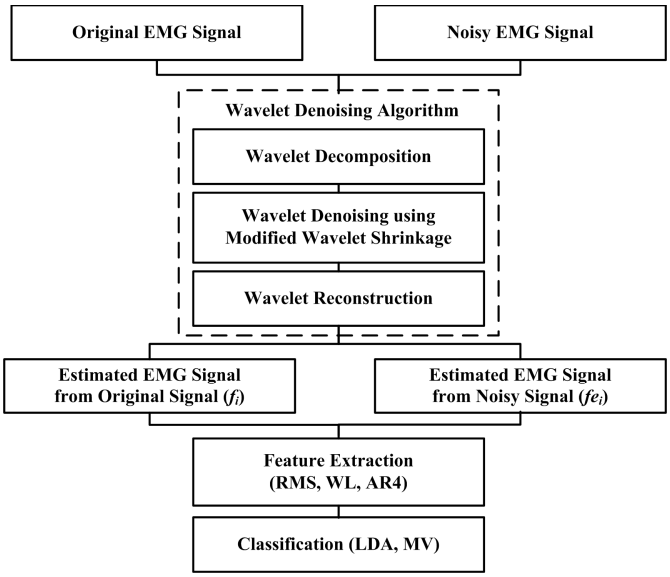

Figure 1. The procedure of improving multifunction myoelectric control system using wavelet denoising algorithm.

forearm. The numbers of motion increase in the second dataset for the performance in pattern recognition. This dataset was acquired by Carleton University in Canada [15]. This system set a band-pass filter of 1-1000 Hz bandwidth and an amplifier with 60 dB gain (Model 15, Grass Telefactor). The EMG signals were sampled at 3 kHz by using an analog-to-digital converter board (PCI-6071E, National Instruments). However, in recognition system, down-sample of EMG signal from 3 kHz to 1 kHz was done. Six trials were collected for each subjects and each trial consisted of four repetitions of each motion. EMG data from three subjects were selected in this study. More details of experiment and data acquisition are described in [15].

C. Evaluation Criterions

Two measured indices are used in this study to illustrate the performance in two criterions. Firstly, *MSE* is used to evaluate the quality of denoising point of view that can be expressed as

$$MSE = \frac{\sum_{i=1}^{N}(f_i - fe_i)^2}{N}, \tag{14}$$

where f_i represents the estimated EMG signal from the original signal and fe_i is estimated EMG signal from the noisy signal.

Secondly, EMG signals that are denoised from all of wavelet shrinkage method were sent to upper limb motions recognition system. Features of the estimated EMG signals are extracted in this study including root mean square (RMS), waveform length (WL), and the fourth order of auto regressive coefficients (AR4). As a result, six members were formed as a feature vector. Classifier is linear Discriminant analysis (LDA) and majority vote (MV) post processing was performed to improve the classification results. The window size is 256 ms and window slide is 64 ms for real-time constraint in myoelectric control system [16]. The procedure of recognition

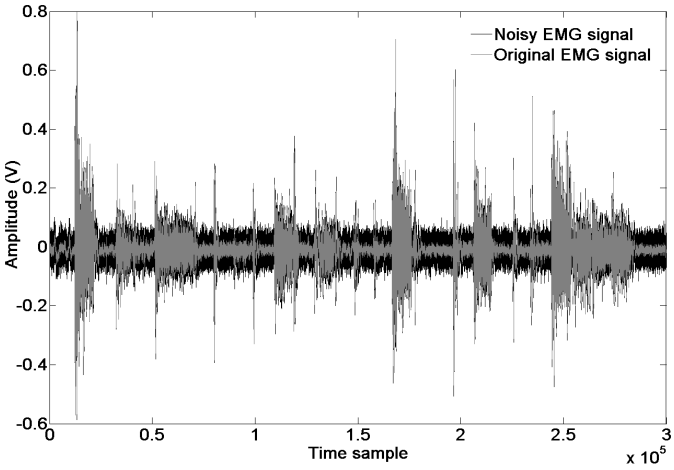

Figure 2. Original EMG signal (gray line) and noisy EMG signal at 5 dB *SNR* (black line) with six upper limb motions [17].

system is shown in Fig. 1. The second index is classification rate (*CR*). It is used to evaluate the quality of the recognition system with the EMG signal that is estimated by using wavelet denoising. To clearly show observation results, improved classification rate (*ICR*) is calculated to demonstrate the improvement of the modified wavelet shrinkage methods. It can be defined as

$$ICR = CR_{denoised} - CR_{no-denoised}, \tag{15}$$

where $CR_{denoised}$ and $CR_{no\text{-}denoised}$ are the *CR* resulting from with and without wavelet denoising procedures, respectively. The performance of algorithms is better when *ICR* is higher. It means that useful information in EMG signal is remained and undesirable parts of EMG signal are removed. To guarantee the best wavelet shrinkage method achieved and optimized for estimated useful EMG signal, we calculated *MSE* and *CR* averages for each motion with 5 times of additional WGN and in each time the WGN was varied from 20-0 dB *SNRs*. We can observe the effect of noise by adding different levels of noise. The example of original EMG signal and original EMG signal with WGN at 5 dB *SNR* are shown in Fig. 2. The *SNR* is calculated by

$$SNR = 10\log\frac{P_{clean}}{P_{noise}}, \tag{16}$$

where P_{clean} is the power of original EMG signal and P_{noise} is the power of WGN.

III. Results and Discussion

A. Performance in Denoising Point of View

The result of *MSE* that is used to present the performance of denoising is shown in Fig. 3 in log-lin type of a semi-log graph at different level of WGN. The denoising performance is better when the *MSE* is lower. From the Fig. 3, the *MSE* of 11 wavelet shrinkage methods and no denoising case with only WT are presented. At medium and high noises, *SNR* is lower than 10 dB. All of wavelet shrinkage methods are better

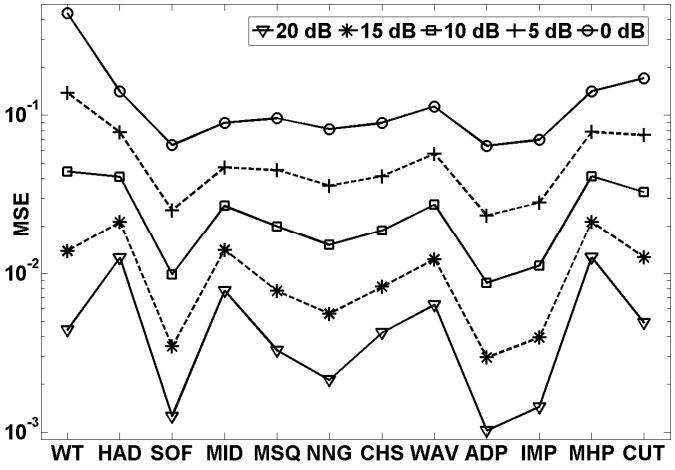

Figure 3. *MSE* of only WT and 11 wavelet shrinkage methods at different level of noise (20-0 dB *SNR*s).

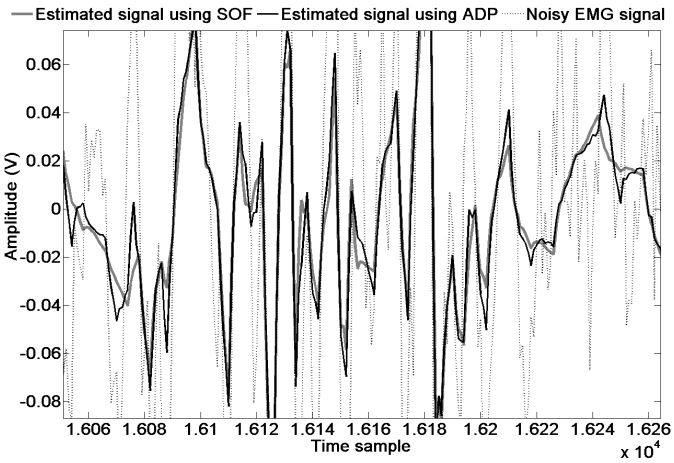

Figure 4. Estimated EMG signal using SOF (gray line) and estimated EMG signal using ADP (black line) with six upper limb motions.

than WT. However, at low noise, 15 dB *SNR*, HAD and MHP are worse than WT. In addition, CUT, WAV, and MID are worse than WT at very low noise, 20 dB *SNR*. Moreover, as *SNR* increases, the *MSE* of each wavelet shrinkage method as well increases.

From the experimental results, the *MSE* of ADP is lowest, followed closely by SOF and IMP. It means that ADP is the best shrinkage in denoising viewpoint. *MSE* of WT is seven times the *MSE* of ADP at low noise and is three times the *MSE* of ADP at high noise. Some responses of wavelet shrinkage methods are presented in Fig. 5(f). However, the *MSE* can be evaluated only for the performance of denoising viewpoint. It may have the different result in the viewpoint of pattern recognition. The same MSE of each wavelet shrinkage method does not mean that the form or shape of estimated EMG signal is similar. We can observe the difference between the estimated EMG signal from the noisy EMG signal at 5 dB *SNR* of SOF (gray line) and ADP (black line) that have the close *MSE* values as shown in Fig. 4. This provides a different value of features in recognition system.

B. Performance in Pattern Recognition Viewpoint

CR and *ICR* were used to present the high performance when *CR* closed to 100 % and *ICR* is high. The results of *CR* and *ICR* of 11 wavelet shrinkage methods at different level of noise (0, 10, and 20 dB *SNR*) are shown in Fig. 5(a-c) respectively. From the observation of *CR* and *ICR* of wavelet shrinkage at different level of *SNR*, it has the same trend. From the Fig. 5(a-c), we can observe that the use of wavelet denoising method to estimate EMG signal before sending to recognition system provides larger *CR* than no denoising EMG signal (black line). The *CR*s of upper limb motions recognition without applying wavelet denoising method are shown in Fig. 5(e) with the square box at each level of noise. When the level of noise increases, *CR* of no denoising rapidly decreases. But the recognition results when using denoising technique still achieved the *CR* larger than 80%. From these experiments, we can confirm that estimated EMG signal that is applied wavelet denoising method before recognition system has better performance than using raw EMG signal in noisy environment. We can get the robust EMG pattern recognition using wavelet shrinkage. It improved about 5% at low level of noise (20 dB *SNR*), about 60% at medium level of noise (10 dB *SNR*), and about 70% at very high level of noise (0 dB *SNR*).

Next, we can see that the best shrinkage is ADP from the observation of the *CR* and *ICR* in Fig. 5(a-c). Its results are summarized in Fig. 5(d) and the comparison with no denoising is shown in Fig. 5(e). However, when level of noise is low, the performance of different kinds of wavelet shrinkage is similar. Moreover, the best wavelet shrinkage method is still ADP. The best *CR* is 98.38% at low noise and 91.62% at very high noise. It is still larger than 90%. Results show that ADP is the best wavelet shrinkage in both of denoising and pattern recognition points of view. The performance of ADP in pattern recognition viewpoint is followed closely by CUT and MHP. These shrinkage methods are better than traditional shrinkage, HAD and SOF. The *CR* of SOF is the lowest. It was expected to perform poorly in recognition viewpoint.

IV. CONCLUSION

Modified wavelets shrinkage methods are introduced and evaluated as an estimation tool to generate useful EMG signal for the pattern recognition in both of class separability and robustness. The evaluation of estimated EMG data confirmed the better results of modified wavelet shrinkage methods over traditional wavelet shrinkage methods. It is able to improve application of multifunction myoelectric control in both of denoising and recognition viewpoints. The results show that the adaptive wavelet shrinkage (ADP) method provides better performance than no denoising and other candidate methods. This paper is a starting idea to find optimal shrinkage method for denoising and estimating EMG signals. In future work, the evaluation of estimated EMG signals with different features and classifiers will be investigated. Moreover, a new equation

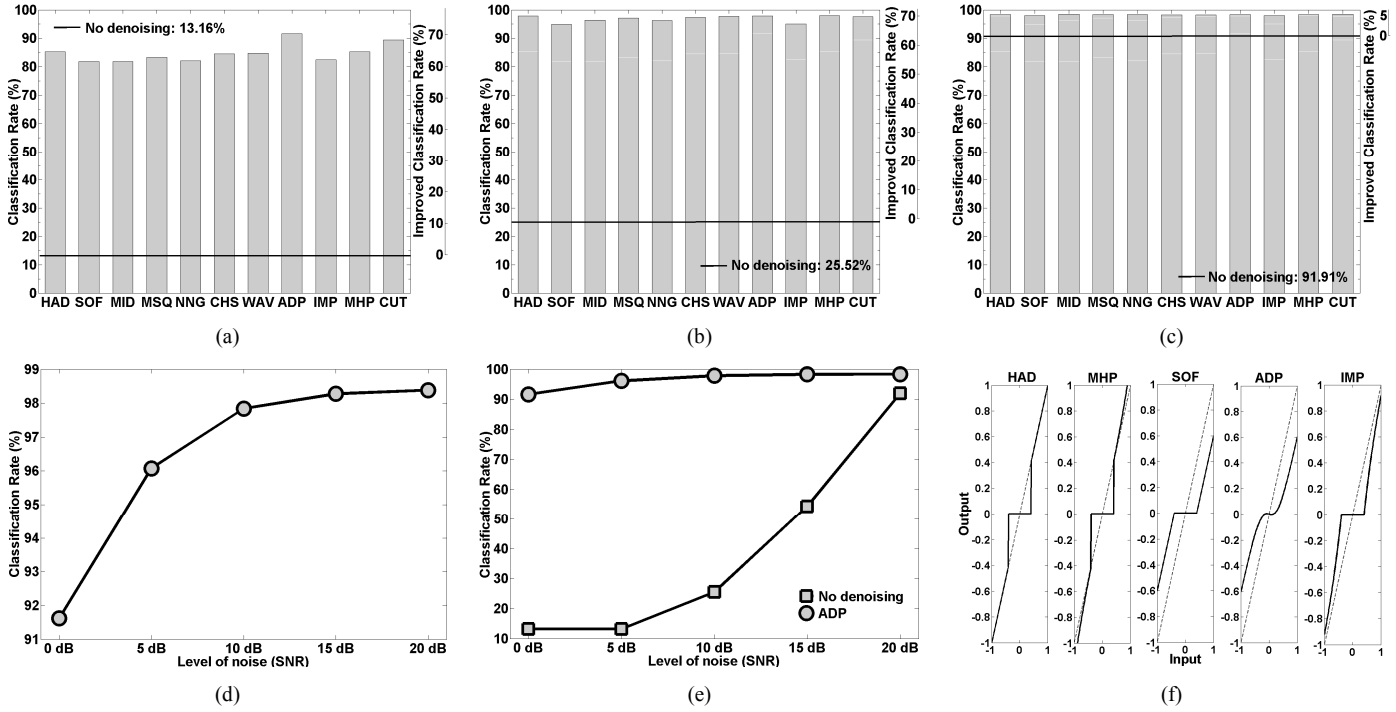

Figure 5. (a-c) *CR* and *ICR* of all wavelet shrinkage methods compared with no denoising method at (a) 0 dB *SNR*. (b) 10 dB *SNR*. (c) 20 dB *SNR*. (d-e) *CR* of ADP and *CR* of ADP with no denoising at 0-20 dB *SNR*, respectively. (f) Responses of five wavelet shrinkage methods with 0.4 threshold value (*THR*) and the diagonal dashed line indicates the input signal.

of wavelet shrinkage method should be formulated only for EMG signals.

ACKNOWLEDGMENT

This work was supported in part by the Thailand Research Fund through the Royal Golden Jubilee Ph.D. Program (Grant No. PHD/0110/2550), and in part by NECTEC-PSU center of excellence for rehabilitation engineering and Faculty of Engineering, Prince of Songkla University. The authors would like to acknowledge the support of Dr. Adrian D.C. Chan from the Carleton University for providing the datasets.

REFERENCES

[1] C.-F. Jiang and S.-L. Kuo, "A comparative study of wavelet denoising of surface Electromyographic signals," in *Proc. 29th IEEE Ann. Int. Conf. Engineering in Medicine and Biology*, Lyon, 2007, pp. 1868-1871.

[2] A. Phinyomark, C. Limsakul, and P. Phukpattaranont, "A comparative study of wavelet denoising for multifunction myoelectric control," in *Proc. Int. Conf. Computer and Automation Engineering (ICCAE 2009)*, Bangkok, 2009, pp. 21-25, doi:10.1109/ICCAE.2009.57.

[3] D.L. Donoho and I.M. Johnstone, "Ideal spatial adaptation by wavelet shrinkage," *Biometrika*, vol. 81, no. 3, pp. 425-455, 1994.

[4] X. Guo, P. Yang, Y. Li, and W.L. Yan, "The SEMG analysis for the lower limb prosthesis using wavelet transformation," in *Proc. 26th IEEE Ann. Int. Conf. Engineering in Medicine and Biology*, San Francisco, 2004, pp. 341-344.

[5] Z. Qingju and L. Zhizeng, "Wavelet de-noising of Electromyography," in *Proc. IEEE Int. Conf. Mechatronics and Automation*, Luoyang, 2006, pp. 1553-1558.

[6] A. Phinyomark, C. Limsakul, and P. Phukpattaranont, "An optimal wavelet function based on wavelet denoising for multifunction myoelectric control," in *Proc. 6th Int. Conf. Electrical Engineering /Electronics, Computer, Telecommunications and Information Technology (ECTI-CON 2009)*, Pattaya, Chonburi, 2009, pp. 1098-1101, doi:10.1109/ECTICON.2009.5137236.

[7] D.B. Percival and A.T. Walden, *Wavelet methods for time series analysis*, Cambridge University Press, 2000.

[8] S. Guoxiang and Z. Ruizhen, "Three novel models of threshold estimator for wavelet coefficients," in *Proc. 2nd Int. Conf. Wavelet Analysis and Its Applications*, Hong Kong, vol. 2251, December 2001, pp. 145–150.

[9] B. Vidakovic, *Statistical Modeling by Wavelets*. Wiley Toronto, ON, Canada, 1999.

[10] H.-Y. Gao, "Wavelet shrinkage denoising using the nonnegative garrote," *J. Comput. Graph. Statist.*, vol. 7, no. 4, pp. 469-488, 1998.

[11] Q. Tianshu, W. Shuxun, C. Haihua, and D. Yisong, "Adaptive denoising based on wavelet thresholding method," in *Proc. 6th Int. Conf. Signal Processing*, Beijing, August 2002, pp. 120-123.

[12] L. Su and G. Zhao, "De-noising of ECG signal using translation-invariant wavelet de-noising method with improved thresholding," in *Proc. 27th IEEE Ann. Int. Conf. on Engineering in Medicine and Biology*, Shanghai, 2005, pp. 5946-5949.

[13] S. Poornachandra, N. Kumaravel, T.K. Saravanan, and R. Somaskandan, "WaveShrink using modified hyper-shrinkage function," in *Proc. 27th IEEE Ann. Int. Conf. Engineering in Medicine and Biology*, Shanghai, 2005, pp. 30-32.

[14] B.-J. Yoon and P.P. Vaidyanathan, "Wavelet-based denoising by customized thresholding," in *Proc. IEEE Int. Conf. Acoustics, Speech, and Signal Processing*, Montreal, May 2004, pp. ii-925-8.

[15] A.D.C. Chan and G.C. Green, "Myoelectric control development toolbox," in *Proc. 30th Conf. Canadian Medical and Biological Engineering Society*, Toronto, 2007.

[16] K. Englehart, B. Hudgins, and P.A. Parker, "A wavelet-based continuous classification scheme for multifunction myoelectric control," *IEEE Transactions on Biomedical Engineering*, vol. 48, no. 3, pp. 302-311, 2001.

[17] A. Phinyomark, C. Limsakul, and P. Phukpattaranont, "A novel feature extraction for robust EMG pattern recognition," *Journal of Computing*, vol.1, issue 1, pp. 71-80, 2009.

Evaluation of EMG Feature Extraction for Hand Movement Recognition Based on Euclidean Distance and Standard Deviation

A. Phinyomark, S. Hirunviriya, C. Limsakul, P. Phukpattaranont
Department of Electrical Engineering, Faculty of Engineering, Prince of Songkla University
110/5, Kanchanavanid Road, Hat Yai, Songkhla 90112 Thailand
E-mail: angkoon.p@hotmail.com, saowaluck_121@hotmail.com, chusak.l@psu.ac.th, pornchai.p@psu.ac.th

***Abstract*-In EMG hand movement recognition, the first and the most important step is feature extraction. The optimal feature is important for the achievement in EMG analysis and control. In this paper, we present a statistical criterion method using the ratio between Euclidean distance and standard deviation, which can response the distance between two scatter groups and directly address the variation of feature in the same group as a selection tool to find the optimal EMG feature. Fifteen features that have been widely used to classify EMG signals were used. The optimal feature is conducted to demonstrate the validity of the proposed index. The major advantages of this method are simplicities of implementation and computation. Moreover, the results of proposed method are the same trend with classification results of the achievement classifiers in EMG recognition. From the experimental results, waveform length is the best feature comparing with the other features. Root mean square, mean absolute value, Willison amplitude, and integrated EMG are useful augmenting features for a more powerful feature vector. From these results, it demonstrates that the proposed method can be used for an EMG feature evaluation index.**

I. INTRODUCTION

Electromyography (EMG) signals have the properties of nonstationary, nonlinear, complexity, and large variation. These lead to difficulty in analyzing EMG signals. In the EMG hand movement recognition, there are two main points, namely feature selection and classifier design that should be paid more attention. In this paper, we focus on the first point. In general, the methods of feature selection can be divided into two types: the measure of classification accuracy and the evaluation using statistical criterion [1]. The first selection method has major disadvantage that the evaluation of EMG features depend on the classifier type but the second selection method is not problematic in this way and tries to quantify the suitableness of the feature space [2]. From the literatures, there are many existing selection methods based on statistic criterion for EMG feature evaluation such as Davies-Bouldin index [1-6], scattering index [5], Fishers linear discriminate index [6], Bhattacharyya distance [7], and fuzzy-entropy-based feature evaluation index [8]. However, the complexity of computation and implementation is drawback of the existing methods.

In this paper, we used two fundamental methods which can evaluate distance between two scatter groups (separation index) and directly address the variation of feature in the same group (compactness index), the ratio between Euclidean distance and standard deviation. The most significant advantage of this method is that it is simple to be implemented and computed. After that the selection of the best features based on the proposed statistical criterion method is investigated. For this purpose, we evaluate different kinds of features that have been widely used in EMG hand movement recognition and there are up-to-date to available techniques today [1-8]. The results of this evaluation and the proposed statistic method can be widely used in EMG applications such as control of EMG robots and prostheses or the EMG diagnosis of nerve and muscle diseases.

Many research works have explored the extraction of features from EMG signal for hand movement recognition. Various features were found in the literatures [1-9]. For example, features based on time domain are mean absolute value, modified mean absolute value, root mean square, integrated of EMG, simple square integral, variance, mean absolute value slope, waveform length, zero crossing, slope sign change, Willison amplitude, and auto-regressive model. Moreover, features based on frequency domain such as mean frequency and median frequency are proposed. All of these feature candidates are selected to be evaluated in this paper. Accordingly, we select six kinds of frequently used hand movements to be classified. In addition, two muscle positions of electrodes are selected based on the relations between muscle location and hand movements to obtain the meaningful EMG signals.

The rest of this paper is organized as follows. Section 2 illustrates experiments and data acquisition. In Section 3, the detail of fifteen kinds of selected features candidates will be introduced. In the later of this section, the detail of proposed statistic criterion method is illustrated. Section 4, experimental results are reported and discussed. Finally, we have some conclusion remarks in Section 5.

II. EXPERIMENTS AND DATA ACQUISITION

Varieties of EMG signals from six hand movements and two muscle positions are used as representative data in this study. Six hand movements were performed by a healthy subject. The six different types of hand movements are performed. They are typical movements of the most frequency use for human beings. They are wrist flexion (wf), wrist extension (we), hand close (hc), hand open (ho), forearm pronation (fp), and forearm

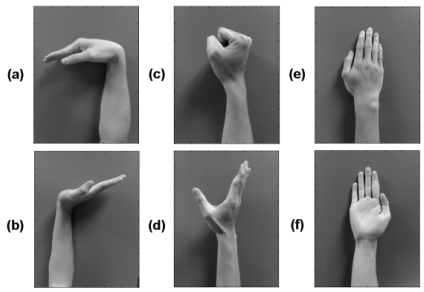

Figure 1. Six different types of hand movements to be classified (a) wf (b) we (c) hc (d) ho (e) fp (f) fs [9].

supination (fs) as shown in Fig. 1. Ten datasets were collected for each hand movement from two channels by two pairs of bipolar Ag/AgCl electrodes (3M red dot solid gel). Therefore, there were 120 datasets of EMG signals in subject. One pair of muscle position was placed over the flexor carpi radialis (ch1) and the other was placed over the extensor carpi radialis longus (ch2). The top side of wrist is used as the reference muscle position. All disc electrodes were put on the skin surface of the right forearm of the subject. Each bipolar pair of electrodes was spaced from a center to center by 20 mm. Moreover, to avoid the cross interference between two muscles, 5 mm diameter electrodes was used.

Differential amplifiers were set with 60 dB gain and band-pass filters of 10-500 Hz bandwidth were used to remove high random frequency interferences and the motion artifacts at low frequency. Sampling frequency was set at 1000 Hz using a 16 bit analog-to-digital converter board (NI, DAQCard-6024E). In the analysis, the window length of EMG samples was set for 256 ms with the objective of real-time signal processing. In other words, the maximum permissible delay for EMG hand prosthesis control should be less than 300 ms [10].

III. METHODOLOGY

A. Feature Extraction Stage

Fifteen features from time domain and frequency domain are used in evaluation. Time domain features are measured as a function of time. Because of their implementation and computation simplicity, time domain features are the most popular in EMG hand movement recognition. All features in time domain can be implemented in real-time. Normally, features in this group are used for detecting muscle contraction, muscle activity, and onset detection. Thirteen features based on time domain are described as follows.

1) *Integrated EMG (IEMG):* IEMG is normally used as an onset detection index that is related to EMG signal sequence firing point. IEMG is the summation of the absolute values of EMG signal amplitude, which can be expressed as

$$\mathrm{IEMG} = \sum_{n=1}^{N} |x_n| . \tag{1}$$

where x_n represents the EMG signal in a segment and N denotes the length of the EMG signal.

2) *Mean Absolute Value (MAV):* MAV is similar to IEMG that normally used as an onset index to detect the muscle activity. MAV is the average of the absolute value of EMG signal amplitude. MAV is a popular feature used in EMG hand movement recognition application. It is defined as

$$\mathrm{MAV} = \frac{1}{N}\sum_{n=1}^{N} |x_n| . \tag{2}$$

3) *Modified Mean Absolute Value 1 (MAV1):* MAV1 is an extension of MAV. MAV1 uses weighting window function (w_n) to improve the robustness of MAV. It is calculated by

$$\mathrm{MAV1} = \frac{1}{N}\sum_{n=1}^{N} w_n |x_n|, \qquad w_n = \begin{cases} 1, & if\ 0.25N \le n \le 0.75N \\ 0.5, & otherwise . \end{cases} \tag{3}$$

4) *Modified Mean Absolute Value 2 (MAV2):* MAV2 is related to MAV1. Moreover, continuous weighting window function (w_n) in this feature is used to improve the smoothness of weighting function. The equation can be defined as

$$\mathrm{MAV2} = \frac{1}{N}\sum_{n=1}^{N} w_n |x_n|, \qquad w_n = \begin{cases} 1, & if\ 0.25N \le n \le 0.75N \\ 4n/N, & if\ 0.25N > n \\ 4(n-N)/N, & if\ 0.75N < n . \end{cases} \tag{4}$$

5) *Mean Absolute Value Slope (MAVS):* MAVS is a modified version of MAV. The differences between the MAVs of adjacent segments are determined. It can be defined as

$$\mathrm{MAVS}_i = \mathrm{MAV}_{i+1} - \mathrm{MAV}_i ; \quad i = 1, \ldots, I-1. \tag{5}$$

where I is the number of segments covering EMG signal. When the number of segments increases, it may improve the representation of the original signal over the traditional MAV.

6) *Simple Square Integral (SSI):* SSI captures the energy of the EMG signal as a feature. It can be expressed as

$$\mathrm{SSI} = \sum_{n=1}^{N} |x_n|^2 . \tag{6}$$

7) *Variance (VAR):* VAR captures the power of EMG signal as a feature. Normally, variance is mean of square of deviation of that variable. However, mean value of EMG signal is close to zero. Therefore, variance of EMG signal can be defined as

$$\mathrm{VAR} = \frac{1}{N-1}\sum_{n=1}^{N} x_n^2 . \tag{7}$$

8) *Root Mean Square (RMS):* RMS is related to constant force and non-fatiguing contraction. Generally, it similar to *SD*, which can be expressed as

$$\mathrm{RMS} = \sqrt{\frac{1}{N}\sum_{n=1}^{N} x_n^2} . \tag{8}$$

9) *Waveform length (WL):* WL is the cumulative length of waveform over time segment. WL is similar to waveform amplitude, frequency and time. The WL can be formulated as

$$\mathrm{WL} = \sum_{n=1}^{N-1} \left| x_{n+1} - x_n \right| . \tag{9}$$

10) *Zero crossing (ZC):* ZC is the number of times that the amplitude values of EMG signal crosses zero in x-axis. In EMG feature, threshold condition is used to avoid from background noise. ZC provides an approximate estimation of frequency domain properties. The calculation is defined as

$$\mathrm{ZC} = \sum_{n=1}^{N-1} \left[\mathrm{sgn}\left(x_n \times x_{n+1} \right) \cap \left| x_n - x_{n+1} \right| \geq threshold \right];$$
$$\mathrm{sgn}(x) = \begin{cases} 1, & if\ x \geq threshold \\ 0, & otherwise . \end{cases} \tag{10}$$

11) *Slope Sign Change (SSC):* SSC is related to ZC. It is another method to represent the frequency domain properties of EMG signal calculated in time domain. The number of changes between positive and negative slope among three sequential segments are performed with threshold function for avoiding background noise in EMG signal. It is given by

$$\mathrm{SSC} = \sum_{n=2}^{N-1} \left[f\left[\left(x_n - x_{n-1} \right) \times \left(x_n - x_{n+1} \right) \right] \right];$$
$$f(x) = \begin{cases} 1, & if\ x \geq threshold \\ 0, & otherwise . \end{cases} \tag{11}$$

12) *Willison amplitude (WAMP):* WAMP is the number of time resulting from the difference between EMG signal amplitude of two adjoining segments that exceeds a predefined threshold, which is used to reduce background noises like in the calculation of ZC and SSC. It is given by

$$\mathrm{WAMP} = \sum_{n=1}^{N-1} f\left(\left| x_n - x_{n+1} \right| \right);$$
$$f(x) = \begin{cases} 1, & if\ x \geq threshold \\ 0, & otherwise . \end{cases} \tag{12}$$

WAMP is related to the firing of motor unit action potentials and muscle contraction level. The suitable value of threshold parameter of features in ZC, SSC, and WAMP is normally chosen between 10 and 100 mV that is dependent on the setting of gain value of instrument. However, the optimal threshold suitable for EMG analysis is discussed later.

13) *Auto-regressive (AR) coefficients:* AR model described each sample of EMG signals as a linear combination of previous EMG samples (x_{n-i}) plus a white noise error term (w_n). In addition, p is the order of AR model. AR coefficients (α_i) are used as features in EMG hand movement recognition. The definition of AR model is given by

$$x_n = -\sum_{i=1}^{p} a_i x_{n-i} + w_n , \tag{13}$$

Moreover, two features in frequency domain are evaluated in this study. Normally, frequency domain features are used to detect neural abnormalities and muscle fatigue. Moreover, these features are used in EMG hand movement recognition. Details of all features are as follows.

14) *Median Frequency (MDF):* MDF is frequency at which the spectrum is divided into two regions with equal amplitude. It can be expressed as

$$\sum_{j=1}^{\mathrm{MDF}} P_j = \sum_{j=\mathrm{MDF}}^{M} P_j = \frac{1}{2} \sum_{j=1}^{M} P_j , \tag{14}$$

where P_j is EMG power spectrum at frequency bin j.

15) *Mean Frequency (MNF):* MNF is average frequency. It is calculated as the sum of the product of power spectrum and frequency divided by the total sum of spectrum intensity, which can be expressed as

$$\mathrm{MNF} = \sum_{j=1}^{M} f_j P_j \Big/ \sum_{j=1}^{M} P_j , \tag{15}$$

where f_j is frequency of spectrum at frequency bin j.

B. Feature Selection Stage

The good quality in class separability point of view means that the result of misclassification rate is the lowest or the highest of separation between classes is obtained and the small value of variation in subject experiment is reached. From the explanation above, feature selection methods can be obtained based on either classifier or statistic measurement index. From the drawback of evaluation using classifier in the first type that the evaluation results are dependent on the classifier [5, 11]. We investigate the selection of features based on statistical index in this study. We introduce the statistic criterion method which can evaluate distance between two scatter groups (separation index) and directly address the variation of feature in the same group (compactness index). Normally, the statistical index should be addressed in both of separation and compactness index [8]. Euclidean distance (*ED*) and standard deviation (*SD*) are the simple method that is selected in this study to address two properties above.

ED is the most common use of distance. It is calculated as the root of square differences between co-ordinates of a pair of objects. We used *ED* as a separation index. In addition, *SD* is the most robust and widely used measure of the variability. *SD* is used as a compactness index. The *ED*(p,q) is defined as

$$ED(p,q) = \sqrt{\left(p_{\mathrm{ch1}} - q_{\mathrm{ch1}} \right)^2 + \left(p_{\mathrm{ch2}} - q_{\mathrm{ch2}} \right)^2} , \tag{16}$$

where p and q is the feature mean of two motions from six hand motions with two dimensional spaces (two muscles). In addition, the equation of *SD* is given by

$$SD = \sigma = \sqrt{\frac{\sum_{w=1}^{N_W} (r_w - \mu)^2}{N_W}} , \tag{17}$$

where r is the feature of the w^{th} window of N_W and μ is the feature mean of all windows. The ratio between *ED* and *SD* that we called RES_{pq} index is used as a statistic measured index in this paper. The RES_{pq} index can be expressed as

$$RES_{pq} = \frac{ED(p,q)}{\bar{\sigma}} , \tag{18}$$

where the $\bar{\sigma}$ is the average between standard deviation of two motions (p and q) with two dimensional spaces (two muscle positions, ch1 and ch2). In addition, the EMG features are normalized before calculating the *ED* and *SD* values. The normalization in this study refers to allow feature values on different scales to be compared. In order to negate that variable's effect on the EMG features, the normalized features (r_{norm}) are performed which can be expressed as

$$r_{norm} = \frac{r + \min(r)}{\max(r + \min(r))}, \tag{19}$$

The best performance of classification is obtained when the *ED* value is high and the *SD* value is low. Therefore the RES_{pq} index should be large to obtain better performance. In order to confirm the results, the average of RES_{pq} from fifteen possible combinations of six hand movements (*RES* index) is performed. The most significant advantage of the proposed statistic method is that it is simple to implement and compute. Moreover, in order to confirm that it can directly indicate the best feature with the classification results. We compared the results of proposed method with the classification results of the achievement classifiers in EMG recognition. We used the results of support vector machine (SVM) classifier in [12] to compare.

IV. Results and Discussion

In order to demonstrate the classification performance, the scatter plots between EMG features from two muscles of six movements are used to confirm the distance between two scatter groups and the variation of feature in the same group. From Fig. 2(a), scatter plot of WL feature shows that the data points in each motion are clear separation and compactness. It will be easily grouped when used for pattern recognition. However, from the Fig. 2(b), scatter plot of AR1 is observed that pattern for different motions are much fluctuated. In practice, it is hard to classify these patterns to reach maximum rate. In this paper, we used *RES* index to indicate the quality of separation instead of using the observation from scatter plot.

From the experimental results, WL is the best feature compared with the other features as we can observe from the Fig. 3. WL obtains the *RES* index as 11.764. It is higher than the secondary feature about 2.337. RMS, WAMP, MAV, and IEMG are the secondary features group. Their *RES* index are greater than 9.3. Moreover, they provide only one feature per channel which is small enough to combine with other features to make a more powerful feature vector but it does not increase the computational burden for the classifier. VAR, SSI, MAV1 are closed by the secondary features group. For time domain features that contained frequency information, WAMP has better cluster separability than ZC and SSC. The optimal threshold value of WAMP is about 30 mV but the optimal threshold value of ZC and SSC is about 10 mV.

The modified version of MAV is worse than the traditional MAV. In addition, the whole features in frequency domain show poor class separability. MNF and MDF obtain *RES* index

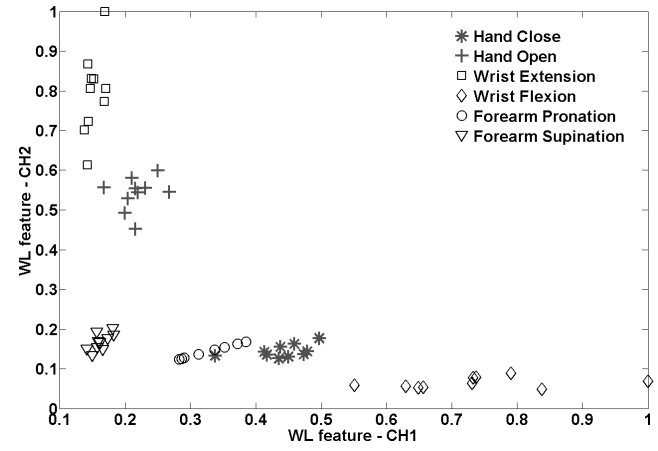

(a)

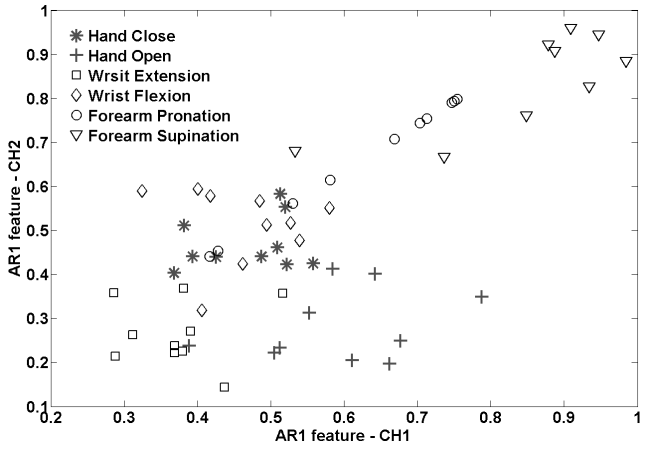

(b)

Figure 2. Scatter plot of six different movements of (a)WL features - (b) AR1 features - from two muscles (ch1 and ch2).

merely about 4.6 and AR1 obtain *RES* index only about 3.7. *RES* index of WL feature is three times the *RES* index of whole frequency domain features. Furthermore, MAVS is the worst classifier performance compared to the other features. Its *RES* index is only 2.901. The *RES* index of WL feature is four times the *RES* index of the worst case, MAVS. Additionally, AR and MAVS in this study used the first order and two segments for obtaining only one feature per channel. Therefore, the increasing of AR order and MAVS segments may improve the classification results.

The results of the proposed method are the same trend with the SVM classifier in [12]. The classification results of SVM classifier in [12] showed that it is better than the other successful classifier, namely linear Discriminant analysis and multilayer perceptron neural network. The best single feature is WL in [12] that is similar to the results from *RES* index. In addition, other results in [12] are similar with the results of RES index such as the better performance of RMS over MAV, the improvement of WAMP over ZC and SSC, the betterment of original MAV over modified version of MAV, or the poor class separability of EMG features in frequency domain.

Moreover, Fig. 4(a-b) shows the value of *ED* and *SD* that ZC has the highest *ED* but the *SD* of ZC is very poor. Hence, the

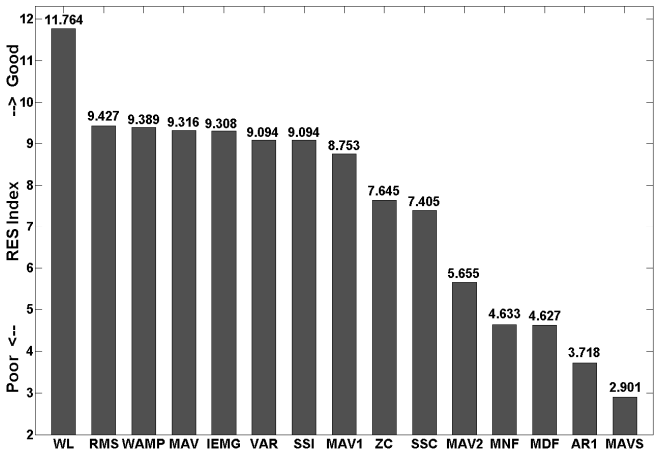

Figure 3. Bar plot of *RES* index of fifteen features with the six different movements and two muscles.

RES index of ZC is not good. MDF and WAMP are the same trend with ZC that *ED* is high but *SD* is high too. The *ED* of WL follows the best group. Furthermore, *SD* of WL is smallest. For this cause, the *RES* index of WL is higher than other features. For the worst case, MAVS obtained both of smallest *ED* and highest *SD*.

V. Conclusion

From the *RES* index, WL has the best overall performance. RMS and WAMP are the better ones that can use with WL for a useful feature vector. The results of *RES* index are same trend with the classification results of SVM classifier. From the experiments demonstrate that *RES* index can be used as an EMG feature evaluation index. In future work, other features that have been reported in literatures should be evaluated to find the better one. Moreover, the combination of some useful features should be tested using the proposed index and the achievement classifiers to find optimal feature vector for EMG recognition. In addition, the assessment of the *RES* index with the larger EMG datasets is ongoing research..

Acknowledgment

This work was supported in part by the Thailand Research Fund through the Royal Golden Jubilee Ph.D. Program (Grant No. PHD/0110/2550), and in part by NECTEC-PSU center of excellence for rehabilitation engineering and Faculty of Engineering, Prince of Songkla University.

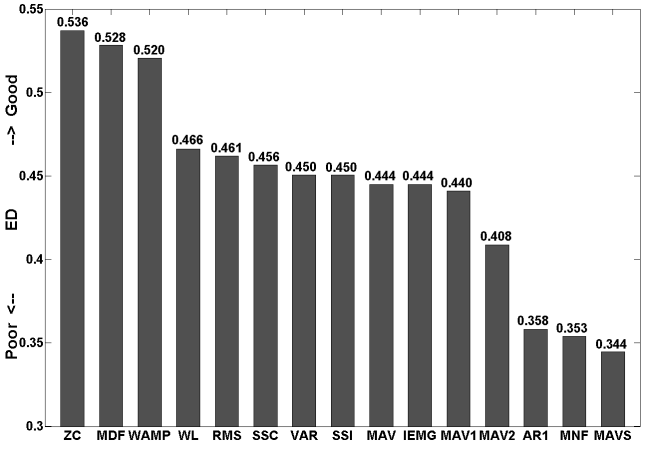

(a)

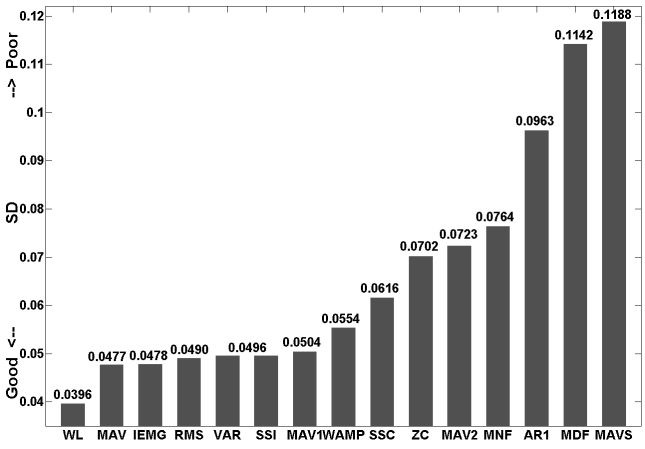

(b)

Figure 4. Bar plot of (a) *ED* - (b) *SD* - of fifteen features with the six different movements and two muscles.

References

[1] M. Zardoshti-Kermani, B.C. Wheeler, K. Badie, and R.M. Hashemi, "EMG feature evaluation for movement control of upper extremity prostheses," *IEEE Transactions on Rehabilitation Engineering*, vol. 3, no. 4, pp. 324-333, December 1995.

[2] H. Han-Pang and C. Chun-Yen, "Development of a myoelectric discrimination system for a multi-degree prosthetic hand," in *Proc. IEEE Int. Conf. Robotics and Automation*, vol. 3, 1999, pp. 2392-2397.

[3] G. Wang, Z. Wang, W. Chen, and J. Zhuang, "Classification of surface EMG signals using optimal wavelet packet method based on Davies-Bouldin criterion," *Medical and Biological Engineering and Computing*, vol. 44, no. 10, pp. 865-872, October 2006.

[4] M.C. Santa-Cruz, R. Riso, and F. Sepulveda, "Optimal selection of time series coefficients for wrist myoelectric control based on intramuscular recordings," *in Proc. 23rd Ann. Int. Conf. IEEE Engineering in Medicine and Biology Society*, vol. 2, 2001, pp. 1384-1387.

[5] R. Boostani and M.H. Moradi, "Evaluation of the forearm EMG signal features for the control of a prosthetic hand," *Physiological Measurement*, vol. 24, no. 2, pp. 309-319, May 2003.

[6] M.A. Oskoei and H. Hu, "GA-based Feature Subset Selection for Myoelectric Classification," in *Proc. IEEE Int. Conf. Robotics and Biomimetics*, 2006, pp. 1465-1470.

[7] S.H. Park and S.P. Lee, "EMG pattern recognition based on artificial intelligence techniques," *IEEE transactions on rehabilitation engineering*, vol. 6, no. 4, pp. 400-405, December 1998.

[8] H.-P. Huang, Y.-H. Liu, and C.-S. Wong, "Automatic EMG feature evaluation for controlling a prosthetic hand using a supervised feature mining method: an intelligent approach," in *Proc. IEEE Int. Conf. Robotics and Automation*, 2003, pp. 220-225.

[9] A. Phinyomark, C. Limsakul, and P. Phukpattaranont, "A novel feature extraction for robust EMG pattern recognition," *Journal of Computing*, vol. 1, issue 1, pp. 71-80, December 2009.

[10] K. Englehart, B. Hudgins, and P.A. Parker, "A wavelet-based continuous classification scheme for multifunction myoelectric control," *IEEE Transactions on Biomedical Engineering*, vol. 48, no. 3, pp. 302-311, March 2001.

[11] R.N. Khushaba and A. Al-Jumaily, "Channel and feature selection in multifunction myoelectric control," in *Proc. 29th Ann. Int. Conf. IEEE Engineering in Medicine and Biology Society*, 2007, pp. 5182-5185.

[12] M.A. Oskoei and H. Hu, "Support vector machine-based classification scheme for myoelectric control applied to upper limb," *IEEE Transactions on Biomedical Engineering*, vol. 55, no. 8, pp. 1956-1965, August 2008.

4.2 ความคงทนต่อสัญญาณรบกวน

ในแง่มุมของการทนต่อสัญญาณรบกวนได้ดีที่สุด คณะผู้วิจัยได้เริ่มศึกษาเพิ่มเติมในขั้นของการเตรียมสัญญาณ ก่อนนำมาคำนวณหาวิธีการวัดลักษณะเด่นของสัญญาณ โดยการใช้การลดสัญญาณรบกวนด้วยวิธีการแปลงเวฟเล็ต (บทความที่ 1 และ 2) ซึ่งทำให้ยังคงค่าความแม่นยำในการระบุท่าทางการเคลื่อนไหวอยู่ได้ แม้ขณะที่มีสัญญาณรบกวนเข้ามาในระบบ ตั้งแต่ระดับ สัญญาณหลักต่อสัญญาณรบกวนที่ 20 จนถึง 0 dB ดังนั้นในกรณีที่ระบบมีสัญญาณรบกวนเข้ามามาก การใช้การลดสัญญาณรบกวนก่อนการหาลักษณะเด่นของสัญญาณก็จะเป็นการทำให้ระบบมีความคงทนต่อสัญญาณรบกวนได้สูงขึ้น นอกจากนี้ คณะวิจัยได้มีการปรับปรุงวิธีการวัดลักษณะเด่นของสัญญาณเชิงความถี่สองวิธี คือ Modified Mean Frequency (MMNF) และ Modified Median Frequency (MMDF) (บทความที่ 4) โดยพบว่าเมื่อเทียบกับวิธีการวัดลักษณะเด่นของสัญญาณที่มีอยู่เดิม ซึ่งกล่าวถึงในหัวข้อที่ 4.1 จำนวน 15 วิธีแล้วได้เพิ่มวิธีการวัดลักษณะเด่นของสัญญาณอีก 1 วิธีในแกนเวลา คือ วิธี Histogram of EMG (HIST) ซึ่งจากผลการทดลอง พบว่าวิธีที่ปรับปรุงขึ้นมาใหม่ให้ผลในการทนต่อสัญญาณรบกวนได้ดีกว่าวิธีการเดิมทั้ง 16 วิธี สำหรับวิธีการวัดลักษณะเด่นของสัญญาณวิธีที่มีอยู่เดิมพบว่า วิธีการ Willison Amplitude และวิธีการ HIST ให้ผลทนต่อสัญญาณรบกวนในระดับที่น่าพอใจ

บทความที่ 4 เรื่อง A Novel Feature Extraction for Robust EMG Pattern Recognition

A Novel Feature Extraction for Robust EMG Pattern Recognition

Angkoon Phinyomark, Chusak Limsakul, and Pornchai Phukpattaranont

Abstract—Varieties of noises are major problem in recognition of Electromyography (EMG) signal. Hence, methods to remove noise become most significant in EMG signal analysis. White Gaussian noise (WGN) is used to represent interference in this paper. Generally, WGN is difficult to be removed using typical filtering and solutions to remove WGN are limited. In addition, noise removal is an important step before performing feature extraction, which is used in EMG-based recognition. This research is aimed to present a novel feature that tolerate with WGN. As a result, noise removal algorithm is not needed. Two novel mean and median frequencies (MMNF and MMDF) are presented for robust feature extraction. Sixteen existing features and two novelties are evaluated in a noisy environment. WGN with various signal-to-noise ratios (SNRs), i.e. 20-0 dB, was added to the original EMG signal. The results showed that MMNF performed very well especially in weak EMG signal compared with others. The error of MMNF in weak EMG signal with very high noise, 0 dB SNR, is about 5-10% and closed by MMDF and Histogram, whereas the error of other features is more than 20%. While in strong EMG signal, the error of MMNF is better than those from other features. Moreover, the combination of MMNF, Histrogram of EMG and Willison amplitude is used as feature vector in classification task. The experimental result shows the better recognition result in noisy environment than other success feature candidates. From the above results demonstrate that MMNF can be used for new robust feature extraction.

Index Terms—Electromyography (EMG), Feature extraction, Pattern recognition, Robustness, Man-machine interfaces.

1 Introduction

SURFACE Electromyography (sEMG) signal is one of the electrophysiological signals, which is extensively studied and applied in clinic and engineering. In this research, the application of sEMG signal in assistive technology and rehabilitation engineering is paid attention. Main application of these fields is the control of the prosthesis or other assistive devices using the different patterns of sEMG signal [1-2]. Nevertheless, the major drawback of EMG pattern recognition is the poor recognition results under conditions of existing noises especially when the frequency characteristic of noise is random. Major types of noise, artefact and interference in recorded sEMG signal are electrode noise, electrode and cable motion artifact, alternating current power line interference, and other noise sources such as a broad band noise from electronic instrument [3-4]. The first three types of noise can be removed using typical filtering procedures such as band-pass filter, band-stop filter, or the use of well electrode and instrument [3-4] but the interferences of random noise that fall in EMG dominant frequency energy is difficult to be removed using previous procedures. Generally, white Gaussian noise (WGN) is used to represent the random noise in sEMG signal analysis [5-6]. Adaptive filter or wavelet denoising algorithm, advance digital signal filter, has been received considerable attention in the removal of WGN [7-8]. However, WGN cannot be removed one hundred percent and sometimes some important part of sEMG signals are removed with noise even if we use adaptive filter and wavelet denoising algorithm. The broad band and random frequency characteristic of noise in this group is a main reason that make it difficult to be removed. Moreover, the amplitude of noise is bigger than the sEMG signal amplitude; the amplitude of raw signal is about 50 μV-100 mV [9].

In EMG-based pattern recognition, sEMG signal is preprocessed the spectral frequency component of the signal and extracted some features before performing classification [1]. Normally, in preprocessing and signal condition procedure, method to remove noise is a significant step to reduce noises and improve some spectral component part [3]. Next important step, feature extraction, is used for highlighting the relevant structures in the sEMG signal and rejecting noise and unimportant sEMG signal [5]. The success of EMG pattern recognition depends on the selection of features that represent raw sEMG signal for classification. This study is motivated by the fact that the limitation of the solutions to remove WGN in the preprocessing step and EMG-based gestures classification need to do the extraction step. The selection of feature that torelance of WGN and the modified of existing EMG feature to improve the robust property are proposed. As a result, WGN removal algorithms in the preprocessing step are not needed.

- *Angkoon Phinyomark is with Department of Electrical Engineering, Prince of Songkla University, Songkhla, Thailand 90112.*
- *Chusak Limsakul is with the Department of Electrical Engineering, Prince of Songkla University, Songkhla, Thailand 90112.*
- *Pornchai Phukpattaranont is with the Department of Electrical Engineering, Prince of Songkla University, Songkhla, Thailand 90112.*

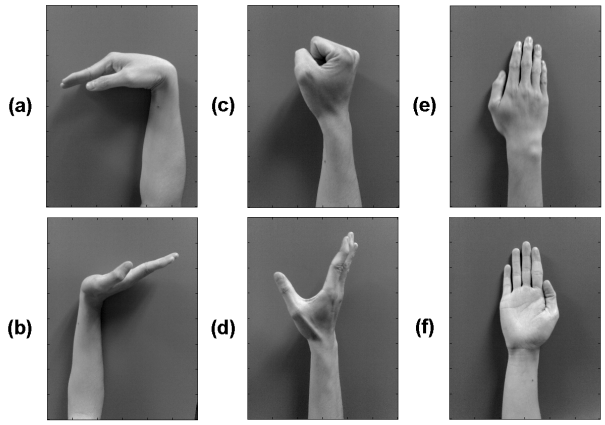

Fig. 1. Estimated six upper limb motions (a) wrist flexion (b) wrist extension (c) hand close (d) hand open (e) forearm pronation (d) forearm supination.

From the literatures, the development of robust feature extractions in speech, texture, and image are presented [10-11] but there is no selection and modification of robust EMG feature extraction. There are some evaluations about the effect of noise with EMG features [5, 12-14]. However, these literatures attend to the quality of EMG features in maximum class separability point of view. The description and discussion about the robustness are inferiority. Furthermore, features that used to evaluate in the literatures are not fair with the available methods today. In 1995, Zardoshti-Kermani et al. [5] evaluated seven features in time domain and frequency domain. WGN with 0 to 50% of rms amplitude signal are used to test the effect of noise. The cluster separability index and classification result are presented that histrogram of EMG is the better feature in very high noise (50% of rms amplitude signal). Later, in 2003, thirteen features with combination and various orders are tested the robustness property by Boostani et al. [12]. One level, one tenth of sEMG peak-to-peak amplitude, of 50 Hz interference and random noise is considered and the sensitivity of feature is reported. In addition, our previous work [13-14] compared the effect of eight features and their relevant features with 50 Hz interference and WGN. The results of mean square error (*MSE*) criterion show that Willison amplitude with 5 mV threshold parameter is the best feature compared to the other features.

However, there is an increase in EMG feature methods that is published in many literatures this day. In this paper, sixteen features in time domain and frequency domain from the literatures [5, 12-17] are used to test the robustness with the additive WGN at various signal-to-noise ratios (*SNR*s). Moreover, the effect of the level of signal amplitude was tested. Eighteen features that used in this research represent most features in EMG pattern recognition. Generally, most of the attempts to extract features from sEMG signal can be classified into three categories including time domain, frequency domain, and time-frequency domain [1]. We considered only former two categories because they have computational simplicity and they have been widely used in research and in clinical practice. In addition, two novel feature calculations using frequency properties are presented. We modified the mean frequency and median frequency by calculating the mean and median of amplitude spectrum instead of power spectrum that we called Modifed Mean Frequency (MMNF) and Modified Median Frequency (MMDF). This paper is organized as follows. Experiments and data acquisition are presented in Section 2. Section 3 presents a description of EMG feature extraction methods in time domain and frequency domain. In addition, the evaluation criterion is introduced. Results and discussion are reported in Section 4, and finally the conclusion is drawn in Section 5.

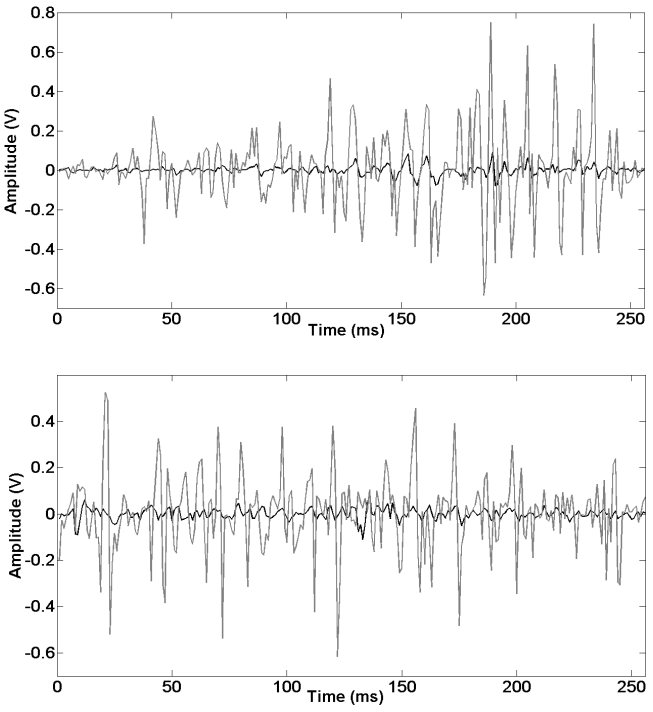

Fig. 2. Strong sEMG signal (gray line) and weak sEMG signal (black line) of (a) wrist extension motion. (b) hand open motion.

2 Experiments and Data Acquisition

In this section, we depict our experimental procedure for recording sEMG signals. The sEMG signal was recorded from flexor carpi radialis and extensor carpi radialis longus of a healthy male by two pairs of Ag-AgCl Red Dot surface electrodes on the right forearm. Each electrode was separated from the other by 2 cm. A band-pass filter of 10-500 Hz bandwidth and an amplifier with 60 dB gain was used. Sampling frequency was set at 1 kHz using a 16 bit analog-to-digital converter board (National Instruments, DAQCard-6024E).

A volunteer performed four upper limb motions including hand open, hand close, wrist extension, and wrist flexion as shown in Fig. 1 (a-d). In this study, the effect of signal strength was performed by divided the sEMG signal to two types: strong sEMG signal and weak sEMG signal. Strong sEMG signals were collected from extensor carpi radialis longus in hand close and wrist flexion and

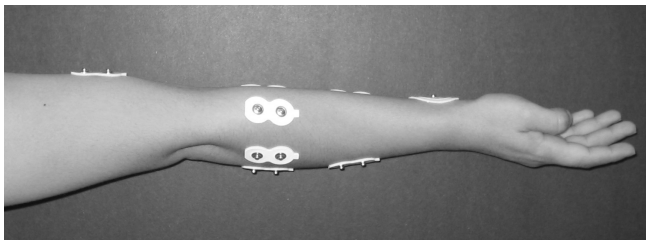

Fig. 3. The eight electrode placements of the right forearm.

were collected from flexor carpi radialis in hand open and wrist extension as shown in Fig. 2 (gray line). In addition, the others motion and electrode channel are weak sEMG signals as shown in Fig. 2 (black line). Ten datasets were collected for each motion. The sample size of the sEMG signals is 256 ms for the real-time constraint that the response time should be less than 300 ms. This dataset was used for the *MSE* criterion that represent the effect of noise with the value of EMG features.

The second dataset is used to evaluate the performance of the classification results of EMG features in noisy environment. Seven upper limb motions including hand open, hand close, wrist extension, wrist flexion, forearm pronation, forearm supination and resting as shown in Fig. 1 and eight electrode positions on the right forearm as shown in Fig. 3 were used in the classification procedure to measure the performance of the EMG feature space quality with WGN. This dataset was acquired by the Carleton University in Canada [17]. A duo-trode Ag-AgCl surface electrode (Myotronics, 6140) was used and an Ag-AgCl Red-Dot surface electrode (3M, 2237) was placed on the wrist to provide a common ground reference. This system set a bandpass filter with a 1–1000 Hz bandwidth and amplifier with a 60 dB (Model 15, Grass Telefactor). The sEMG signals were sampled by using an analog-to-digital converter board (National Instruments, PCI-6071E), and the sampling frequency was 3 kHz. However, in pattern recognition, downsample of EMG data from 3 kHz to 1 kHz was done. Each trial of the database consisted of four repetitions of each motion. There are six trials in each subject. Three subjects were selected in this study. More details of experimentals and data acquisition are described in [17].

3 METHODOLOGY

Eighteen time domain features and frequency domain features are described in this section. Thirteen time domain variables are measured as a function of time. Because of their computational simplicity, time domain features or linear techniques are the most popular in EMG pattern recognition. Integrated EMG, Mean absolute value, Modified mean absolute value 1, Modified mean absolute value 2, Mean absolute value slope, Simple square integral, Variance of EMG, Root mean square, Waveform length, Zero crossing, Slope sign change, Willison amplitude, and Histogram of EMG are used to test the performance. All of them can be done in real-time and electronically and it is simple for implementation. Features in this group are normally used for onset detection, muscle contraction and muscle activity detection. Moreover, features in frequency domain are used to represent the detect muscle fatigue and neural abnormalities, and sometime are used in EMG pattern recognition. Three traditional and two modified features in frequency spectrum are performed namely autoregressive coefficients, mean and median frequencies, modified mean and median frequencies. Afterward, the evaluation methods of two criterions that used to measure the robustness property of the whole features are introduced.

3.1 Time Domain Feature Extraction

3.1.1 Integrated EMG

Integrated EMG (IEMG) is calculated as the summation of the absolute values of the sEMG signal amplitude. Generally, IEMG is used as an onset index to detect the muscle activity that used to oncoming the control command of assistive control device. It is related to the sEMG signal sequence firing point, which can be expressed as

$$\mathrm{IEMG} = \sum_{n=1}^{N} \left| x_n \right| , \tag{1}$$

where N denotes the length of the signal and x_n represents the sEMG signal in a segment.

3.1.2 Mean Absolute Value

Mean Absolute Value (MAV) is similar to average rectified value (ARV). It can be calculated using the moving average of full-wave rectified EMG. In other words, it is calculated by taking the average of the absolute value of sEMG signal. It is an easy way for detection of muscle contraction levels and it is a popular feature used in myoelectric control application. It is defined as

$$\mathrm{MAV} = \frac{1}{N} \sum_{n=1}^{N} \left| x_n \right| . \tag{2}$$

3.1.3 Modified Mean Absolute Value 1

Modified Mean Absolute Value 1 (MMAV1) is an extension of MAV using weighting window function w_n. It is shown as

$$\mathrm{MMAV1} = \frac{1}{N} \sum_{n=1}^{N} w_n \left| x_n \right| ,$$
$$w_n = \begin{cases} 1, & if\ 0.25N \le n \le 0.75N \\ 0.5, & otherwise . \end{cases} \tag{3}$$

3.1.4 Modified Mean Absolute Value 2

Modified Mean Absolute Value 2 (MMAV2) is similar to MMAV1. However, the smooth window is improved in this method using continuous weighting window function w_n. It is given by

$$\mathrm{MMAV2} = \frac{1}{N} \sum_{n=1}^{N} w_n \left| x_n \right| , \tag{4}$$

$$w_n = \begin{cases} 1, & if\ 0.25N \le n \le 0.75N \\ 4n/N, & if\ 0.25N > n \\ 4(n-N)/N, & if\ 0.75N < n \end{cases}.$$

3.1.5 Mean Absolute Value Slope

Mean Absolute Value Slope (MAVSLP) is a modified version of MAV. The differences between the MAVs of adjacent segments are determined. The equation can be defined as

$$\mathrm{MAVSLP_i = MAV_{i+1} - MAV_i}\ . \quad (5)$$

3.1.6 Simple Square Integral

Simple Square Integral (SSI) uses the energy of the sEMG signal as a feature. It can be expressed as

$$\mathrm{SSI} = \sum_{n=1}^{N} \left| x_n \right|^2\ . \quad (6)$$

3.1.7 Variance of EMG

Variance of EMG (VAR) uses the power of the sEMG signal as a feature. Generally, the variance is the mean value of the square of the deviation of that variable. However, mean of EMG signal is close to zero. In consequence, variance of EMG can be calculated by

$$\mathrm{VAR} = \frac{1}{N-1} \sum_{n=1}^{N} x_n^2\ . \quad (7)$$

3.1.8 Root Mean Square

Root Mean Square (RMS) is modeled as amplitude modulated Gaussian random process whose RMS is related to the constant force and non-fatiguing contraction. It relates to standard deviation, which can be expressed as

$$\mathrm{RMS} = \sqrt{\frac{1}{N} \sum_{n=1}^{N} x_n^2}\ . \quad (8)$$

The comparison between RMS and MAV feature is reported in the literatures [3, 18]. Clancy et al. experimentally found that the processing of MAV feature is equal to or better in theory and experiment than RMS processing. Furthermore, the measured index of power property that remained in RMS feature is more advantage than MAV feature.

3.1.9 Waveform Length

Waveform length (WL) is the cumulative length of the waveform over the time segment. WL is related to the waveform amplitude, frequency and time. It is given by

$$WL = \sum_{n=1}^{N-1} \left| x_{n+1} - x_n \right|\ . \quad (9)$$

All of these features above, 3.1.1-3.1.9, are computed based on sEMG signal amplitude. From the experimental results, the pattern of these features is similar. Hence, we selected the robust feature representing for the other features in this group. The results and discussion is presented in Section 4.1.

3.1.10 Zero Crossing

Zero crossing (ZC) is the number of times that the amplitude value of sEMG signal crosses the zero y-axis. In EMG feature, the threshold condition is used to abstain from the background noise. This feature provides an approximate estimation of frequency domain properties. It can be formulated as

$$\mathrm{ZC} = \sum_{n=1}^{N-1} \left[\mathrm{sgn}\left(x_n \times x_{n+1} \right) \cap \left| x_n - x_{n+1} \right| \ge threshold \right];$$
$$\mathrm{sgn}(x) = \begin{cases} 1, & if\ x \ge threshold \\ 0, & otherwise \end{cases}. \quad (10)$$

3.1.11 Slope Sign Change

Slope Sign Change (SSC) is similar to ZC. It is another method to represent the frequency information of sEMG signal. The number of changes between positive and negative slope among three consecutive segments are performed with the threshold function for avoiding the interference in sEMG signal. The calculation is defined as

$$\mathrm{SSC} = \sum_{n=2}^{N-1} \left[f\left[\left(x_n - x_{n-1} \right) \times \left(x_n - x_{n+1} \right) \right] \right];$$
$$f(x) = \begin{cases} 1, & if\ x \ge threshold \\ 0, & otherwise \end{cases}. \quad (11)$$

3.1.12 Willison Amplitude

Willison amplitude (WAMP) is the number of times that the difference between sEMG signal amplitude among two adjacent segments that exceeds a predefined threshold to reduce noise effects same as ZC and SSC. The definition is as

$$\mathrm{WAMP} = \sum_{n=1}^{N-1} f\left(\left| x_n - x_{n+1} \right| \right);$$
$$f(x) = \begin{cases} 1, & if\ x \ge threshold \\ 0, & otherwise \end{cases}. \quad (12)$$

WAMP is related to the firing of motor unit action potentials (MUAP) and the muscle contraction level.

The suitable value of threshold parameter of features in ZC, SSC, and WAMP is normally chosen between 10 and 100 mV that is dependent on the setting of gain value of instrument. Nevertheless, the optimal threshold that suitable for robustness in sEMG signal analysis is evaluated and discussed in Section 4.1.

3.1.13 Histogram of EMG

Histogram of EMG (HEMG) divides the elements in sEMG signal into b equally spaced segments and returns the number of elements in each segment. HEMG is an extension version of the ZC and WAMP features. The effect of various segments is tested and expressed in Section 4.1.

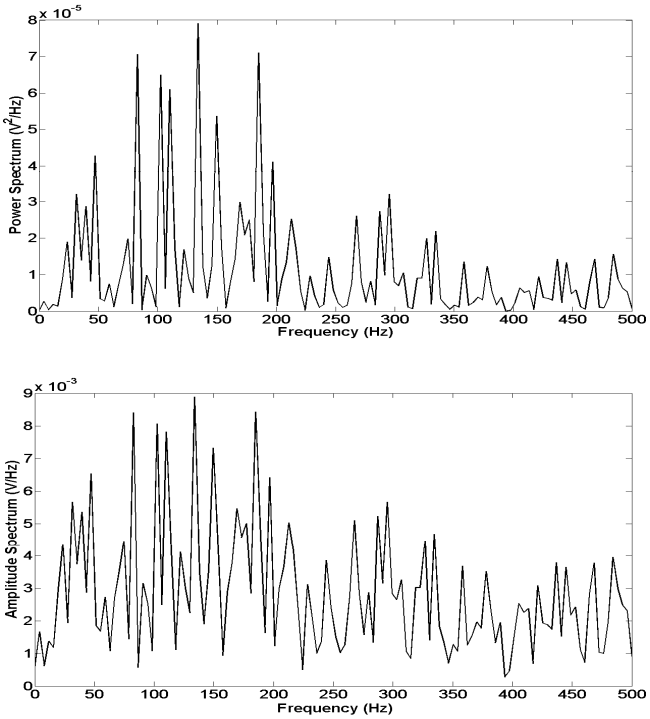

Fig. 4. Power spectrum (×10^{-5}) (top) and amplitude spectrum (×10^{-3}) (bottom) of noisy sEMG signal at 20 dB *SNR* in hand close motion.

3.2 Frequency Domain Feature Extraction

3.2.1 Autoregressive Coefficients

Autoregressive (AR) model described each sample of sEMG signal as a linear combination of previous samples plus a white noise error term. AR coefficients are used as features in EMG pattern recognition. The model is basically of the following form:

$$x_n = -\sum_{i=1}^{p} a_i x_{n-i} + w_n \,, \tag{13}$$

where x_n is a sample of the model signal, a_i is AR coefficients, w_n is white noise or error sequence, and p is the order of AR model.

The forth order AR was suggested from the previous research [19]. However, the orders of AR between the first order and the tenth order are found. The results are discussed in Section 4.1.

3.2.2 Modifed Median Frequency

Modified Median Frequency (MMDF) is the frequency at which the spectrum is divided into two regions with equal amplitude. It can be expressed as

$$\sum_{j=1}^{\text{MMDF}} A_j = \sum_{j=\text{MMDF}}^{M} A_j = \frac{1}{2}\sum_{j=1}^{M} A_j \,, \tag{14}$$

where A_j is the sEMG amplitude spectrum at frequency bin j.

3.2.3 Modifed Mean Frequency

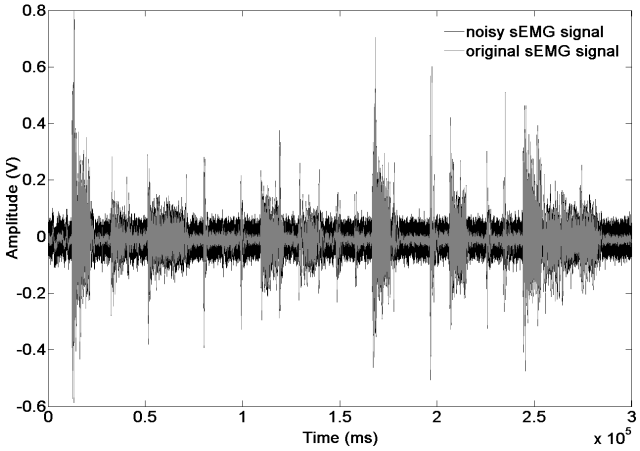

Fig. 5. Original sEMG (gray line) signal and noisy sEMG signal at 5 dB *SNR* (black line) in six upper limb motions.

Modified Mean Frequency (MMNF) is the average frequency. MMNF is calculated as the sum of the product of the amplitude spectrum and the frequency, divided by the total sum of spectrum intensity, as in

$$\text{MMNF} = \sum_{j=1}^{M} f_j A_j \Big/ \sum_{j=1}^{M} A_j \,, \tag{15}$$

where f_j is the frequency of spectrum at frequency bin j.

3.2.4-3.2.5 Mean Frequency and Median Frequency

Traditional median frequency (MDF) and traditional mean frequency (MNF) are calculated based on power spectrum. We can calculate using the sEMG power spectrum Pj instead of amplitude spectrum A_j. They can be expressed as

$$\sum_{j=1}^{\text{MDF}} P_j = \sum_{j=\text{MDF}}^{M} P_j = \frac{1}{2}\sum_{j=1}^{M} P_j \,, \tag{16}$$

$$\text{MNF} = \sum_{j=1}^{M} f_j P_j \Big/ \sum_{j=1}^{M} P_j \,. \tag{17}$$

The outline of amplitude spectrum and power spectrum is similar but the amplitude value of amplitude spectrum is larger than amplitude value of power spectrum as shown in Fig. 4. Moreover, the variation of amplitude spectrum is less than the power spectrum. For that reason, variation of MMNF and MMDF is also less than traditional MNF and MDF.

3.3 Evaluation methods

The percentage error (*PE*) is used to evaluate the quality of the robust of WGN of EMG features, as in

$$PE = \left| \frac{feature_{clean} - feature_{noise}}{feature_{clean}} \right| \times 100\% \,, \tag{18}$$

where $feature_{clean}$ denotes the feature vector of the original sEMG signal and $feature_{noise}$ represents the feature vector of the noisy sEMG signal. WGN at different level is added

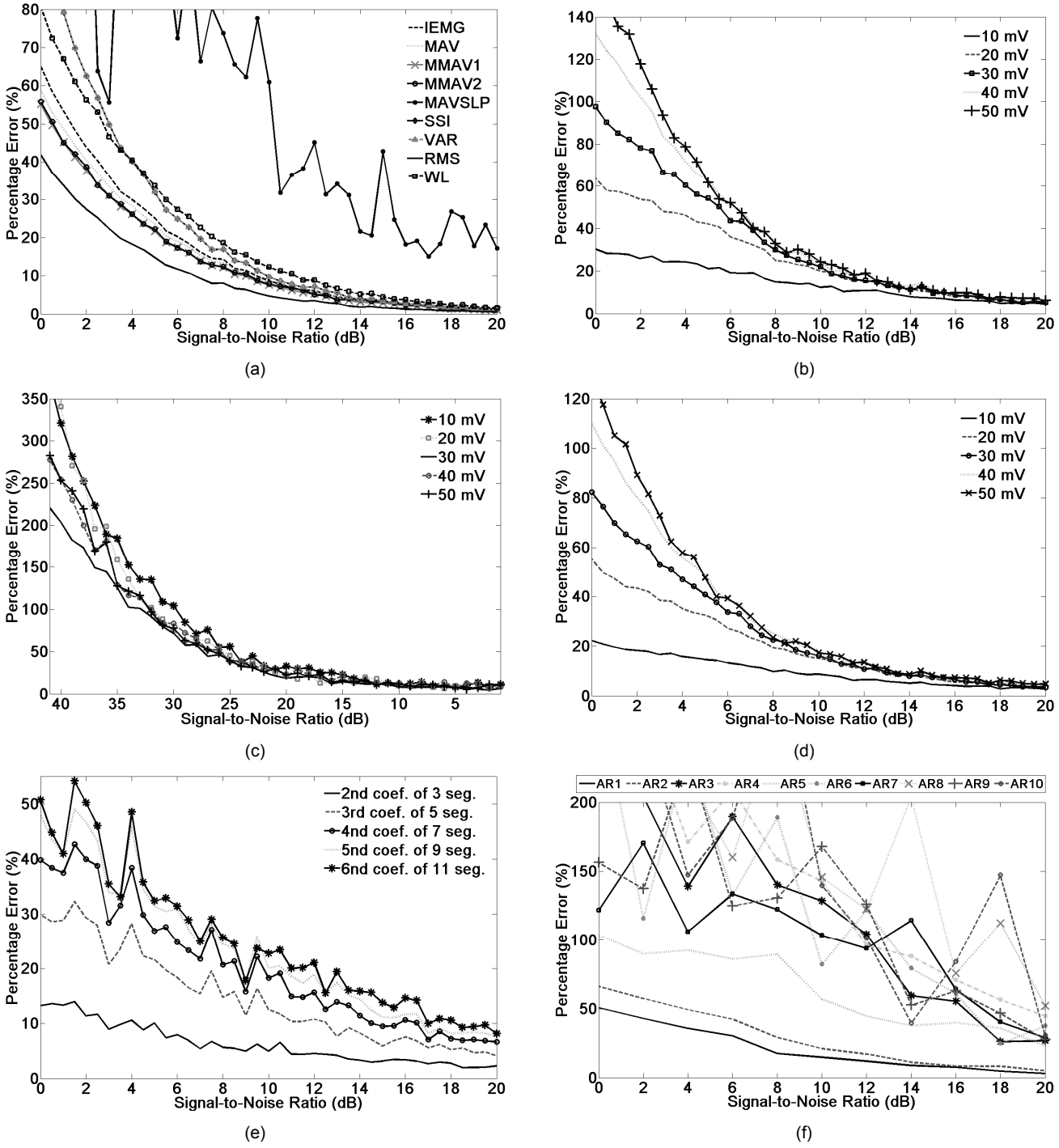

Fig. 6. Average *PE* of sEMG signals of (a) features in time domain based on signal amplitude, 3.1.1-3.1.9 (b) ZC with various threshold value (10-50 mV) (c) SSC with various threshold value (10-50 mV) (d) WAMP with various threshold value (10-50 mV) (e) HEMG with various segment parameters (3, 5, 7, 9, 11 segments) (f) AR coefficients with various orders (1-10) at various signal-to-noise ratios (20-0 dB) in four motions.

to the original sEMG signal.

The performance of the methods is the best when *PE* is the smallest value. We calculated average *PE* for each motion with ten repeated datasets. Therefore, there are 80 datasets with four motions and two channels for each feature and noise level was varied from 20 to 0 dB *SNR* for each dataset. Moreover, WGN was added 10 times in each noise level to confirm the results. *SNR* is calculated by

$$SNR = 10\log\frac{P_{clean}}{P_{noise}}, \tag{19}$$

where P_{clean} is power of the original sEMG signal and P_{noise} is power of WGN.

The classification rate (*CR*) is used to evaluate the quality of the recognition system with the noisy environment of sEMG signal. The performance of the methods is the

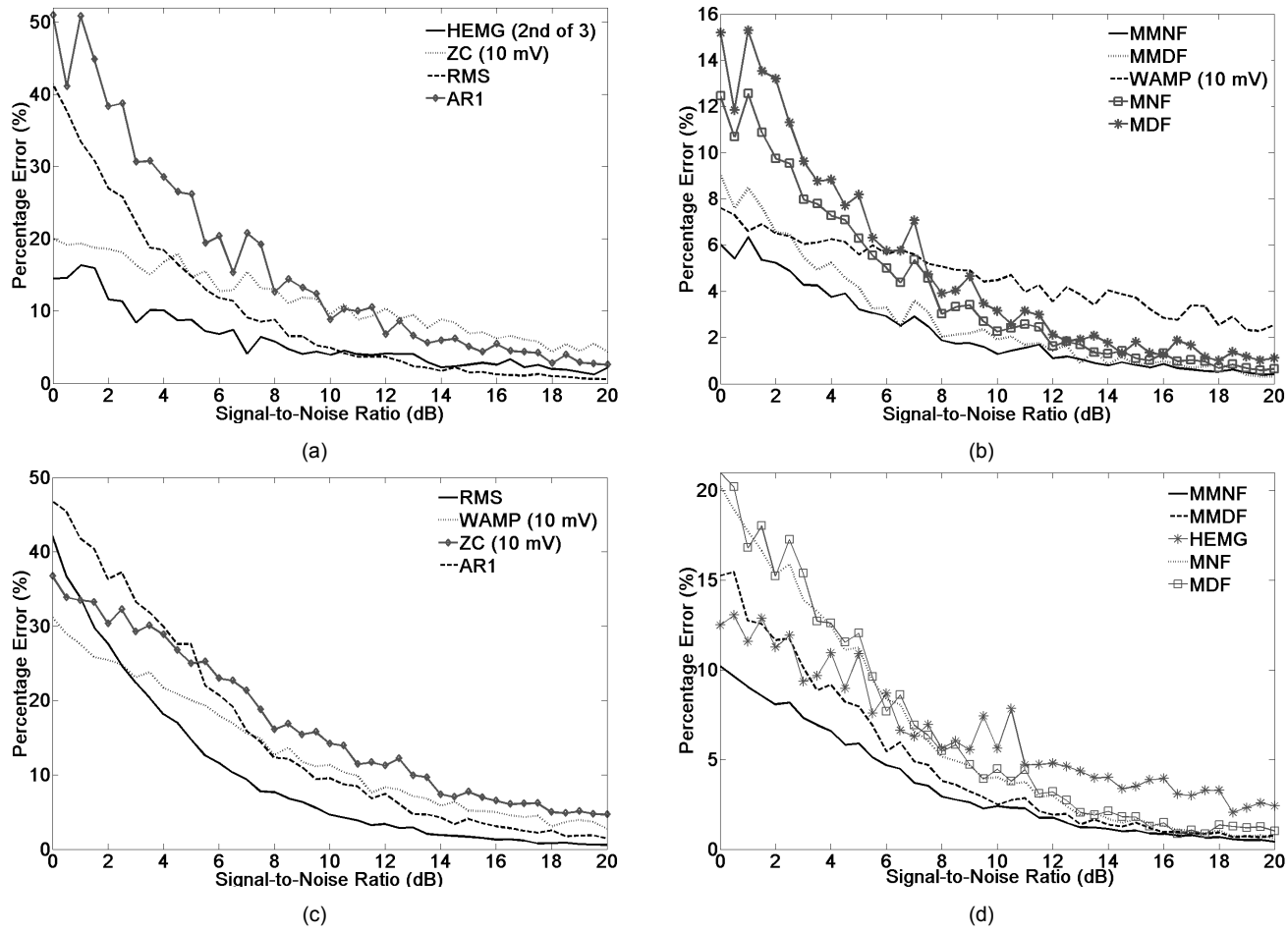

Fig. 7. (a-b) Average *PE* of strong sEMG signals of nine selected features at various signal-to-noise ratios (20-0 dB *SNR*s) in four motions. (c-d) Average *PE* of weak sEMG signals of nine selected features at various signal-to-noise ratios (20-0 dB *SNR*s) in four motions.

best when the *CR* values still have the same value with the noisy sEMG signals. Original sEMG signal and noisy sEMG signal were sent to hand movement recognition. In this study, we evaluated the performance of robust features in pattern recognition view point with Myoelectric Control development (MEC) toolbox [17]. The window size is 256 ms and window slide is 64 ms for the real-time constraint that the response time should be less than 300 ms. The feature vector of selected robust features was evaluated by linear discriminant anslysis classifier (LDA) and majority vote (MV) post-processing was performed in this study. In summary, the robust features should have the small value of *PE* and still have maximum classification accuracy.

4 Results and Discussion

4.1 The Quality of the Robustness of EMG Features with WGN

To test the robustness of sixteen traditional features and two novel features, we measured the *PE* with sEMG signal with additive WGN. The results of *PE* are plotted for *SNR*s from 20 dB to 0 dB, as shown in Fig. 6-7, in practice; we can select feature extraction to be suitable for each application depend on the level of interference of sEMG system. For the easy way to describe the results of a large number of features, we discussed and evaluated the features that have the same pattern in recognition and evaluated some parameter of each feature in Fig. 6. As a result, only nine representatives are discussed as the results shown in Fig. 7.

In Fig. 6 (a), the *PE* of time domain features computed using sEMG signal amplitude demonstrates that RMS results in powerful performance in robust noise tolerance than the other features. Hence, RMS feature is used to represent the features in this group. Fig. 6 (b-d) present the evaluation of suitable value of threshold. Threshold value was chosen between 10 and 50 mV. The optimal threshold is 10 mV for ZC and WAMP but the suitable threshold of SSC is 30 mV. However, the minimum PE of SSC is higher than ZC and WAMP. ZC and WAMP with 10 mV threshold value are selected for the representative features of this group. Afterward, the second bin of the third segment HEMG was adopted from the result in Fig. 6 (e) and the first-order of AR is chosen because the PE of the other AR orders are much bigger than the first one as shown in Fig. 6 (f).

Therefore, we evaluated the performance of robustness of nine representative features namely RMS, ZC and WAMP with 10 mV threshold, HEMG with 2nd bin, AR order 1, MNF, MDF, MMNF, and MMDF. Two types of

TABLE 1
CLASSIFICATION RATE (%) OF 7 EMG FEATURES USING LEAVE-ONE-OUT VALIDATION

Method	Level of SNR noise			
	Clean	20 dB	15 dB	10 dB
HEMG	60.7835	49.1590	41.7926	34.6817
WL	79.3059	34.1707	14.4347	12.5186
WAMP	86.6298	92.2504	47.0087	21.6095
MMNF	41.1326	36.3636	32.6804	17.1386
MAV,WL, ZC,SSC	95.6781	67.4260	22.5676	7.9838
RMS,AR2	96.4871	89.8872	64.8712	25.2714
HEMG,WAMP,MMNF	93.0807	96.1891	64.0622	28.1243

sEMG signal, strong signals and weak signals, are used to evaluate the robust of nine features. The weak sEMG signal has the effect of interference more than the strong sEMG signal. In practice, we can select the robust features to be suitable for each application. Fig. 7 (a) and Fig. 7 (b) show the average *PE* of strong sEMG. For strong sEMG signals and low noise, *SNR* more than 10 dB, MMNF has the smallest average *PE*, followed closely by the MMDF, MNF, and MND. For *SNR* less than 10 dB that showed high noise, the *PE* of MNF and MDF rapidly increased and *SNR* less than 3 dB that showed very high noise, WAMP has the average *PE* close to MMNF. The average error of MMNF in strong sEMG with very high noise, 0 dB *SNR*, is only 6%. Moreover in wrist extension and hand open from extensor carpi radialis longus, it is only 3.5%. HEMG and ZC have slightly larger error compared to the first group in Fig. 7 (b). The *PE* of RMS and AR1 are large that they were expected to perform poorly.

The average *PE* of weak sEMG signals shown in Fig. 7 (c-d) clearly demonstrate that MMNF is the best robustness feature and closed by MMDF and HEMG, whereas the error of other features is more than 20%. In very high noise, 0 dB *SNR*, it provides average *PE* about 10% and the *PE* of wrist extension from flexor carpi radialis is only 5%. Other feature results are similar to the results of strong sEMG signal but the results of *PE* of weak sEMG signal are larger than the *PE* of strong sEMG signal. The results above show that MMNF was the best feature comparing with others in four motions. In summary, MMDF and WAMP can be used with HEMG for multi-feature. Hence, it is compared the classification results in noisy environment with other successful individual feature and multi-feature sets from the literatures [5, 14-15, 20] in Section 4.2.

4.2 The Quality of the Recognition System of EMG Features with the Noisy Environment

Four individual features and three multi-feature sets are examined in this study. The classification results of seven representative features are reported in Table 1. Leave-one-out validation was used to guarantee an exact performance measure for this dataset. The first single robust

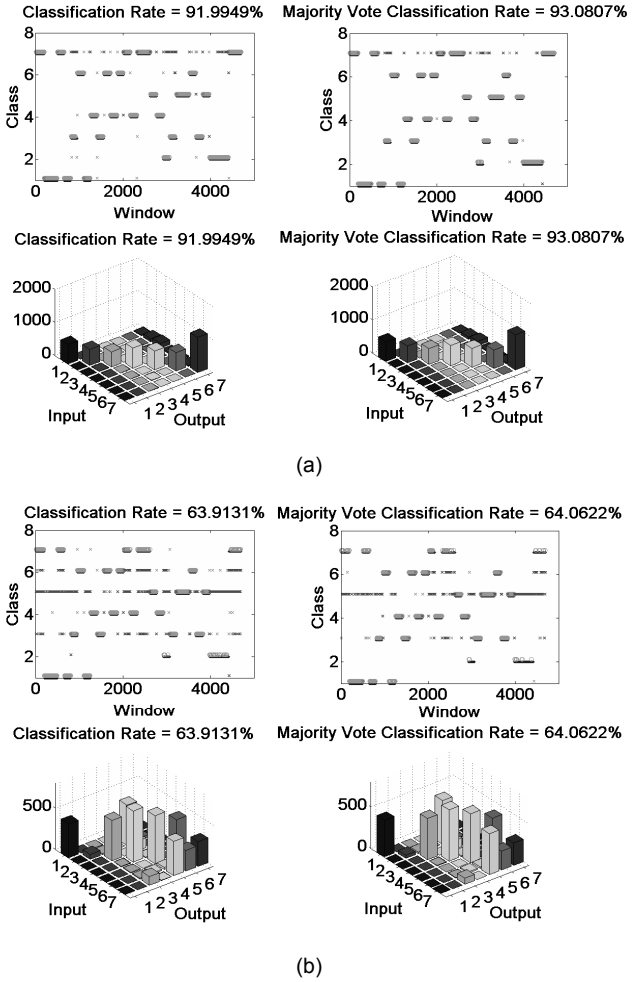

Fig. 8. Plot of the classification results as a function of time (Top) and plot of confusion matrix (Below) of our multi-feature set with (a) original sEMG signal. (b) noisy sEMG signal, 15 dB *SNR*.

feature is HEMG that suggested by Zardoshti-Kermani et al. [5] and is comfirmed with our result in Section 4.1. The second feature, WL is recommended by Oskoei and H. Hu [15] that it is the best single feature in their experiment. Lastly, two individual features, WAMP and MMNF, are aprroved by our previous experiment [14] and the experimental results in this paper. The recognition results of single feature did not perform well but it is commonly used in EMG recognition system. The *CR* of WAMP in clean and low noisy environment is good but its *CR* is rapidly decreased in high noise. The *CR* of HEMG is still stability even if noise increases. In addition, no surprising that the CR of WL in noisy environment is poor that comfired by the result in Section 4.1 and the CR of MMNF is poor because of the limitation of their ability to discriminate between classes. However, in practice, we are usually combined this feature with other features to get the useful information features. Because of only one feature per channel of feature that provided from features in time domain and frequency domain, it is effective and small enough to combine with other features for a more powerful feature vector and avoiding additional significant computational burden.

Therefore, the multi-features are the excellent way to provide the powerful performance in recognition system. The combination of robust features namely, MMNF, WAMP, and HEMG is compared with two successful and popular multi-features that was used by Hudgins et al. [20], MAV, WL, ZC and SSC, and was recommended by Oskoei and H. Hu [15] , conists of RMS and AR2. From the experiment in Table 1, our robust multi-features group provides more excellent discriminatory power for a classifier than Hudgins's and Oskoei's multi-features group in noisy environment. Moreover, the observation from the classification results as a function of time and plot of confusion matrix of our multi-feature set with orginal sEMG signal and noisy sEMG signal are shown in Fig. 8.

5 Conclusion

The objectives of this study were to present a novel feature that tolerate with white Gaussian noise. Sixteen traditional features and two novel features in time domain and frequency domain were tested. Results showed that a modified mean frequency (MMNF) is the best feature comparing with others in the quality of the robustness of EMG features with WGN point of view. MMNF has average error only 6% in strong sEMG signals and 10% in weak sEMG signal at *SNR* value of 0 dB and MMNF has average error only 0.4% in both strong and weak sEMG signals at *SNR* value of 20 dB. In addition, MMNF and other robust features (WAMP and HEMG) are used as an input to the EMG pattern recognition. The experiment shows that these features are the excellent candidates for a multi-source feature vector. From the above experiment results, it is shown that MMNF can be used as feature in augmenting the other features for a more powerful robust feature vector. Future work is recommended to combine the new multi-feature sets with MMNF to be tested in other classifer types.

Acknowledgment

This work was supported in part by the Thailand Research Fund through the Royal Golden Jubilee Ph.D. Program (Grant No. PHD/0110/2550), and in part by NEC-TEC-PSU center of excellence for rehabilitation engineering and Faculty of Engineering, Prince of Songkla University. The authors would like to acknowledge the support of Dr. A.D.C. Chan, from the Carleton University for providing the datasets.

References

[1] M. A. Oskoei and H. Hu, "Myoelectric Control Systems-A Survey," *Biomedical Signal Processing and Control*, vol. 2, no. 4, pp. 275-294, Oct 2007, doi:10.1016/j.bspc.2007.07.009.

[2] P. Parker, K. Englehart, and B. Hudgins, "Myoelectric Signal Processing for Control of Powered Limb Prostheses," *Journal of Electromyography and Kinesiology,* vol. 16, no. 6, pp. 541-548, Dec 2006, doi: 10.1016/j.jelekin.2006.08.006.

[3] E. A. Clancy, E. L. Morin, and R. Merletti, "Sampling, Noise-reduction and Amplitude Estimation Issues in Surface Electromyography," *Journal of Electromyography and Kinesiology,* vol. 12, no. 1, pp. 1-16, Feb 2002, doi:10.1016/S1050-6411(01)00033-5.

[4] M. B. I. Reaz, M. S. Hussain, and F. Mohd-Yasin, "Techniques of EMG Signal Analysis: Detection, Processing, Classification and Applications," *Biological Procedures Online*, vol. 8, no. 1, pp. 11-35, Mar 2006, doi:10.1251/bpo124.

[5] M. Zardoshti-Kermani, B. C. Wheeler, K. Badie, and R. M. Hashemi, "EMG Feature Evaluation for Movement Control of Upper Extremity Prostheses," *IEEE Trans. Rehabilitation Engineering*, vol. 3, no. 4, pp. 324-333, Dec 1995, doi:10.1109/86.481972.

[6] A. Phinyomark, C. Limsakul, and P. Phukpattaranont, "A Comparative Study of Wavelet Denoising for Multifunction Myoelectric Control," *Proc. Int. Conf. Computer and Automation Engineering (ICCAE '09)*, pp. 21-25, Mar. 2009, doi:10.1109/ICCAE.2009.57.

[7] A. Phinyomark, C. Limsakul, and P. Phukpattaranont, "EMG Denoising Estimation Based on Adaptive Wavelet Thresholding for Multifunction Myoelectric Control," *Proc. Conf. Innovative Technologies in Intelligent Systems and Industrial Applications (CITISIA '09)*, pp. 171-176, July 2009, doi:10.1109/CITISIA.2009.5224220.

[8] R. L. Ortolan, R. N. Mori, R. R. Jr. Pereira, C. M. N. Cabral, J. C. Pereira, and A. Jr. Cliquet, "Evaluation of Adaptive/Non-adaptive filtering and Wavelet Transform Techniques for Noise Reduction in EMG Mobile Acquisition Equipment," *IEEE Trans. Neural Systems and Rehabilitation Engineering,* vol. 11, no. 1, pp. 60-69, doi:10.1109/TNSRE.2003.810432.

[9] R. Merletti and P. Parker, *Electromyography Physiology, Engineering, and Noninvasive Applications.* John Wiley Sons, Inc., New York, 2004.

[10] D. -S. Kim, S. -Y. Lee, and R. M. Kil, "Auditory Processing of Speech Signals for Robust Speech Recognition in Real-World Noisy Environments," *IEEE Trans. Speech and Audio Processing*, vol. 7, no. 1, pp. 55-69, Jan 1999, doi:10.1109/89.736331.

[11] Z. Liu and S. Wada, "Robust Feature Extraction Technique for Texture Image Retrieval," *Proc. IEEE Int. Conf. Image Processing (ICIP '05),* pp. I-525-8, Sept. 2005, doi:10.1109/ICIP.2005.1529803.

[12] R. Boostani and M. H. Moradi, "Evaluation of the Forearm EMG Signal Features for the Control of a Prosthetic Hand," *Physiological Measurement,* vol. 24, no. 2, pp. 309-319, May 2003, doi:10.1088/0967-3334/24/2/307.

[13] A. Phinyomark, C. Limsakul, and P. Phukpattaranont, "EMG Feature Extraction for Tolerance of 50 Hz Interference," *Proc. PSU-UNS Int. Conf. Engineering Technologies (ICET '09)*, pp. 289-293, Apr. 2009.

[14] A. Phinyomark, C. Limsakul, and P. Phukpattaranont, "EMG Feature Extraction for Tolerance of white Gaussian noise," *Proc. Int. Work. Symp. Science and Technology (I-SEEC '08)*, pp. 178-183, Dec. 2008.

[15] M. A. Oskoei and H. Hu, "Support Vector Machine-Based Classification Scheme for Myoelectric Control Applied to Upper Limb," *IEEE Trans. Biomedical Engineering*, vol. 55, no. 8, pp. 1956-1965, Aug 2008, doi:10.1109/TBME.2008.919734.

[16] H. –P. Huang and C. –Y. Chen, "Development of a Myoelectric Discrimination System for a Multi-Degree Prosthetic Hand," *Proc. IEEE Int. Conf. Robotics and Automation (ICRA '99)*, pp. 2392-2397, May 1999, doi:10.1109/ROBOT.1999.770463.

[17] A. D. C. Chan and G. C. Green, "Myoelectric Control Development Toolbox," *Proc. thirtyth Conf. Canadian Medical and Biologi-*

cal Engineering Society, 2007.

[18] E. A. Clancy and N. Hogan, "Theoretic and Experimental Comparison of Root-Mean-Square and Mean-Absolute-Value Electromyogram Amplitude Detectors," *Proc. nineteenth Annu. Int. Conf. IEEE Engineering in Medicine and Biology Society (EMBS '97)*, pp. 1267-1270, vol. 3, Oct.-Nov. 1997, doi:10.1109/IEMBS.1997.756605.

[19] O. Paiss and G. F. Inbar, "Autoregressive Modeling of Surface EMG and Its Spectrum with Application to Fatigue," *IEEE Trans. Biomedical Engineering*, vol. 34, no. 10, pp. 761-770, Oct 1987, doi:10.1109/TBME.1987.325918.

[20] B. Hudgins, P. Parker, and R. N. Scott, "A New Strategy for Multifunction Myoelectric Control," *IEEE Trans. Biomedical Engineering*, vol. 40, no. 1, pp. 82-94, Jan 1993, doi:10.1109/10.204774.

Angkoon Phinyomark received the B.Eng. degree in computer engineering with first class honors in 2008 from Prince of Songkla University, Songkhla, Thailand, where he is currently working toward the Ph.D. degree in electrical engineering. His research interests are primarily in the area of biomedical signal processing and rehabilitation engineering. He is a student member of the IEEE.

Chusak Limsakul received the B.Eng. degree in electrical engineering from King Mongkut's Institute of Technology Ladkrabang Bangkok, Thailand in 1978 and D.E.A and D. Ing. from Institute National des Sciences Appliquees de Toulouse, France in 1982 and 1985, respectively. He started working as lecturer at the department of electrical engineering at Prince of Songkla University in 1978. He is currently an associate professor of electrical engineering and vice president for research and graduate studies at Princeof Songkla University. His research interests are biomedical signal processing, biomedical instrumentation and neural network.

Pornchai Phukpattaranont was born in Songkla, Thailand. He received the B. Eng. and M. Eng. degrees in electrical engineering from Prince of Songkla University in 1993 and 1997, respectively, the Ph.D. degree in electrical engineering from the University of Minnesota, in 2004. He is currently an assistant professor of electrical engineering at Prince of Songkla University. His research interests are ultrasound contrast imaging, ultrasound signal processing, medical image processing, and biomedical signal processing. Dr.Phukpattaranont is a member of the IEEE.

4.3 ทรัพยากรและเวลาในการคำนวณ

ในแง่มุมของเวลาในการคำนวณ ทางคณะผู้วิจัยได้ ทำการทดลองหาค่าเวลาในการคำนวณของวิธีการวัดลักษณะเด่นของสัญญาณแต่ละวิธี โดยการเขียนโปรแกรมด้วยโปรแกรม MATLAB และทำการใช้งานฟังก์ชั้น Tic และ Toc เพื่อจับเวลาที่ได้จากการคำนวณ โดยกำหนดให้คำนวณสัญญาณไฟฟ้ากล้ามเนื้อจากหนึ่งช่องสัญญาณ มีขนาดของจำนวนข้อมูล 256 จุดข้อมูล (เวลาในการคำนวณไม่ควรเกิน 300 มิลลิวินาที ในกรณีต้องการให้ทำงานแบบทันเวลาในอุปกรณ์ที่ใช้การควบคุมด้วยสัญญาณไฟฟ้ากล้ามเนื้อ [6]) ทั้งนี้เวลาในการประมวลผลขึ้นกับการใช้งานของเครื่องคอมพิวเตอร์ด้วย จึงกำหนดให้ไม่มีการใช้งานของโปรแกรมอื่นใดนอกจากโปรแกรม MATLAB และค่าที่ได้มากจากการเฉลี่ยของการหาเวลาการคำนวณ 100 ครั้ง โดยรายละเอียดของเครื่องที่นำมาใช้ในการทดลอง คือ เครื่องคอมพิวเตอร์ตั้งโต๊ะ ระบบปฏิบัติการวินโดว์ 7 หน่วยประมวลผล (CPU) Intel Core i5 750 2.67GHz หน่วยความจำชั่วคราว (RAM) ขนาดความจุ 4 GB โดยผลของเวลาแสดงได้ดังตารางที่ 1

ตารางที่ 1 เวลาในการคำนวณของวิธีการวัดลักษณะเด่นของสัญญาณ 16 วิธี

วิธีการวัดลักษณะเด่นของสัญญาณ	เวลาในการคำนวณ (วินาที)
1.Integrated EMG (IEMG)	8.1061×10^{-5}
2.Mean Absolute Value (MAV)	8.2789×10^{-5}
3.Modified Mean Absolute Value 1 (MAV1)	8.3020×10^{-5}
4.Modified Mean Absolute Value 2 (MAV2)	8.4786×10^{-5}
5.Mean Absolute Value Slope (MAVS)	10.0950×10^{-5}
6.Simple Square Integral (SSI)	8.1829×10^{-5}
7.Variance (VAR)	8.2405×10^{-5}
8.Root Mean Square (RMS)	9.1045×10^{-5}
9.Waveform length (WL)	8.2213×10^{-5}
10.Zero crossing (ZC)	9.8495×10^{-5}
11.Slope Sign Change (SSC)	9.3196×10^{-5}
12.Willison amplitude (WAMP)	9.3157×10^{-5}
13.Auto-regressive (AR) coefficients	57.4190×10^{-5}
14.Median Frequency (MDF)	45.1960×10^{-5}
15.Mean Frequency (MNF)	20.7430×10^{-5}

16.Histogram of EMG (HIST)	31.6030×10^{-5}

พบว่าวิธีการวัดลักษณะเด่นของสัญญาณ แบบ Integrated EMG ใช้เวลาในการคำนวณน้อยที่สุด แต่ถึงอย่างไรก็ตามเวลาในการคำนวณของวิธีการวัดลักษณะเด่นของสัญญาณในแกนเวลาวิธีอื่นๆ ก็ใช้เวลาไม่ต่างกันมา กนักโดยต่างกันในระดับ 10^{-5} วินาที ซึ่งถือว่าน้อยมาก ต่างจากวิธีการวัดลักษณะเด่นของสัญญาณบนแกนความถี่ ซึ่งใช้เวลาในการคำนวณสูงกว่าวิธีการวัดลักษณะเด่นของสัญญาณบนแกนเวลาเป็น 10 เท่า แต่ถึงอย่างไรก็ตามวิธีการวัดลักษณะเด่นของสัญญาณบนแกนเวลา ซึ่งสามารถคำนวณได้ทันเวลานั้นจะไม่สามารถเข้าถึงคุณลักษณะ Non-stationary ของสัญญาณได้ แต่วิธีการวัดลักษณะเด่นของสัญญาณแบบทั้งแกนเวลาและความถี่จะสามารถเข้าถึง Non-stationary ของสัญญาณได้ แต่ก็พบว่าจะใช้เวลาในการคำนวณสูงกว่าหลายร้อยเท่า [7] ดังนั้นทางคณะผู้วิจัยจึงได้เลือกทำการศึกษาวิธีการวัดลักษณะเด่นของสัญญาณชนิดใหม่เพิ่มเติม คือ วิธี Detrended Fluctuation Analysis (DFA) ซึ่งเป็นวิธีที่สามารถเข้าถึงความเป็น Non-stationary ของสัญญาณได้เหมือนกับวิธีการวัดลักษณะเด่นของสัญญาณบนแกนเวลาและความถี่ แต่ใช้เวลาในการคำนวณ และความซับซ้อนที่น้อยกว่าวิธีบนแกนเวลาและความถี่มาก และใช้เวลาในการคำนวณสูงกว่าวิธีบนแกนเวลา และวิธีบนแกนความถี่เพียงเล็กน้อย นอกจากนี้วิธี DFA ยังคงให้ความแม่นยำในการระบุท่าทาง และความสามารถในการทนต่อสัญญาณรบกวนที่ดีด้วย

บทความที่ 5 เรื่อง Detrended Fluctuation Analysis of Electromyography Signal to Identify Hand Movement

บทความที่ 6 เรื่อง Effect of Trends on Detrended Fluctuation Analysis for Surface Electromyography (EMG) Signal

DETRENDED FLUCTUATION ANALYSIS OF ELECTROMYOGRAPHY SIGNAL TO IDENTIFY HAND MOVEMENT

A. Phinyomark[1*], M. Phothisonothai[2], C. Limsakul[1], P. Phukpattaranont[1]
[1]Department of Electrical Engineering, Prince of Songkla University, Thailand
[2]Department of Electrical Engineering, Burapha University, Thailand
*Corresponding author: angkoon.p@hotmail.com

ABSTRACT

Recent advances in nonlinear analysis techniques are essential to understand the complexity of surface Electromyography (sEMG) signal. This research examines the use of Detrended Fluctuation Analysis (DFA), a novel parameter, to study the properties of sEMG signal and to use these properties to identify the hand movements. The experimental results of mean and standard deviation show that the scaling exponents of DFA in various hand motions have the significant difference values and small experimental variation. Cluster-to-cluster distance and scatter plot between scaling exponents of hand movements were demonstrated that DFA is suitable for sEMG feature extraction to characterize the sEMG signal. The application of this parameter is use to feature extraction for multifunction myoelectric control.

1. INTRODUCTION

Surface Electromyography (sEMG) signal is one of physiological signal that is very complex, nonlinear, non-stationary, and non-periodic [1]. This is due to the fact that the use of sEMG signal is very easy, fast and convenient, it is currently becoming increasingly a powerful indication to get important information and to diagnose about the muscular and nervous systems. Use of sEMG signal for the measurement of force from hand motions is a powerful indication to apply in rehabilitation system and the control of prosthetic devices. Lots of methods are used to model and analyze sEMG signal that call feature extraction [2]. Time domain feature is first group that is used to describe the characteristics of the sEMG signal. Two well-known time domain features are mean absolute value (MAV) and root mean square (RMS). MAV and RMS are widely used for multifunction myoelectric control. However, time domain features were successful to some limit because these methods assume that sEMG signal is stationary, while the sEMG signal is non-stationary. Thus changing the researcher's trend toward the use of information contained in frequency domain. Mean frequency and median frequency are two characteristic variables in power spectral density that a major role in frequency domain. Later, time-frequency features such as short time Fourier transform, wavelet transform, and wavelet packet transform, were used. Furthermore, all of these features that introduce above are calculated based on linear or statistical analysis.

Recent advances in nonlinear analysis techniques are essential to understand the complexity of biomedical signal [3-4]. They are very useful methods in a range of muscular applications. Nonlinear analysis techniques may be estimated by using entropy, correlation, and fractal dimension. Some methods have been reported for characterization of sEMG signal such as correlation time, Lempel-Ziv complexity, sample entropy, approximate entropy, Lyapunov exponent, and fractal dimension [5-7]. Detrended fluctuation analysis (DFA) is invented by Peng et al. [8]; it has been established as an important tool for detecting long-range correlations in noisy signal. DFA is a method for the determination of fractal scaling exponent and very useful for analyzing non-stationary time series. The DFA method has been successfully applied to various fields such as DNA sequences, cardiac dynamics, human gait, longtime weather records, economics time series, and especially complex medical signals such as EEG (Electroencephalogram) and ECG (Electrocardiogram) signals [3-4, 9]. However, DFA has never been used in the analysis of sEMG signal. Therefore, DFA maybe is a useful tool to characterize the self-similarity of sEMG signal. This paper presents the use of DFA to study the nonlinear properties of sEMG signal and to use these properties to identify hand movements. As a result, this parameter can be used to feature extraction for multifunction myoelectric control.

2. EXPERIMENTS AND DATA ACQUISITION

In this section, we describe our experimental procedure for recording sEMG signal. The sEMG signals were recorded from flexor carpi radialis (channel 1) and extensor carpi radialis longus (channel 2) of a healthy male by two pairs of surface electrodes (3M red dot 2.5 cm. foam solid gel). Each electrode was separated from the other by 20 mm. The frequency range of EMG is within 0-500 Hz, but the dominant energy is concentrated in the range of 10–150 Hz. A band-pass filter of 10-500 Hz bandwidth and an amplifier with 60 dB gain were used. Sampling rate was set at 1000 samples per second using a 16 bit A/D converter board (IN BNC-2110, National Instruments Corporation).

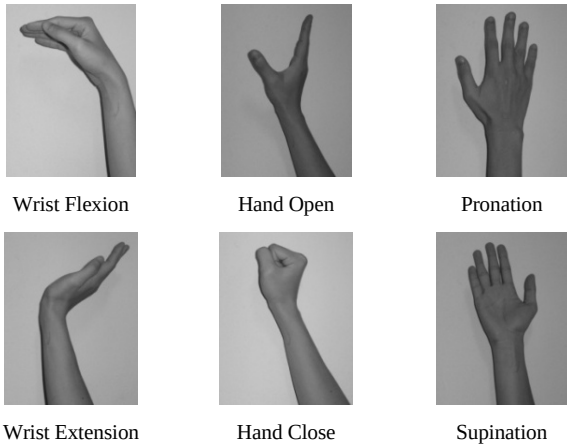

Figure 1. Estimated six hand motions.

A volunteer performed six upper limb motions including hand open (ho), hand close (hc), wrist extension (we), wrist flexion (wf), forearm pronation (fp), and forearm supination (fs) as shown in Fig. 1. Ten datasets were collected for each motion. The sample size of the sEMG signals in this research is 256 ms for the real-time constraint of robot arm control or prosthetic device that the response time should be less than 300 ms.

3. METHODOLOGY

Detrended Fluctuation Analysis (DFA) is a modified root mean square analysis of a random walk to analyze physiological signal. We used the scaling exponent from DFA algorithm to indentify the sEMG signal from hand movement. The scaling exponent of DFA is related with Hurst exponent and fractal dimension. We can convert this exponent to fractal parameters. However, they have the linear relationship. In this study, we considered only the scaling exponent of DFA.

3.1. Detrended Fluctuation Analysis

To exemplify the DFA algorithm, we use the sEMG time series as shown in Fig. 2(a) that be denoted by *{x(t)}*, where *t* is discrete time ranging from 1 to *N* (*N* = 256). The procedure of DFA follows six steps described below.

1) The sEMG time series is first integrated. This integration process converts sEMG signals into a random walk. The integrated series is

$$y(k) = \sum_{t=1}^{k} \left[\{x(t)\} - \overline{x(t)} \right], k = 1, ..., N \ , \qquad (1)$$

where $\overline{x(t)}$ represents the average value of *x(t)*. *y(k)* is called cumulative sum or profile. The example is shown in Fig. 2(b).

2) The integrated series are divided into *L* equal windows or box sizes as shown in Fig. 2(b). In each window has *n* time points, where *n* = integer (*N*/*L*).

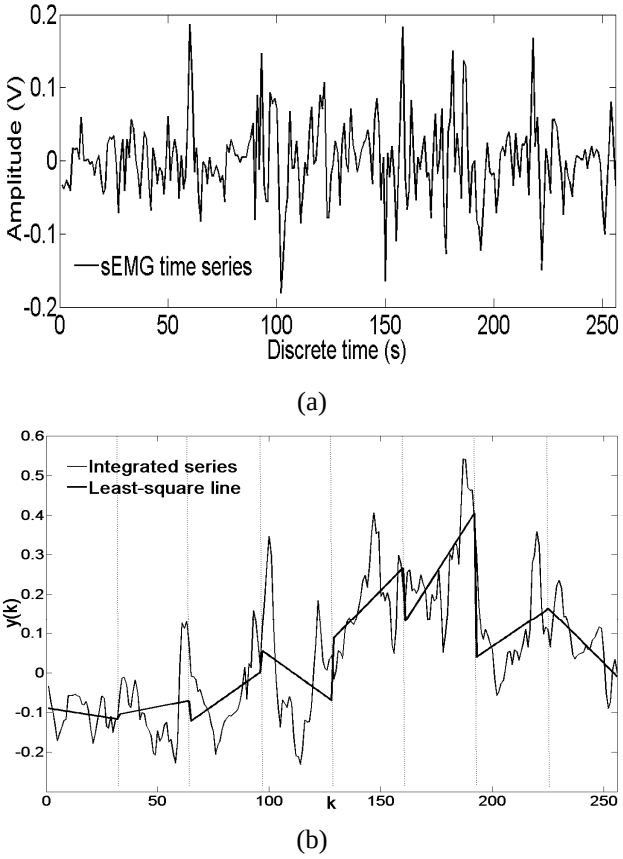

Figure 2. Example of calculate the DFA algorithm of sEMG signal. (a) sEMG time series (b) Integrated series, vertical dotted lines represent window sizes, and solid straight lines represent least-square line.

In this study, we have two experiments or options about window sizes or box sizes.

1. From the experiments of [10], the maximum window should be one-tenth of the signal length (*N*). The window sizes are ranged between 3 and 25 points in this study.
2. In practices [11], the minimum length is around 10, and the maximum is a half length of the signal length (*N*), giving two adjacent intervals. The window sizes are ranged between 8 and 128 points in this study.

Table 1. Options of window sizes.

Option		Window sizes
1	1	Start: 2 Increment: 2 End: 24
	2	Start: 4 Increment: 4 End: 24
	3	Start: 6 Increment: 6 End: 24
	4	Start: 8 Increment: 8 End: 24
2	1	2 ^ k , k = 3, …, 7
	2	2 ^ k , k = 4, …, 7
	3	Start: 8 Increment: 8 End: 128
	4	Start: 16 Increment: 16 End: 128

3) Within each window of length *n*, a least-square is fit to the integrated series ($\{y(k)\}$) as shown in Fig. 2(b). The coefficient of y coordinate is denoted by $y_n(k)$. The least-square line is shown the semi-local trend in that window.
4) The RMS fluctuation of integrated series and detrended time series is calculated by

$$F(n)=\sqrt{\frac{1}{N}\sum_{k=1}^{N}\left[y(k)-y_n(k)\right]^2}\ . \qquad (2)$$

The results are *F(n)* at the window size *n* and window size *n*.
5) The computation is repeated over all window sizes, as define in 2nd step. As a result, the linear relationship between *F(n)* and *n* is plotted in log-log graph.
6) The slope of the line between log *F(n)* and log *n* can be characterized the fluctuation as shown in Fig. 3. This slope is called scaling exponent α. In this study, we used a natural logarithm.

The scaling exponent can be explaining the behavior of time series as:

1) $0<\alpha<1/2$ indicates anti-correlated.
2) $\alpha\cong 1/2$ indicates uncorrelated or white noise.
3) $1/2<\alpha<1$ indicates correlated.
4) $\alpha\cong 1$ indicates 1/f-noise or pink noise.
5) $1<\alpha<3/2$ indicates non-stationary or random walk.
6) $\alpha\cong 3/2$ indicates Brownian noise.

3.2. Evaluation

For multifunction myoelectric control, the selection of feature extraction is a significant stage to achieve optimal performance in classification. In [2] the quality of EMG feature extraction is evaluated by three properties: class separability, robustness, and complexity. In this study, we demonstrate a novel feature, DFA, to identify the hand movement in class separability point view. A high quality of class separability is the maximum class separability or misclassification rate, and small variation in subject experiment. For the class separability, we calculated the mean value of scaling exponent of DFA, ten trials, in each motions and channels. We can observe the different values between six motions and two channels for feature space. The standard deviation of mean (SDM) value is the one way to demonstrate the class separability. When the SDM value is large, it means the maximum class separability. In addition, the scatter plot graph is plotted to observe the pattern of different motions. In this study, we plotted scatter between two features, DFA's scaling exponent and RMS (Root mean square), popular feature.

The other way to indicate class separability is cluster-to-cluster distance. It is distance between mean features of different motions. The performance of classification is

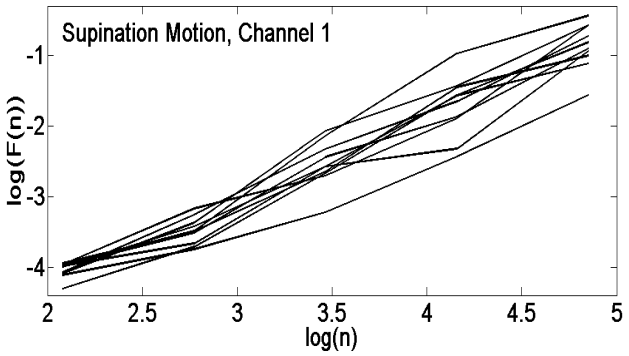

(a)

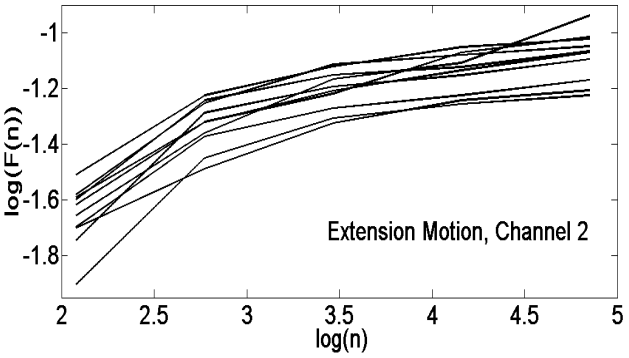

(b)

Figure 3. Plot of log *F(n)* and log *n* for sEMG time series from (a) supination motion and flexor carpi radialis. (b) extension motion and extensor carpi radialis longus. The plots are from a subject with 10 repeated.

the best when the distance is large. The cluster-to-cluster distance (d_{ij}) can be calculated by

$$d_{ij}=\left\|mean_i-mean_j\right\|, \qquad (3)$$

where $mean_i$ ($mean_i$) is the average of DFA's scaling exponent of motion *i* (*j*); *i* and *j* is one of six hand movements and one of two channels.

The second condition, the variation in subject experiment is measured by the standard deviation (SD). In each trial of the same movement, the value of DFA's scaling exponent should have the same value; it means that the variation should be small. The SD of each motions and channels are presented and the mean of all SD (MSD) is shown. The other indication is the observation of the range of the top and bottom of box in box plot graph.

4. RESULTS AND DISCUSSION

The scaling exponents of DFA are calculated from the slope of the line between log *F(n)* and log *n*. The example of the double log plots are shown in Fig. 3. In Fig. 3(a), the double log plot of window size option 2.1 of supination motion and channel 1 is the maximum DFA's scaling exponent. The minimum DFA's scaling exponent is shown in Fig. 3(b) by the double log plot of window size option 2.1 of extension motion and channel 2. From -

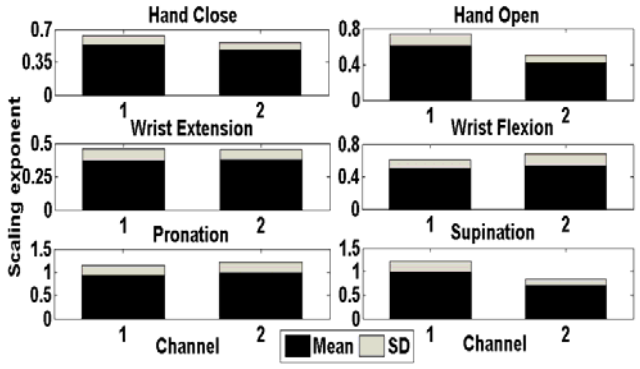

(a)

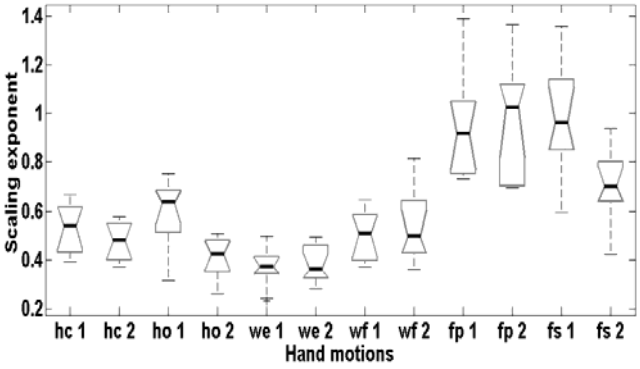

(b)

Figure 4. (a) Bar plot (b) Box plot of Scaling exponent of DFA (option 1.4) for different motions from channel 1 and 2.

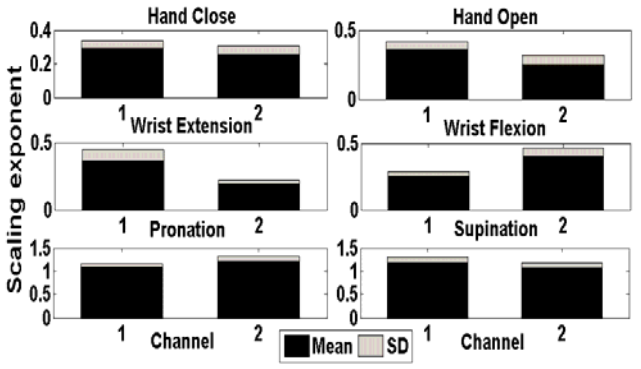

(a)

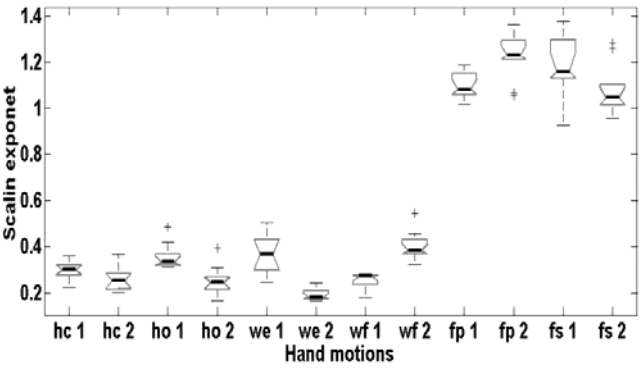

(b)

Figure 5. (a) Bar plot (b) Box plot of Scaling exponent of DFA (option 2.1) for different motions from channel 1 and 2.

the plot, we can see that the pattern of the lines is different for different motions and different channels.

The mean and SD of DFA's scaling exponents in six motions and two channels are presented in Fig. 4(a) and Fig. 5(a) by bar graph and in Fig. 4(b) and Fig. 5(b) by box plot graph. The results that show in Fig. 4 and Fig. 5 are the example results of option 1 and 2, respectively. The best result in this study is meant the balance between the maximum class separability and small experimental variation. The observation of Fig. 4(a) and 5(a) is the different between the DFA's scaling exponent of same motion but different channels and the DFA's scaling exponent of same channel but different motions. Furthermore, the Fig. 4(b) and Fig. 5(b) are confirmed the different between the DFA's scaling exponent of various motions and various channels. The interesting result of DFA's scaling exponents of option 1 is the range of DFA value. When we used window sizes option 1.1, the values of DFA are ranging between 8.5574 and 9.2871 that mean the wrong value of DFA's scaling exponent. However, when the window sizes are setup to option 1.2, 1.3, and 1.4, the range of DFA value will be correct, it ranges between 0.2301 and 1.3909. The option 1.4 has the much bigger range of DFA value, 1.1608, than option 1.2 and 1.3. In the option 2, the range of DFA's scaling exponent is ranged between 1.5363 and 0.0758, the range of option 2.4. The range of option 2 is much bigger than the range of option 1. In this study, the range values of - scaling exponent of DFA varied more than the fractal dimension of [12] that varies between 1.95 and 2.

We are confirmed the quality of the class separability by SD of mean DFA's scaling exponent (SDM) in six motions and two channels and cluster-to-cluster distance (d_{ij}) that are shown in Fig. 6-7 (a) and Fig. 6-7 (b), respectively. The SDM of option 1 increases when the window sizes increase and the option 1.4 has the biggest value of SDM. Moreover, the results of window sizes option 2 are the same trend with option 1. When window sizes increase, the SDM increases. However, some interesting observation is the increasing interval window sizes with the same size interval are better than the increasing interval window sizes with the power of 2.

The cluster-to-cluster distances (d_{ij}) of all window sizes options are shown in Fig. 6(b) and 7(b). We can observe that d_{ij} of all window sizes options of channel 1 is less than d_{ij} of channel 2 except the case of option 1.4. All of these results can confirmed the significant different for different motions and channel. The values of d_{ij} of DFA's scaling exponent in each option in this study are much bigger than the d_{ij} of fractal dimension in [13], in case of the calculation by raw sEMG signals.

In the second condition, the variation in subject experiment direct-change with the maximum class separability. It means that the maximum class separability increases, the variation increases. This is the limitation that should be considered in the practice and applications.

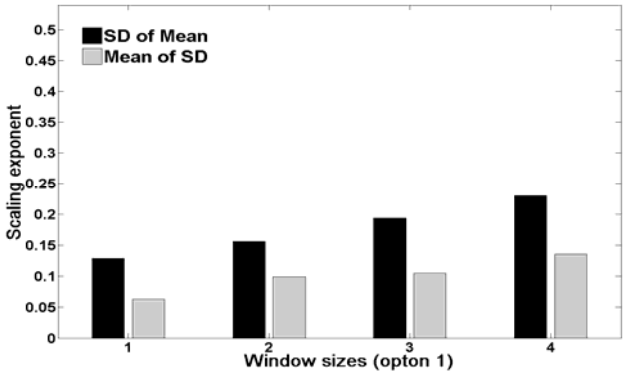

(a)

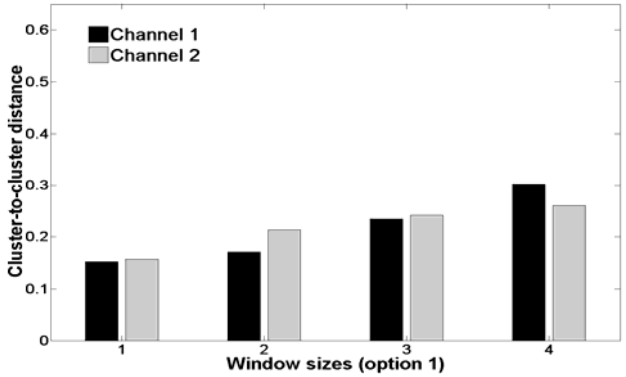

(b)

Figure 6. (a) Bar plot of SD of mean and mean of SD of window sizes (option 1.1 – 1.4) from different motions. (b) Bar plot of average of cluster-to-cluster distance of window sizes (option 1.1 – 1.4) from different motions.

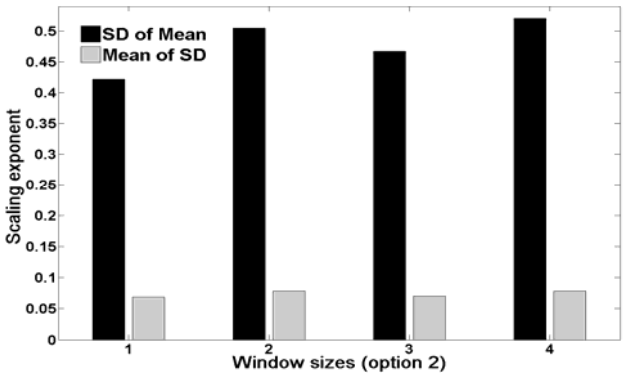

(a)

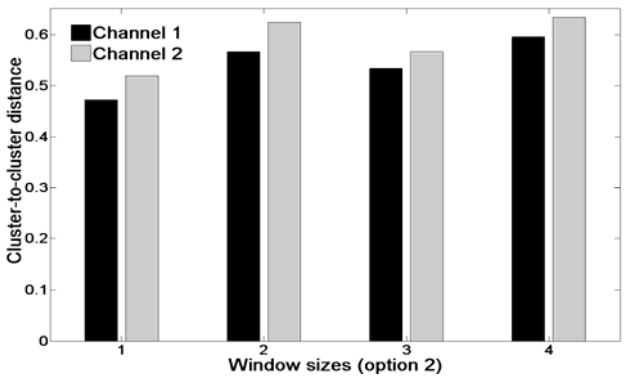

(b)

Figure 7. (a) Bar plot of SD of mean and mean of SD of window sizes (option 2.1 – 2.4) from different motions. (b) Bar plot of average of cluster-to-cluster distance of window sizes (option 2.1 – 2.4) from different motions.

The variation of window sizes option 1 is bigger than the window sizes option 2 that can be observed from Fig. 6-7 (a). The minimum SD is the window sizes option 2.1, 0.0688 and the maximum SD is the window sizes option 1.4, 0.1356. The other indication is the observation of the range of the top and bottom of box in box plot graph, Fig. 4-5(b). From the observation, it is confirmed that the option 2 is much less than the option 1.

The scatter plots between DFA and RMS are shown in Fig. 8. From the Fig. 8(a), the data points in each motion are clear separation. It will be easily grouped when used for pattern recognition. From the Fig. 8(b), it is observed that pattern for different motions are very varied. In practice, it is hard to classify these patterns for maximum rate. From this point, DFA should be combining with other features for a more powerful feature vector.

From the experimental results, we can summary into three points:

1) It is observed that the scaling exponent of DFA of sEMG may be considered as a feature vector for the classification of hand movements. It has the maximum class separability and less variation of subject experimental as compared to existing fractal analysis methods [12-13]. Furthermore, the values of scaling exponent are not depended on the amplitude of sEMG signals same as other features in time domain group such as RMS or MAV (Mean absolute value). In addition, the pattern of DFA's scaling exponents of various hand motions are very different to the patterns of RMS or MAV values that calculated from various hand motions.

2) The optimal window size of DFA algorithm for sEMG signal is the option 2.4 because it is balance between the maximum class separability and less experimental variation.

3) From the values of DFA's scaling exponent of six motions, it is observed that the behavior of wrist extension, wrist flexion, hand close, and hand open are anti-correlated time series. It means that a high amplitude data point is followed by a low amplitude data point, and vice versa. The behavior of DFA's scaling exponent of wrist extension and channel 2 is very high anti-correlated but behavior of DFA's scaling exponent of wrist extension and channel 1 is very low anti-correlated (close to white noise). In addition, the behavior of DFA's scaling exponent of forearm pronation and forearm supination are non-stationary. However, the behavior of DFA's scaling exponent of forearm pronation and channel 1 is associated with pink noise.

5. CONCLUSIONS

Detrended fluctuation analysis (DFA), a novel non-linear analysis, is used to study the properties of sEMG signal.

From the experiments, it is shown that DFA's scaling exponent is the efficient method to make it useful parameter in practical sEMG controlled prostheses. In the future work, the DFA should be tested the performance of class separability with many volunteers that will be answer the variation of this method in inter-subjects. Moreover, the classification of DFA with others feature should be considered for multifunction myoelectric control system.

ACKNOWLEDGMENT

This work was supported in part by the Thailand Research Fund through the Royal Golden Jubilee Ph.D. Program (Grant No. PHD/0110/2550) and in part by NECTEC-PSU center of excellence for rehabilitation engineering and Faculty of Engineering, Prince of Songkla University.

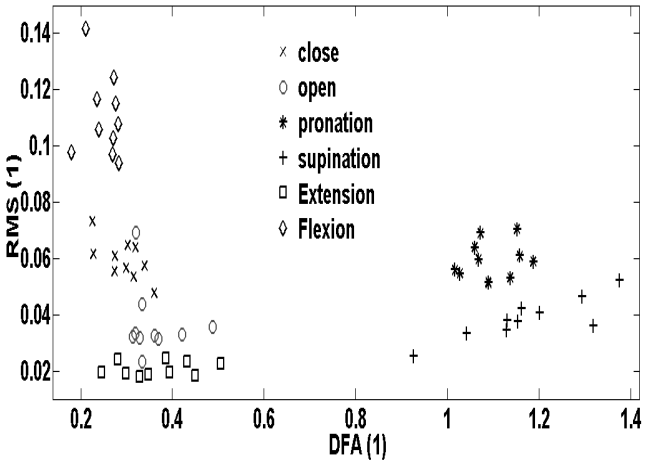

(a)

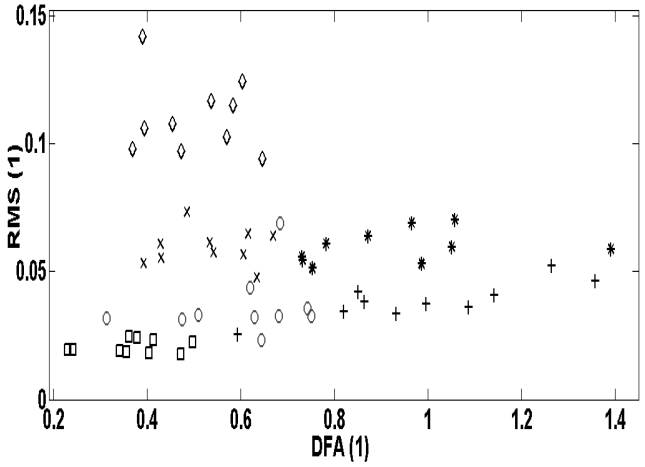

(b)

Figure 8. Scatter plot of different motions between (a) scaling exponent of DFA (option 2.1) and RMS from channel 1. (b) scaling exponent of DFA (option 1.4) and RMS from channel 1.

REFERENCES

[1] R. Merletti, and P. Parker, *Electromyography Physiology, Engineering, and Noninvasive Applications*, John Wiley & Sons, Hoboken, New Jersey, USA, 2004.

[2] R. Boostani, and M.H. Moradi, "Evaluation of the Forearm EMG Signal Features for the Control of a Prosthetic Hand," *Physiological Measurement*, vol. 24, pp. 309-319, Mar. 2003.

[3] M.G. Signorini, M. Ferrario, M. Marchetti, and A. Marseglia, "Nonlinear Analysis of Heart Rate Variability Signal for the Characterization of Cardiac Heart Failure Patients," in *Proc. 28th IEEE Annu. Int. Conf. Engineering in Medicine and Biology*, New York City, USA, pp. 3431-3434, Aug.-Sept. 2006.

[4] M. Obayya, and F. Abou-Chadi, "Classifying Some Cardiac Abnormalities using Heart Rate Variability Signals," in *Proc. 25th National Radio Science Conf.*, Tanta Univ., Egypt, pp. 1-8, Mar. 2008.

[5] J. Zhao, L. Jiang, H. Cai, H. Liu, and G. Hirzinger, "A Novel EMG Motion Pattern Classifier based on Wavelet Transform and Nonlinearlity Analysis Method," in *Proc. IEEE Int. Conf. Robotics and Biomimetics*, Kunming, China, pp. 1494-1499, Dec. 2006.

[6] Y. Meng, B. Liu, and Y. Liu, "A Comprehensive Nonlinear Analysis of Electromyogram," in Proc. 23rd *IEEE Annu. Int. Conf. Engineering in Medicine and Biology*, Istanbul, Turkey, pp. 1078-1081, Oct. 2001.

[7] M. Talebinejad, A.D.C. Chan, A. Miri, and R.M. Dansereau, "Fractal Analysis of Surface Electromyography Signals: A Novel Power Spectrum-based Method," in press *Journal of Electromyography and Kinesiology*, May. 2008.

[8] C.-K. Peng, S. Havlin, H.E. Stanley, and A.L. Goldberger, "Quantification of Scaling Exponents and Crossover Phenomena in Nonstationary Heartbeat Time Series," *Chaos*, vol. 5, no. 1, pp. 82-87, 1995.

[9] D. Abásolo, R. Hornero, J. Escudero, and P. Espino, "A Study on the Possible Usefulness of Detrended Fluctuation Analysis of the Electroencephalogram Background Activity in Alzheimer's Disease," *IEEE Transaction Biomedical Engineering*, vol. 55, no. 9, pp. 2171-2179, Sept. 2008.

[10] K. Hu, P. Ch. Ivanov, Z. Chen, P. Carpena, and H.E. Stanley, "Effect of Trends on Detrended Fluctuation Analysis," *Physical Review E*, Stat. Phys. Plasmas Fluids Relat. Interdiscip. Top., vol. 64, pp. 011114-1–011114-19, Jul. 2001.

[11] M. Phothisonothai, and M. Nakagawa, "Fractal-based EEG Data Analysis of Body Parts Movement Imagery Tasks," *Journal of Physiological Science*, vol. 57, no. 4, pp. 217–226, Aug. 2007.

[12] S.P. Arjunan and D.K. Kumar, "Fractal Based Modelling and Analysis of Electromyography (EMG) to Identify Subtle Actions," in Proc. 29th *IEEE Annu. Int. Conf. Engineering in Medicine and Biology*, Lyon, France, pp. 1961-1964, Aug. 2007.

[13] X. Hu, Z.-Z. Wang, and X.-M. Ren, "Classification of Surface EMG Signal with Fractal Dimension," Journal of Zhejiang University SCIENCE, vol. 6B, no. 8, pp. 844-848, May. 2005.

The Eighth PSU Engineering Conference
22-23 APRIL 2010

Effect of Trends on Detrended Fluctuation Analysis for Surface Electromyography (EMG) Signal

Angkoon Phinyomark[1]* Montri Phothisonothai[2] Chusak Limsakul[1] Pornchai Phukpattaranont[1]
[1]Department of Electrical Engineering, Faculty of Engineering, Prince of Songkla University,
Hat Yai, Songkhla 90112
[2]College of Research Methodology and Cognitive Science, Burapha University,
Bangsaen, Chonburi 20131
E-mail: angkoon.p@hotmail.com*

Abstract
Detrended Fluctuation Analysis (DFA), a novel nonlinear analysis, is a useful tool to study and understand the properties and complexity of surface Electromyography (sEMG) signal. Many noises that contaminate sEMG signals in real applications display trends that become difficult to analyze sEMG signal. The different types of trend fitting of DFA algorithm are used to eliminate these problems. In this study, the performance of DFA algorithm for sEMG-based control is presented. Moreover, the six types of trend, namely linear, quadratic, cubic, fourth order, fifth order, and sixth order polynomial functions are evaluated. The experimental results show that the scaling exponents of linear trend in various hand movements have the significant different values and small experimental variation. Hence, linear trend is a suitable trend fitting for sEMG signal. However, the interesting result is when we considered the scaling exponent of each pair of EMG hand movements; the appropriate trend is changed. Therefore, the selection of optimal trend fitting will improve the effectiveness in analysis of sEMG signals and become the useful tool to extract feature in sEMG-based control. Moreover, the DFA relate to the fractal analysis. The better performance of DFA algorithm over the other fractal parameters in sEMG-based control is shown.
Keywords: Electromyography (EMG), Detrended Fluctuation Analysis (DFA), Feature extraction, Noise, Man-machine interfaces

1. Introduction
Surface Electromyography (sEMG) signal is one of electrophysiological signal that is measured the muscle activity and gives a useful information for study of many clinical and biomedical engineering applications. Use of sEMG signal as a distinguishing tool to identify neuromuscular diseases and disorders of motor control is the currently increasing the importance and also used as an effective control signal for the prosthetic devices. The significant step to achieve the control performance is the extraction of feature from the sEMG signal [1]. Because of lots of information from the raw sEMG signal, the optimal feature will provide the better performance in sEMG-based control. Normally, feature extraction in sEMG analysis can be divided into three groups [1]. The first feature group is based on time domain and linear technique. Two popular features in this group are Mean Absolute Value (MAV) and Root Mean Square (RMS). These features are vastly used in both of diagnostic tool and assistive device control. Even so time domain feature were limited success because these methods presume that the sEMG signal is stationary, while sEMG signal is non-stationary. The second feature group attended to use the frequency information. Mean Frequency (MNF) and Median Frequency (MDF) are two major characteristic variables in frequency domain. There are useful in fatigue analysis but performance in control signal viewpoint is very poor. Subsequently, time-frequency features such as Wavelet Transform (WT) and Wavelet Packet Transform (WPT) were used as the third feature group. The good ability in class separability viewpoint of this feature group is presented in many literatures. Nevertheless, the drawbacks of their complexity and computational time are main limitation of feature in this group. Moreover, all of these features that introduce above are calculated based on linear or statistical analysis but the properties of sEMG signal are very complex, non-linear, non-stationary, and non-periodic [2].

Non-linear analysis technique is necessary to comprehend the complexness of sEMG signal [2]. Detrended Fluctuation Analysis (DFA) is one of non-linear analysis method that is an effective method in a range of biological, forecasting, and medical applications. Peng et al. [3] invented DFA as an important tool for detection of long-range correlations in time series of noisy signal. The fractal scaling exponent is determined by DFA and it is very helpful parameter for non-stationary time series analysis. From the literatures, the success of DFA algorithm in many fields such as DNA sequences, human gait, cardiac dynamics, economics time series, and longtime weather records are reported. In addition, fractal analysis of complex medical signals such as Electroencephalogram (EEG) and Electrocardiogram (ECG) signal are well performed [4]. However, the usefulness of DFA in EMG analysis has been started in our previous work [7]. In [7], DFA is a beneficial

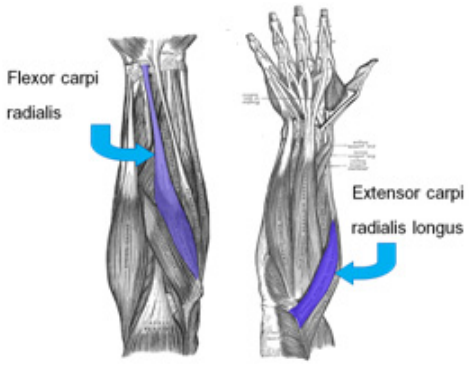

Figure 1. Two muscle position on the forearm [5-6].

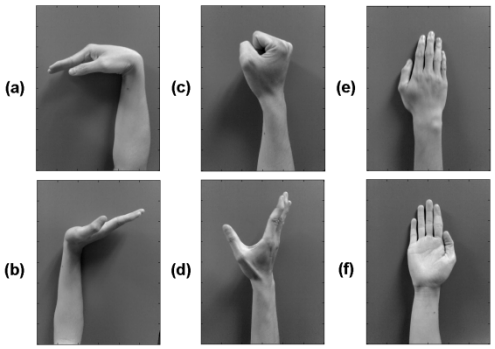

Figure 2. Six different types of hand movement (a) wrist flexion (b) wrist extension (c) hand close (d) hand open (e) forearm pronation (f) forearm supination [8].

tool to characterize the self-similarity of sEMG signal and extract the novel feature that has the different pattern from popular feature such as RMS or MAV. Besides the effect of window size parameter of DFA is evaluated. In this paper, the usefulness of DFA algorithm to study the nonlinear properties of sEMG signal is still discovered. In addition, the effects of trend in fitting procedures are evaluated to eliminate different orders of noisy trend in sEMG signals. The variety of the sEMG signals recorded from six hand movements and two muscle positions are used as representative sEMG signals.

This paper is organized as follows. In Section 2, the experiments and data acquisition are introduced in detail. The proposed algorithm, DFA, is defined in Section 3 with the evaluation methods. In Section 4, the comparative analysis of DFA's trend is reported and discussed. Finally, the concluding remarks are drawn.

2. Experiments and Data Acquisition

Two channels of sEMG signals were recorded by two pairs of bipolar Ag/AgCl electrodes (3M red dot solid gel). One pair was placed over the flexor carpi radialis (Ch1) and the other was placed over the extensor carpi radialis longus (Ch2), as shown in Fig. 1. The top side of the wrist is used as the reference electrode position. All disc electrodes were put on the skin surface of the right forearm of volunteer. Each bipolar pair of electrodes was spaced from a center to center by 20 mm. In addition, to avoiding the cross interference between two channels, 5 mm diameter electrodes were used. Differential amplifiers were set with 60 dB gain and band-pass filters of 10-500 Hz bandwidth were used to remove the high random frequency noises and movement artifacts at low frequency. Sampling frequency was set at 1000 Hz using a 16 bit analog-to-digital converter board (NI, DAQCard-6024E).

A healthy volunteer was asked to perform six different types of movement: wrist flexion (WF), wrist extension (WE), hand close (HC), hand open (HO), forearm pronation (FP), and forearm supination (FS), as shown in Fig. 2. The size of sEMG samples were recorded for 256 ms with the aim of real-time signals processing (the maximal allowable delay for prosthetic control should be less than 300 ms [9]). A volunteer was instructed to repeat each hand movement category ten times. Hence, there were 120 datasets of two channels of sEMG signals in total.

3. Methodology

DFA is an alterable RMS of a random walk to study electrophysiological signal. We used the fractal scaling exponent from DFA algorithm to distinguish the sEMG signal with hand movements. The scaling exponent of DFA is one of the fractal parameters. It relates to Hurst exponent and fractal dimension. The conversion between DFA's scaling exponent and other fractal parameters is easy with linear equation. Hence we considered only DFA's scaling exponent which can be widely used in non-linear analysis.

3.1 Detrended fluctuation analysis

To illustrate the procedure of DFA algorithm, we use the sEMG time series as shown in Fig. 3(a) that be signified by $\{x(t)\}$, where t is the discrete time in the range [1, N] where N is the sample length of time series. The scheme of DFA follows six steps described below.

1. The sEMG time series is first integrated. This integration process is used to convert sEMG signals into a random walk. The integrated series or profile is

$$y(k) = \sum_{t=1}^{k} \left[\{x(t)\} - \overline{x(t)} \right], k = 1, ..., N \ , \qquad (1)$$

where $\overline{x(t)}$ represents the average value of $x(t)$. $y(k)$ is called cumulative sum or profile. The example results are shown in Fig. 3(b-c) in dotted lines.

2. The profiles are divided into L equal window sizes as shown in Fig. 3(b-c) in dashed lines. In each window has an n time points, where n is defined as int(N/L). Instead of focusing on the selection of window sizes, we have already presented in our previous work that the optimal window size are in the range [16, 128] with 16 time intervals [7].

3. Inside each window of length n, a least-square is fit to the profile ($\{y(k)\}$) as shown in Fig. 3(b-c) in solid lines. The coefficient of y coordinate is referred

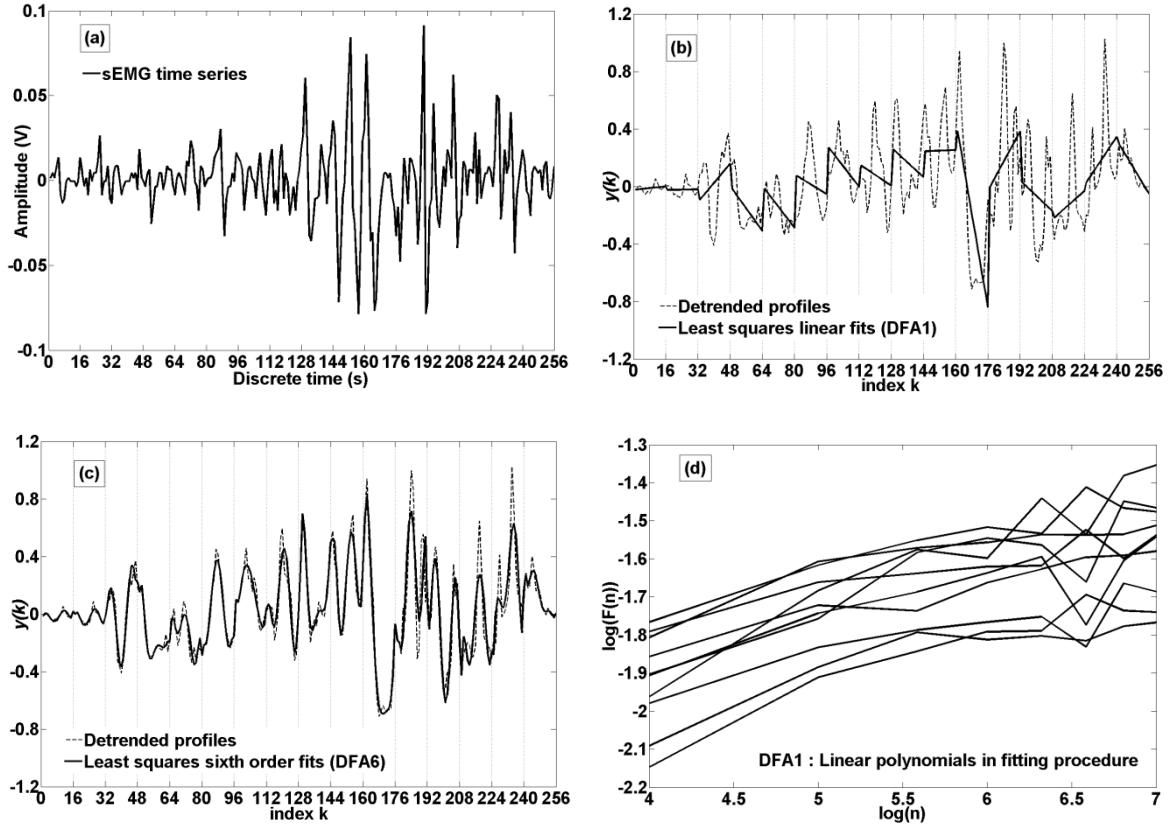

Figure 3. Example of calculate the DFA of sEMG signal (a) sEMG time series (b-c) Detrended profiles (dotted lines), window sizes (dashed lines), and least squares fits (solid lines) (b) DFA1 (c) DFA6 (d) plot of log *F(n)* and log *n* for sEMG time series with 10 repetition.

by $y_n(k)$. The least-square fits are shown the semi-local trend in that window. In this study, the various orders of polynomial function are evaluated the effect of detrending. Six types of fitting procedure are linear (DFA-1), quadratic (DFA-2), cubic (DFA-3), forth order (DFA-4), fifth order (DFA-5), and sixth order (DFA-6) polynomial functions.

4. The RMS fluctuation of the profiles and detrended time series are calculated by

$$F(n) = \sqrt{\frac{1}{N}\sum_{k=1}^{N}\left[y(k) - y_n(k)\right]^2}. \qquad (2)$$

5. The computation is repeated over all window sizes, as define in the second step. As a result, the linear relationship between $F(n)$ and n is plotted in log-log graph.

6. The slope of the line between log $F(n)$ and log n can be characterized the fluctuation as shown in Fig. 3(d). This slope is called scaling exponent α and it is used as a feature parameter in this study. The natural logarithm is applied in this work.

Mainly the regular DFA uses linear polynomial to fit and detrend the sEMG profiles. The linear fitting can eliminate only constant trend in the noisy sEMG signal. However, due to the varieties of noise are not only in constant form or trend, the different orders of trend fitting of DFA algorithm are used to resolve a problem. We will explain in described case, linear fitting (n = 1). The linear fittings are applied to the profile as shown in Fig. 3(b), so we call DFA-1. Due to the profiles (dotted lines) in Fig. 3(b), DFA-1 can eliminate the constant trend in original ($x(t)$) signal. Therefore, the DFA of order n can remove trend of order $n-1$. If the noisy signal is contaminated with the linear trend, it means the quadratic fitting or DFA-2 is needed. In this study, we vary the order of trend fitting of DFA algorithm from 1 to 6, because DFA-6 polynomial fits shows more similarity with sEMG signal.

3.2 Evaluation method

For sEMG-based control, the selection of feature is an important stage to succeed optimal performance in classification. In [1], the evaluation of the quality of EMG feature is measured by three criterions: class separability, robustness, and complexity. In this study, we demonstrate a novel feature extraction, DFA's scaling exponent, to recognize the hand movement in class separability point of view. Moreover, the effect of trend in DFA feature does not only enhance the class separability property also enhance the usefulness of the DFA feature with noisy environment. The robustness criterion is discussed with the effect of DFA's order and behavior of time series. The better quality in sEMG-based control is performed when the representative feature can reach the high recognition rate and get the small variation in subject experiment. For the class separability viewpoint, the statistical

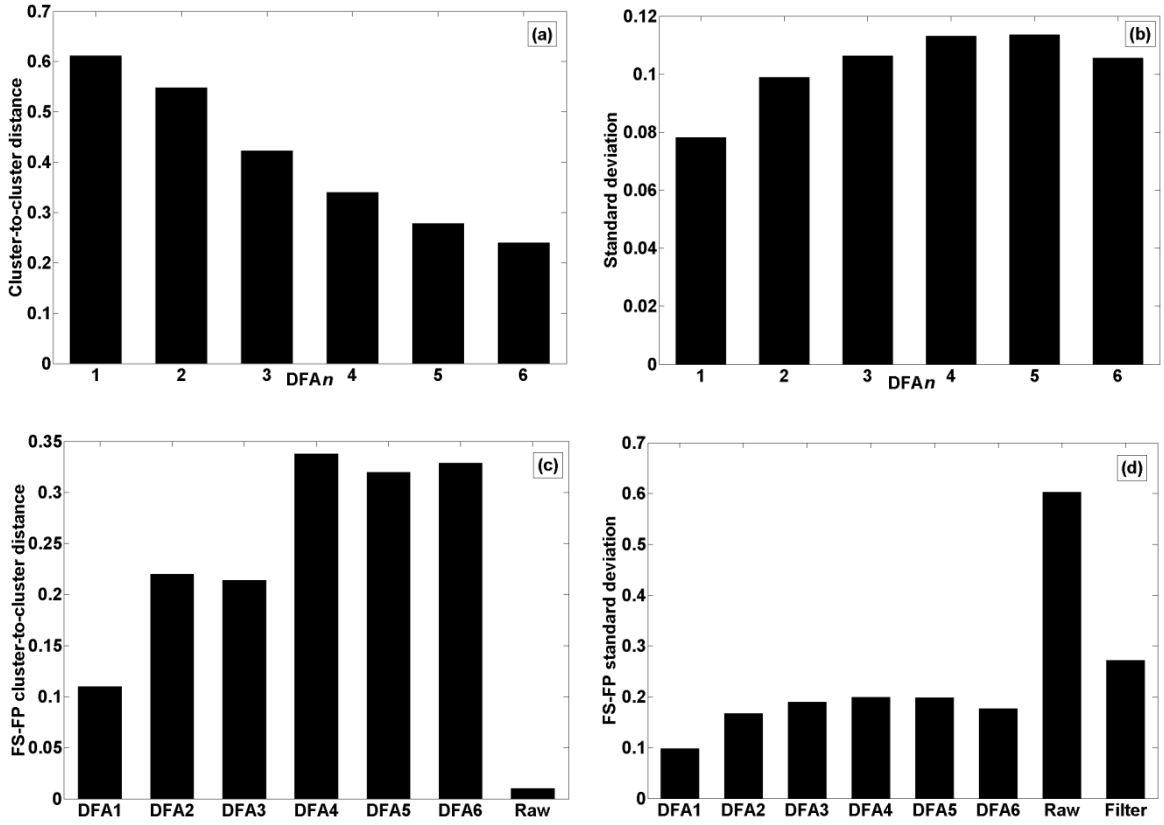

Figure 4. (a) Bar plot of d_{ij} of various types of DFA*n* (b) Bar plot of σ of various types of DFA*n* (c) Bar plot of d_{ij} of FS and FP movements (d) Bar plot of σ of FS and FP movements (Raw and Filter in (c) and (d) is meant fractal parameters calculated based on raw and filtered sEMG signals, respectively in [11]).

indication can be used same as the measuring of recognition rate using classifier. The first method has advantage that the evaluation of features is not dependent on the statistic types as in the second method that is dependent on the classifier types. Cluster-to-cluster distance (d_{ij}) is a statistic indication that is used to illustrate the difference between two scatter groups [11]. It calculates the distance between mean features of different movements as defined by

$$d_{ij} = \left\| mean_i - mean_j \right\|, \quad (3)$$

where $mean_i$ ($mean_j$) is the average of DFA's scaling exponent of movement i (j); i and j is one of six hand movements and one of two channels.

In this study, the averaging of d_{ij} of the possible combination between two movements from the total six hand movements and two channels is performed to confirm the results. The performance of recognition is best when the averaged distance (d_{ij}) is large. The other condition that should be considered is the variation in subject experiment. Normally, standard deviation (σ) is the measured index of the variation. In practice, each trial of the same movement, the value of DFA's scaling exponent should be the same value. It means that the variation should be small, in other words, the σ should be as small as possible. The σ of each movements and channels are averaged to confirm the results.

4. Results and Discussion

4.1 Class separability criterion

The value of DFA's scaling exponents in six movements and two channels of the various fitting orders are presented. The results show the usefulness of DFA features same as the results in [7]. The effect of six trend types are evaluated and discussed in this study. The best result is meant that the balance between the maximum class separability (d_{ij}) and the small experimental variation (σ). From the observation of d_{ij} of six trend types as shown in Fig. 4(a), DFA-1 has the maximum value of d_{ij} that means it obtained the maximum class separability. In addition, we observed that the performance of class separability is reduced when the order of DFA increases. Note that the d_{ij} as shown in Fig. 4(a) is calculated with the sEMG signals in six movements and two channels.

However, if we considered the d_{ij} of each pair of EMG hand movements, we found that the suitable order is changed. For example, the d_{ij} between HO and HC movements obtains the highest value when the trend fitting is DFA-6 and the d_{ij} between WE and WF movements obtains the highest value when the trend fitting is DFA-1. Therefore, in practice, the selection of optimal trend fitting with the selected sEMG signal will improve the effectiveness in the analyzing of sEMG analysis and become the useful

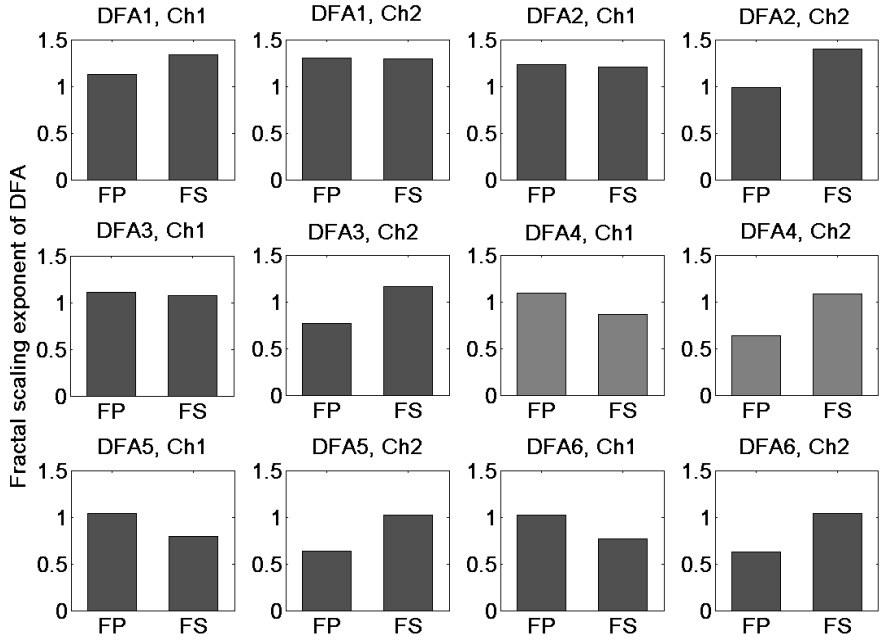

Figure 5. Bar plot of DFA's scaling exponent for FP-FS movements from two channels with six different orders.

tool to extract feature in sEMG-based control.

From the theory, the DFA algorithm relates to the fractal analysis. The other fractal parameters used in the previous literatures [10-11] are compared with the fractal scaling exponent from the DFA algorithm. In [10], the values of fractal parameter are only ranging between 1.950 and 2.000 for four movements and four muscles but the DFA's scaling exponent with DFA-1 in this study are varied from 0.075 to 1.536. So the interval of our DFA value is bigger than the interval of fractal parameter reported in [10]. It is guaranteed the discriminate ability. Furthermore, the values of d_{ij} of DFA's scaling exponent in each trend in this study are much bigger than the d_{ij} of fractal dimension in [11], in case of the calculation by raw sEMG signals as the results shown in Fig. 4(c).

In the second condition, the variation in subject experiment is discussed. Normally, the maximum class separability directly changes with the variation in subject experiment. It means that the maximum class separability increases, the variation increases. This is the limitation that should be considered in the practice and real-world applications. However, the effect of the variation of DFA is not normality. The variation of DFA-1 is smaller than other trends that can be observed from Fig. 4(b). It guarantees that the optimal order of fitting procedure for DFA algorithm in analysis of EMG signal is the DFA-1 or linear polynomial function. The maximal σ is obtained when the fitting procedure is DFA-4 and DFA-5.

The interesting results are shown in Fig. 4 (c-d). The figures show the comparison of d_{ij} and σ between the six trends in this study and in [11]. The results of literature calculate the fractal parameter of FS and FP. We compare only two movements (FS and FP) of our results with results in [11] that used the same muscle position. In the d_{ij} results, DFA-4 has the maximum value, followed closely by DFA-6 and DFA-5. On the other hand, the d_{ij} of fractal-based on raw sEMG data in [11] is very small. It is expected to perform poor class separability. Moreover, the σ of fractal-based on both raw and filtered sEMG data in [11] are bigger than each trend in this study. Therefore, estimation of fractal parameter with DFA algorithm is better than the estimation of fractal parameter with Higuchi's fractal dimension and correlation dimension that used in [10] and [11], respectively.

For the class separability point of view, we can summarize into two points:

1. It is observed that the fractal scaling exponent of DFA method may be considered as a feature vector for the classification of EMG hand movements. It has the maximum class separability and less variation of subject experiment as compared to the existing fractal methods to estimate fractal parameters [10-11]. In addition, the values of fractal scaling exponent are not dependent on the amplitude of sEMG signals like as other features in time domain group such as MAV or RMS. Furthermore, the patterns of fractal scaling exponents of many kinds of hand movements are very different to the patterns of RMS or MAV features that calculated from various hand movements.

2. The optimal trend of fitting procedure for DFA algorithm with sEMG signal is DFA-1 or linear polynomial function because it obtains the better results in both of maximum class separability viewpoint and less experimental variation viewpoint.

4.2 Robustness criterion

The scaling exponent α is an indicator of the

nature of the fluctuations in the sEMG signal that can be explicating the behavior of sEMG time series. If $0 < \alpha < 0.5$, the correlation in the time series are antipersistent, while if $0.5 < \alpha < 1$, the correlation in the time series are persistent. Furthermore, when $1 < \alpha < 1.5$, the behavior of the time series is non-stationary or random walk. The fractal-like signal (1/f noise) or pink noise results in $\alpha \cong 1$, the uncorrelated or white noise results in $\alpha \cong 0.5$, and the Brownian noise in $\alpha \cong 1.5$.

For the robustness point of view, we can use the advantage of higher order (4^{th}, 5^{th}, and 6^{th}) that has better class separability (high d_{ij}) than the lower order. The behavior of the sEMG signal in various hand movements can describe this advantage point. It is observed that the behavior of WE, WF, HC, and HO are anti-correlated time series. It means that a high amplitude data point is followed by a low amplitude data point, and vice versa. However, the behavior of FP and FS are non-stationary or random walk in most trends (DFA's scaling exponent values are more than one). The amplitudes of these movements are very small. Although, MAV or RMS features (popular features in sEMG-based control) in FP and FS are calculated features based on amplitude. Therefore, the value of MAV and RMS is close to zero. If the sEMG signal is contaminated, it becomes difficult to analyze. However, the higher order of the DFA generate the crucial difference between two channels of FP and FS as shown in Fig. 5 that normally has the same values in the most of EMG features. In other way, we can observe the d_{ij} value of FP and FS movements as shown in Fig. 4(c). This advantage point is strongly recommended to extract features in movements that have the small amplitude.

5. Conclusion

A novel non-linear and fractal method analysis, Detrended fluctuation analysis (DFA) is used to study the non-stationary characteristics of sEMG signal. From the results, the fractal scaling exponent that estimated with DFA is the powerful method to make it useful parameter in practical sEMG-based control such as prosthetic or robot arm. The selection of detrended with specific sEMG signal will be improve the effective in processing. Extraction of DFA feature on higher order trends is recommended to use with the sEMG signals with small amplitude property. In the future work, the DFA feature should be tested the performance of movement separability with many volunteers that will be answering the variation of this method in inter-subjects. Moreover, the classification of DFA based on the small order for high amplitude movements and high order for low amplitude movements should be considered for sEMG-based control.

Acknowledgments

This work was supported in part by the Thailand Research Fund through the Royal Golden Jubilee Ph.D. Program (Grant No. PHD/0110/2550), in part by College of Research Methodology and Cognitive Science, Burapha University and in part by NECTEC-PSU center of excellence for rehabilitation engineering and Faculty of Engineering, Prince of Songkla University.

References

[1] Boostani, R. and Moradi, M.H. 2003. Evaluation of the Forearm EMG Signal Features for the Control of a Prosthetic Hand. Physiological Measurement, 24: 309-319.

[2] Talebinejad, M., Chan, A.D.C., Miri, A. and Dansereau, R.M. 2008. Fractal Analysis of Surface Electromyography Signals: A Novel Power Spectrum-based Method. Journal of Electromyography and Kinesiology, In Press.

[3] Peng, C.-K., Havlin, S., Stanley, H.E. and Goldberger, A.L. 1995. Quantification of Scaling Exponents and Crossover Phenomena in Nonstationary Heartbeat Time Series. Chaos, 5: 82-87.

[4] Hu, K., Ivanov, P.Ch., Chen, Z., Carpena, P. and Stanley, H.E. 1999. Effect of Trends on Detrended Fluctuation Analysis. Physical Review E, 64: 011114.

[5] Flexor carpi radialis muscle, Wikipedia. [Online]. Available: http://en.wikipedia.org/wiki/Flexor_carpi_radialis.

[6] Extensor carpi radialis longus muscle, Wikipedia. [Online]. Available: http://en.wikipedia.org/wiki/Extensor_carpi_radialis_longus_muscle.

[7] Phinyomark, A., Phothisonothai, M., Limsakul, C. and Phukpattaranont, P. 2009. Detrended Fluctuation Analysis of Electromyography Signal to Identify Hand Movement. Proceedings of the Second Biomedical Engineering International Conference, Phuket, Thailand, Aug. 13-14, 2009: 324-329.

[8] Phinyomark, A., Limsakul, C. and Phukpattaranont, P. 2009. A Novel Feature Extraction for Robust EMG Pattern Recognition. Journal of Computing, 1(1): 71-80.

[9] Englehart, K., Hudgins, B. and Parker, P.A. 2001. A Wavelet-Based Continuous Classification Scheme for Multifunction Myoelectric Control. IEEE Transactions on Biomedical Engineering, 48(3): 302-311.

[10] Arjunan, S.P. and Kumar, D.K. 2007. Fractal Based Modelling and Analysis of Electromyography (EMG) to Identify Subtle Actions. Proceedings of the 29th Annual International Conference of the IEEE Engineering in Medicine and Biology Society, Lyon, France, Aug. 22-26, 2007: 1961-1964.

[11] Hu, X., Wang, Z.-Z. and Ren, X.-M. 2005. Classification of Surface EMG Signal with Fractal Dimension. Journal of Zhejiang University Science B, 6(8): 844-848.

5. สรุปผลการวิจัย

ในการประเมินหาวิธีการวัดลักษณะเด่นของสัญญาณที่ดีที่สุดนั้น ได้แบ่งการประเมินออกเป็น 3 ประเด็น คือ 1. ความแม่นยำในการระบุท่าทางการเคลื่อนไหว 2. ความสามารถในการทนต่อสัญญาณรบกวน 3. เวลาและความซับซ้อนในการคำนวณ ซึ่งในทั้ง 3 ประเด็นนั้น จะมีการหาวิธีการวัดลักษณะเด่นของสัญญาณ ทั้งจากการประเมินวิธีการวัดลักษณะเด่นของสัญญาณที่มีการใช้งานอยู่ในปัจจุบัน ด้วยวิธีทางสถิติ และวิธีใช้ตัวจำแนก การปรับปรุงวิธีการวัดลักษณะเด่นของสัญญาณที่มีอยู่เดิม ให้มีคุณสมบัติบางประการที่ดีขึ้น รวมถึงการหาวิธีการวัดลักษณะเด่นของสัญญาณชนิดใหม่ที่ดีมาประยุกต์ใช้งาน อย่างไรก็ตามจากข้อจำกัดที่ว่า ไม่มีวิธีการวัดลักษณะเด่นของสัญญาณชนิดใดที่จะได้ผลดีที่สุดในทั้ง 3 ประเด็นนั้น ในขั้นของการทดลอง และสรุปผลวิธีการวัดลักษณะเด่นของสัญญาณที่ดีที่สุด จึงแยกวิเคราะห์ในแต่ละประเด็น โดยในการนำไปประยุกต์ใช้งานจริง มีความจำเป็นต้องเลือกใช้เหมาะสมกับงานต่อไป สำหรับวิธีการวัดลักษณะเด่นของสัญญาณที่นำมาประเมินในงานวิจัยมีด้วยกัน 16 วิธี มีการปรับปรุงวิธีการวัดลักษณะเด่นของสัญญาณ 2 วิธี และนำเสนอวิธีการวัดลักษณะเด่นของสัญญาณชนิดใหม่ 1 วิธี ซึ่งสามารถสรุปผลการวิจัยแบ่งตามบทความได้ดังนี้

บทความที่ 1 และ 2 พบว่าการรวมกลุ่มวิธีการวัดลักษณะเด่นของสัญญาณ 3 ชนิด ประกอบด้วย วิธี Root Mean Square วิธี Waveform Length และวิธี Auto Regressive อันดับที่ 4 ให้ผลค่าความแม่นยำในการจำแนกท่าทาง ขณะไม่มีสัญญาณรบกวนสูงถึง 98-99% โดยการประเมินด้วยตัวจำแนกชนิด Linear Discriminant Analysis นอกจากนี้ในบทความทั้งสองยังได้ทำการพัฒนาวิธีการในการเตรียมข้อมูลก่อนการหาลักษณะเด่นของสัญญาณด้วยวิธี Wavelet Transform พร้อมการลดสัญญาณรบกวน ซึ่งทำให้ระบบยังคงค่าความแม่นยำในการจำแนกสูงกว่าไม่มีการลดสัญญาณรบกวนเมื่อมีสัญญาณรบกวนเข้ามาในระบบได้ตั้งแต่ 6.5 จนถึง 78.5% ขึ้นกับระดับของสัญญาณรบกวนในระบบ

บทความที่ 3 เมื่อทำการประเมินด้วยวิธีทางสถิติ เพื่อเป็นการยืนยันผลของการประเมินด้วยตัวจำแนก พบว่าวิธีการวัดลักษณะเด่นของสัญญาณแบบ Waveform Length ให้ผลดีที่สุด โดยการใช้วิธีการวัดทางสถิติแบบอัตราส่วนระหว่างค่าของ Euclidean distance และ Standard deviation นอกจากนี้วิธีการอื่นๆ ที่ให้ผลรองลงมาได้แก่ วิธี Root Mean Square และวิธี Willison Amplitude

ดังนั้นจากบทความทั้ง 3 ข้างต้น จะพบได้ว่า ในแง่มุมของความแม่นยำในการระบุท่าทาง สามารถสรุปได้ว่าวิธีการวัดลักษณะเด่นของสัญญาณแบบ Waveform Length ให้ผลดีที่สุด แต่ถึงอย่างไรก็ตามในการนำไปประยุกต์ใช้งานจริงมีความจำเป็นต้องรวมกลุ่มของวิธีการวัดลักษณะเด่นของสัญญาณ ตัวอย่างของกลุ่มที่นำเสนอในบทความที่ 1 และ 2 ก็ถือเป็นกลุ่มวิธีการวัดลักษณะเด่นของสัญญาณที่ให้ผลดี แนะนำให้นำไปใช้งานได้ต่ออีกกลุ่มหนึ่ง

บทความที่ 4 มีการปรับปรุงวิธีการวัดลักษณะเด่นของสัญญาณเชิงความถี่ 2 วิธี คือ วิธี Modified Mean Frequency และวิธี Modified Median Frequency ซึ่งพบว่าสามารถเพิ่มประสิทธิภาพในการทนต่อสัญญาณรบกวนได้ดีขึ้น โดยวิธีการของ Modified Mean Frequency ที่ถูกปรับปรุงให้ผลดีกว่าวิธีการของ Modified Median Frequency และยังให้ผลดีกว่าวิธีการวัดลักษณะเด่นของสัญญาณชนิดเดิม สำหรับวิธีการวัดลักษณะเด่น

ของสัญญาณชนิดเดิมที่ให้ผลในการทนต่อสัญญาณรบกวนรองลงมาได้แก่ วิธี Willison Amplitude และวิธี Histogram of EMG

บทความที่ 5 และ 6 ได้มีการหาวิธีการคัดเลือกลักษณะเด่นของสัญญาณชนิดใหม่ คือ วิธี Detrended Fluctuation Analysis ซึ่งเป็นวิธีที่สามารถเข้าถึงความเป็น Non-stationary ของสัญญาณไฟฟ้ากล้ามเนื้อได้เหมือนกับวิธีการวัดลักษณะเด่นของสัญญาณบนแกนเวลาและความถี่ แต่ใช้เวลาในการคำนวณและความซับซ้อนที่น้อยกว่า โดยในการวิจัยพบว่าวิธีดังกล่าวยังคงให้ความแม่นยำในการระบุท่าทาง และความสามารถในการทนต่อสัญญาณรบกวนที่ดีด้วย

บรรณานุกรม

[1] M. Asghari Oskoei and H. Hu “Myoelectric Control Systems-A Survey,” Biomedical Signal Processing and Control, vol. 2, no. 4, Oct 2007, pp. 275-294.

[2] P. Parker, K. Englehart, and B. Hudgins “Myoelectric Signal Processing for Control of Powered Limb Prostheses,” Journal of Electromyography and Kinesiology, vol. 16, 2006, pp. 541-548.

[3] M. Zecca, S. Micera, M.C. Carrozza, and P. Dario “Control of Multifunctional Prosthetic Hands by Processing the Electromyographic Signal,” Critical Reviews in Biomedical Engineering, vol. 30, no. 4-6, 2002, pp. 459-485.

[4] B. Hudgins, P. Parker, and R.N. Scott “A New Strategy for Multifunction Myoelectric Control,” IEEE Transaction on Biomedical Engineering, vol. 40, no.1, 1996, pp. 82-94.

[5] M.C. Santa-Cruz, R. Riso and F. Sepulveda “Optimal Selection of Time Series Coefficients for Wrist Myoelectric Control based on Intramuscular Recordings,” Proceeding of the 23rd Annual EMBS International Conference, Turkey, October 2001, pp. 1384-1387.

[6] K. Englehart, B. Hudgins, and P.A. Parker “A Wavelet-Based Continuous Classification Scheme for Multifunction Myoelectric Control,” IEEE Transaction on Biomedical Engineering, vol. 48, no. 3, Mar 2001, pp. 302-311.

[7] R. Boostani and M. Hassan Moradi “Evaluation of the Forearm EMG Signal Features for the Control of a Prosthetic Hand,” Physiology Measurement, vol. 24, 2003, pp. 309-319.

[8] M. Zardoshti-Kermani, B.C. Wheeler, K. Badie, and R.M. Hashemi “EMG Feature Evaluation for Movement Control of Upper Extremity Prostheses,” IEEE Transaction on Rehabilitation Engineering, vol. 3, no. 4, Dec 1995, pp. 324-333.